Novel Biomarker Identification in Pancreatic Cancer using Raman Spectroscopy

Miss Hawwa Ahmed Bham

This dissertation is submitted for the fulfilment for the requirements of an intercalated degree of Master of Science by Research at Lancaster University.

August 2018

Declaration

I declare that this thesis is my own original work, and has not been submitted for a higher degree course at any other institution.

Word Count: 33,918

Acknowledgements

First, I would like to thank the patients who have provided consent for their tissue to be collected for this research and the staff involved in the collection of the tissue. This work would not have been possible without their samples. I would also like to thank University Hospitals of Morecambe Bay for the funding which enabled this project.

I would like to thank my supervisor, Dr Jemma Kerns for her excellent guidance and support throughout this research; her close tuition, encouragement and wealth of experience made this research possible. I would also like to thank Mr Georgios Sgourakis for his advice and support.

Ms Rebecca Shepherd's and Dr Nur Adeelah Tantowi's experience and tuition with histology and ELISA were extremely helpful when learning these techniques. Dr Lorna Ashton and Mr Pedro Elston provided advice and their support and wealth of experience with Raman spectroscopy was invaluable when conducting experiments.

Finally, I would like thank the students in the office and laboratories, for their encouragement and friendship over the course of this project.

Abstract

Pancreatic cancer presents an increasing mortality burden, with little improvement in survival rates since 1970, largely because of the non-resectable status of most tumours at diagnosis and high rate of recurrence after resection. Currently, there are significant problems with accurately identifying tumour margins, both during surgery and through histopathology, causing limitations in clinical practice and research. This presents a need for clinically applicable research, to improve detection and differentiation of healthy and cancerous tissue in the exocrine pancreas.

SPARC has been shown to play a role and be expressed in the development of pancreatic cancer and has recently been identified as a potential biomarker for the disease. Raman spectroscopy is an emerging technology, showing promise in the detection and surgical guidance of many cancers. There is, however, limited research on its use in pancreatic cancer.

This study aims to investigate the utility of Raman spectroscopy in identifying and exploring the development of pancreatic cancer and differences between healthy and cancerous pancreatic tissue, which could eventually allow translation to clinical practice.

This study identifies differences between healthy and cancerous pancreatic tissue, using Raman spectroscopy in human tumour resections and blood samples. Differences are seen due to proline and nucleic acids in fresh tissue and collagen in fixed tissue. It further utilises a 2D cell-line model, Raman spectroscopy and ELISA, providing greater understanding of the interactions between cancer and stellate cells, including the production of SPARC and collagen, in pancreatic cancer.

This study concludes by proposing a hypothesis, highlighting the importance of collagen, SPARC and their potential roles in causing biochemical changes to cancer cells and as possible biomarkers. Overall, it demonstrates the potential utility of Raman spectroscopy in pancreatic cancer, providing the basis for further research

and translation to clinical practice, improving survival rates and reducing the mortality burden currently associated with the disease.

Contents

List of Figures

List of Tables

Chapter 1- Introduction

1.1 Pancreatic Cancer

Cancers of the exocrine pancreas comprise of ductal adenocarcinomas (PDAC), acinar cell carcinomas, solid pseudopapillary neoplasms and pancreatoblastomas, making up 95% of all pancreatic cancers. About 5% of malignancies occur in the endocrine pancreas in the form of neuroendocrine tumours.(1) PDAC is the most common form making up more than 80% of all pancreatic cancers. Although a rare cancer, accounting for 3% of all new cancer cases in the UK, incidence rates have increased by 14% since 1990 and over 80% are diagnosed at a late stage.(1) It is the fifth most common cause of cancer related death, with mortality rates remaining at 7% and a 10-year survival rate of less than 1%, figures unchanged since 1970.(2) (Cancer Research UK)

1.2 The normal pancreas – anatomy and histology

The normal pancreas is a retroperitoneal organ made up of a head, body and tail, which extends from the duodenum to the hilum of the spleen. The head contains an additional projection, the uncinate process which projects medially from the inferior section of the head and lies under the body of the pancreas and posterior to the superior mesenteric vessels.(3) The tail is the only section of the pancreas which is intraperitoneal, lying in the splenorenal ligament, alongside the splenic vessels.

The head of the pancreas lies inferior to the origin of the coeliac axis and just superior to the origin of the superior mesenteric axis; both major arterial sources to the gastrointestinal tract.(4) The aorta and inferior vena cava pass posteriorly to the head of the pancreas. Lying in the curve of the duodenum it is medial to the gall bladder and liver and in close proximity to these organs and their ducts.(4)

It connects to the duodenum via two ducts; the pancreatic duct and an accessory duct. The pancreatic duct empties in to the ampulla of Vater, where it joins the common bile duct to form the hepatobiliary duct before emptying in to the

duodenum. The accessory duct empties into the duodenum through the minor duodenal papilla lying superior to the ampulla of Vater. The minor duodenal papilla does not always have a working sphincter (the sphincter of Helly) and patent duct (the accessory pancreatic duct of Santorini). In 10% of cases, the minor duodenal papilla is the principal duct for drainage of the pancreas.(5) Secretions are controlled by the sphincter of Oddi.

It receives a blood supply from the pancreatic branches of the splenic artery. The head has an additional blood supply from the superior and inferior pancreaticoduodenal arteries, which are branches of the gastroduodenal artery, a terminal branch of the common hepatic artery, and the superior mesenteric artery.(3) The body and neck of the pancreas drain into the splenic vein while the head drains into the superior mesenteric and portal veins.
The head of the pancreas drains into the pancreaticoduodenal, the hepatoduodenal ligament, and the pre-pyloric and post-pyloric lymph nodes.(3) The body and tail drain into the lymph nodes around the middle colic artery and the hepatic and splenic arteries. Ultimate drainage ensues into coeliac, superior mesenteric, and para-aortic and aortocaval lymph nodes.(3, 6)

At a cellular and functional level, the pancreas splits into an endocrine and exocrine portion. The exocrine portion consists of acini, glandular epithelial cells, which secrete pancreatic juice.(7) The acini cells are connected by intercalated ducts running into a network of intralobular collecting ducts, which in turn drain into the main pancreatic duct. These cells secrete pancreatic juice, composed of enzymes for digestion including pancreatic amylase, pancreatic lipase, various proteases and trypsinogen.(7) The trypsinogen is stored in zymogen granules, also found in the pancreas, and activated to trypsin on meeting enterokinase.(7)

The endocrine portion is made up of islets of Langerhans, forming approximately 2% of the pancreatic parenchyma, which secrete hormones involved in digestion, appetite and metabolism, including mainly insulin, glucagon and somatostatin.(4) Several other hormone-secreting cells also exist.

1.3 Pathology

1.3.1 Gross Features of PDAC

Infiltrating ductal adenocarcinomas form white-yellow fibrotic or sclerotic masses, which obscure the normal lobar structure of the pancreas whereas non-neoplastic lesions tend to form lobular units surrounded by grape-like clusters of acini. Neoplastic glands or ducts also form, ranging from well-formed glands to partially formed glands to focal intracellular mucin production from singly infiltrating poorly orientated cells to solid sheets of neoplastic cells.(8) These glands are often adjacent to the muscular arteries and do not contain pancreatic parenchyma, with 25% of head of pancreas tumours extending to the duodenal wall.(9) 20% of patients have multiple tumours and in advanced tumours it can be difficult to differentiate between the pancreas, ampulla and common bile duct as the origin of the tumour.(9) These factors make diagnosis of pancreatic cancer and determining the origin of the cancer difficult, even with histological examination and staging.

The tumours have the ability to invade perineural and vascular structures, often growing on the intimal surface of vessels. Vascular invasion can mimic pancreatic epithelial neoplasia (PanIN) in almost 70% of cases and is associated with increased tumour size, lymph node metastasis and perineural invasion, all of which confer a poorer prognosis.(10) In a clinical context this is particularly important due to the anatomical proximity of the head of the pancreas to the coeliac and superior mesenteric arteries. As two thirds of PDAC tumours arise in the head of the pancreas, proximity to and invasion of the vascular structures may make many tumours unable to be surgically resected.(11)

1.3.2 Histological Features of PDAC

The nuclei of invasive PDAC cell are pleomorphic, with the area varying by more than 4 to 1 in a single gland (8) and show visible mitotic figures and loss of polarity.(9) The lumen of the gland contains necrotic debris and is usually incompletely lined by epithelial cells; luminal contents appear to be in direct contact with the stroma. Glands can also be in direct contact with adipose tissue with no intervening stroma.

The stroma in PDAC is often abundant and highly desmoplastic. It is composed of mesenchymal cells, cancer associated fibroblasts, endothelial cells, ECM proteins (T1 collagen) nerve cells, pericytes and bone marrow derived cells and immune cells. (12)

In moderate to poorly differentiated tumours abortive tubular structures, abortive mucin production and frequent mitosis can be seen.(9) These tumours often have a deeply infiltrative growth pattern.

Beyond the tumour mass, the background pancreas can also show signs of high grade PanIN, atrophic changes, chronic inflammatory infiltrate, fibrosis and ductal dilation, all of which are also likely signs of a pre-cancerous or stage of early pancreatic cancer.(9)

1.3.3 Histological Grading

PDAC can be histologically graded using a system developed by Kloppel, which incorporates glandular differentiation, mucin production, nuclear atypia and the mitotic count.(8, 13)This grading, however, has minimal prognostic significance.

The TNM histological grading system is more commonly used and recommended by the College of American Pathologists. It is based in the extent of glandular differentiation ranging from G1 (well differentiated >95% tumour composed of glands) to G4 (minimal or no differentiation).(14-16)

1.3.4 Pancreatic Intraepithelial Neoplasms (PanIN)

PanIN is recognised as a microscopic precursor lesion to PDAC.(8) They are defined as neoplastic epithelial proliferation in smaller calibre pancreatic ducts and are divided into 3 grades (Figure 1).

The existence of these precursor lesions suggests that it should be possible to detect and treat these lesions at a non-invasive stage before the development of an invasive carcinoma in an asymptomatic individual. However, as these lesions are sessile, they

are currently undetectable using radiographic imaging and the lack of a specific diagnostic biomarker renders them currently undetectable.

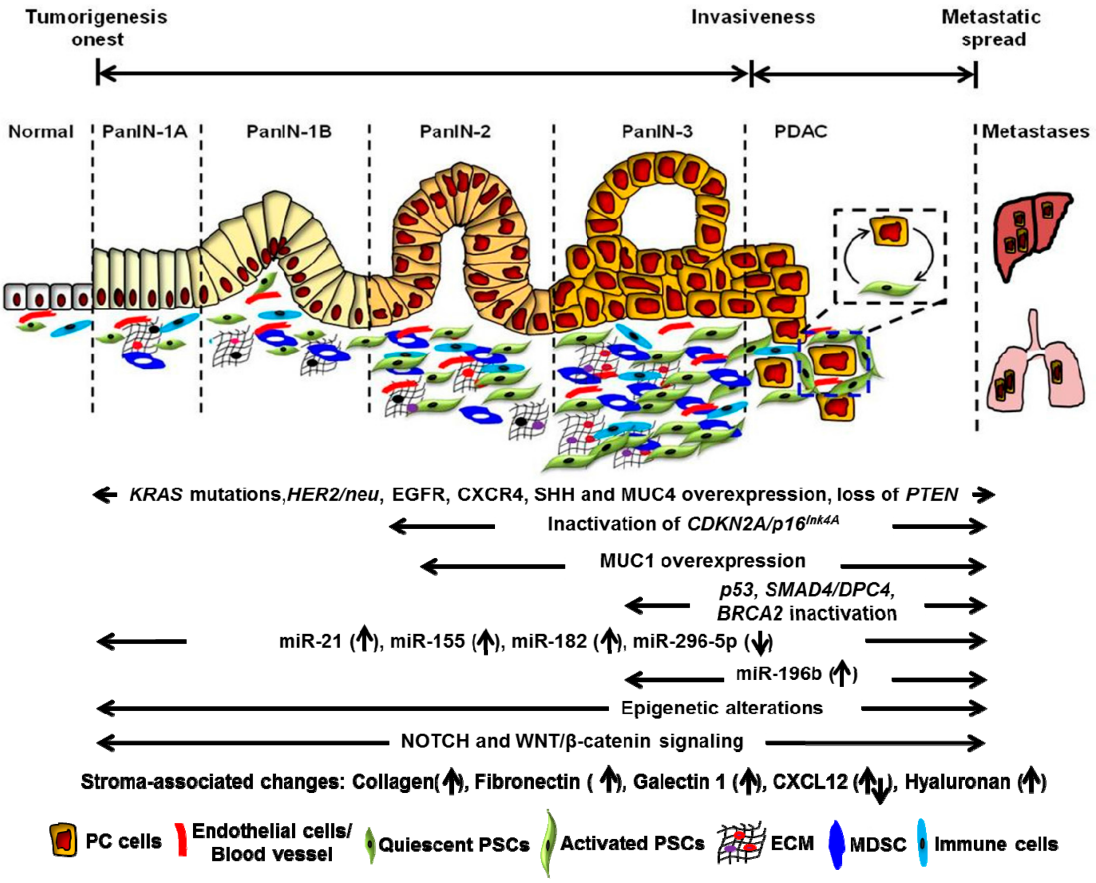

Figure 1: Progression of PanIN to PDAC, image taken from Khan et al 2017(17)

1.4 Pathogenesis

While PDAC tumours are thought to arise from PanIN precursor lesions the exact cell type giving rise to PDAC is currently unknown; murine models suggest both ductal and acinar cells could give rise to PDAC.(18) Recent literature suggests that the cell of origin can affect tumour development and the phenotype of the resultant PDAC. (18)

It is thought that chronic inflammation may play a role in the development of PDAC, with activation of stellate cells and development of pancreatic fibrosis leading to an increase in reactive oxygen species, cytokine release and an increase in the regulation of pro-inflammatory transcription factors.(19) These mediators of inflammation induce genetic damage, cell proliferation and inhibition of apoptosis.

The induction of stroma formation further facilitates growth of transformed cells through the production of pro-invasive factors.(19)

PDAC displays a strong desmoplastic reaction, with invading cancer cells releasing matrix metalloproteinases, which cause the release of growth factors including transforming growth factor B (TGF-B), fibroblast growth factors (FGF), platelet-derived growth factor (PDGF) and insulin-like growth factor-1 (IGF-1).(12) These become included and stored in the stroma and the desmoplastic reaction leads to tumour invasion, metastasis and chemo-resistance.

Following chronic inflammation, there is thought to be metaplasia of normal cuboidal cells lining the duct to mature squamous transitional cells. This leads to PanIN; sessile, non-invasive lesions which progress through a precursor stage to the infiltrating ductal adenocarcinoma. Acinar to duct metaplasia (ADM), also resulting from inflammation, can also be pre-invasive lesions leading to PDAC.(12) The resultant duct cells go on to form PanIN and eventually PDAC.

Epithelial-mesenchymal transition (EMT), where epithelial cells attain mesenchymal phenotype as a result of genetic and epigenetic changes in the tumour microenvironment, occurring in some cancers, appears to be a pivotal event in the cancer progression and metastasis.(12) This mesenchymal phenotype means cells have improved migratory capacity, invasiveness, resistance to apoptosis and production of extracellular matrix (ECM).

Inflammation is thought to play a role in this transition although the exact mechanism has yet to be understood. It is thought that the recruitment of inflammatory cells and formation of a reactive stroma, releases transition inducing signals.(12) A number of cell types within the stroma release growth factors which may release these signals, including cancer associated fibroblasts, of which pancreatic stellate cells (PSC) are the main type. The release of FGF from these fibroblasts is a known inducer of EMT.(12) As it is known that cancer associated fibroblasts and PDAC cancer cells enhance each other’s proliferation, FGF production

leading to EMT appears to be an event in PDAC progression and metastasis.(12) EMT is also thought to play a role in the development of chemo-resistance; cancer cells without the mesenchymal phenotype display increased sensitivity to 5-fluorouracil, gemcitabine and cisplatin.(12)

1.5 Clinical Features

Pancreatic cancer has an insidious onset, presenting initially with non-specific symptoms including weight loss, anorexia and gastrointestinal symptoms, leading to cachexia. Painless jaundice is well known as the most characteristic sign; however, this is often indicative of an advanced tumour blocking the bile duct. NICE guidelines recommend patients are referred for urgent investigation when over the age of 40 and presenting with painless jaundice.(20) A referral should be considered for patients over the age of 60 presenting with weight loss and gastrointestinal symptoms.(20)

Recent research suggests that new onset diabetes, defined as diabetes diagnosed in those over 50 within 2 years of diagnosis of PDAC, is also a symptom of early PDAC.(21, 22) The majority of patients with PDAC were diagnosed with diabetes within 2 years before diagnosis of PDAC and resection of the pancreatic tumours ameliorates the diabetes.(21) In particular rapidly deteriorating diabetes or sudden onset diabetes in patients who have previously shown little sign of diabetes or prediabetes is more likely to be a symptom of PDAC. Although Type 2 diabetes is a very common pathology whereas PDAC is rare, new onset diabetes could be a useful marker of asymptomatic or early stage PDAC and may be an area for further research.

Clinically, tumours are staged according to location and proximity to vessels as well as metastasis, which determines suitability for surgery.(22)

1.6 Clinical Staging

Pancreatic cancer is staged as stages 1 to 4. In stage 1 cancer the cancer is contained within the pancreas; stage 1A suggests the cancer is smaller than 2cm and stage 1B is cancer greater than 2cm.(14) Cancer which has progressed to grow in to the surrounding structures such as the bile duct or duodenum is classed as stage 2. Stage 2A is a cancer which has infiltrated these surrounding structures but not yet spread

to surrounding lymph nodes and stage 2B cancer is found in local lymph nodes.(14) Stage 3 cancer is considered to be either unresectable or borderline resectable as it is locally advanced, having spread to the stomach, spleen, large intestine or larger blood vessels.(14) The resectability status at this stage is often dependent on which of these structures the cancer has advanced to, with particular importance placed on the blood vessels impacted. A stage 4 cancer is one which has metastasised, often to the liver or lungs and treatment for this is usually palliative.(14)

The TNM staging can also be used and offers a similar outline of staging (Table 1).(14, 15)

Tumour

T1	Cancer within pancreas <2cm	
	T1A	Cancer <0.5cm in any direction
	T1B	Cancer >0.5cm but <1cm in any direction
	T1C	Cancer >1cm but <2cm in any direction
T2	Cancer with pancreas >2cm but < 4cm	
T3	Cancer advanced to local tissues but not blood vessels Cancer >4cm	
T4	Cancer has advanced to local blood vessels	

Lymph nodes

N1	No spread to local lymph nodes
N1	Spread to 1-3 local lymph nodes
N2	Spread to >4 lymph nodes

Metastasis

M0	No metastasis
M1	Metastasis to distant organs

Table 1: TNM staging of pancreatic cancer(14, 15)

1.7 Risk Factors

The development of pancreatic cancer, similarly to any cancer, is multifactorial, with risk factors including age and genetics. Smoking, family history, particularly of hereditary pancreatitis, diabetes mellitus and obesity are all well-established risk factors.(1, 8) It is thought that 37% of pancreatic cancer cases each year are linked to major lifestyle factors; smoking is linked to an estimated 29% of cases in the UK and obesity linked to approximately 12%.(1) Age is also a major risk factor with 80% of pancreatic cancers diagnosed in patients between the ages of 60 and 80.(1) Some medical conditions and infections, including chronic pancreatitis and diabetes, appear to be linked to pancreatic cancer risk, however evidence is unclear.(1) An estimated 4% of chronic pancreatitis sufferers will develop pancreatic cancer and 1.34% of pancreatic cancers are thought to be attributed to chronic pancreatitis.(1) However the epidemiology of chronic pancreatitis is unclear, as care is often in the community and the disease is associated with high alcohol intake, creating a stigma which makes identifying and following patients up difficult.(23) (Cancer Research UK)

1.8 Investigations and Diagnosis

1.8.1 NICE Recommendations

The NICE recommendations suggest a referral for a computed tomography scan (CT) with contrast (pancreatic protocol CT) for patients over the age of 40 presenting with painless jaundice.(24) They further recommend considering a referral for patients aged 60 and over, presenting with weight loss and gastrointestinal symptoms.(20) Where the diagnosis remains unclear and for staging, further investigation can include magnetic resonance imaging (MRI), fluorodeoxyglucose-positron emission tomography/CT or endoscopic ultrasound (EUS), where biopsies can be taken through US guided fine needle aspiration or a staging laparoscopy.(24, 25)

1.8.2 Sensitivity and Specificity of Current Diagnostic Methods

A recent meta-analysis has shown CT to have a sensitivity of 90%, specificity of 87% and diagnostic accuracy of 89%.(25) The same meta-analysis reported variation in the results of studies of EUS, but suggested an overall sensitivity, specificity and diagnostic accuracy of 91%, 86% and 89% respectively, independent of fine needle aspiration.(25) While CT and EUS are currently the most sensitive and specific methods, MRI has the greatest potential to give clinically relevant information, such as degree of vascular involvement and detection of metastasis, because of the volume of information collected.(25)

Although these current diagnostic techniques show high sensitivity and specificity, they are dependent on patients presenting with symptoms of pancreatic cancer, by which time the cancer may be at an advanced stage. Further it is estimated that for every 2000 CT scans performed, 1 patient will develop a fatal cancer attributable to the CT procedure.(25) The risks associated with exposure to radiation from CT, and the invasive nature of EUS, which in itself can carry a risk of pancreatitis, also mean that it is inappropriate to subject patients to these tests without significant clinical suspicion of PDAC.

Moreover, the National Comprehensive Cancer Network guidelines state that where there is a high clinical suspicion of PDAC a non-diagnostic biopsy should not delay surgical resection.(22) Although EUS has the potential to be highly specific and sensitive when combined with a biopsy by fine needle aspiration the highly invasive nature of EUS and need for sedation means not all patients are fit for such investigation at the time of diagnosis. Therefore, decisions to proceed to treatment are currently largely based on clinical judgement, which may be subjective, due to the difficulties in diagnosing PDAC.

1.8.3 Current Biomarkers

CA19-9 is currently the most commonly used serum biomarker in monitoring progression of disease and in directing diagnostic decisions. CA19-9 response after induction chemotherapy alongside Response Evaluation Criteria in Solid Tumours (RECIST), a radiologic criteria, seems useful in determining which patients with non-progressive Locally Advanced Pancreatic Cancer should undergo exploratory surgery.(26) It has a sensitivity of 78.2% and 82.8% specificity.(27) However, there are a number of limitations preventing its use as a diagnostic marker. While it is raised in PDAC, there is also significant rise in a number of other benign hepatobiliary conditions making it a poor diagnostic marker due to the lack of specificity.(27) Furthermore, it has been shown to be ineffective in detecting small malignant tumours, meaning in early disease it is not sensitive. As a sialylated Lewis blood group antigen, patients who are Lewis negative, approximately 6% of the Caucasian population, cannot generate the antigen and so in these patients the test could be a false negative.(27) CEA is the second most commonly utilised marker, with a sensitivity of 54% and specificity of 79%.(27)

1.9 Treatment and Management

Patients with a clinical suspicion of PDAC are initially referred for a CT scan. Where a mass is seen on this imaging and there is no metastatic disease, the patient may be considered to be a candidate for surgery.(22, 24) Of these patients those with jaundice and symptoms suggestive of cholangitis or fever are initially given antibiotics and a self-expanding metal stent during ERCP, before a preoperative CA19-9 is taken.(22) Suitability for surgery is considered taking into account the size and location of the tumour, in particular its proximity and any contact to vascular structures. CA 19-9 serum levels can also provide important information with regards to prognosis, overall survival, and response to chemotherapy as well as predicting post-operative recurrence. However, non-specific expression in several benign and malignant diseases, false negative results in Lewis negative genotype and an increased false positive results in the presence of obstructive jaundice severely limit the universal applicability of serum CA 19-9 levels in pancreatic cancer management.

Notably, 6-9% of pancreatic resections are inappropriately carried out on patients with pancreatitis, who have suspected pancreatic cancers, in part due to lack of specificity seen with CA19-9.(28)

Tumours considered to be borderline resectable are first biopsied during an EUS or staging laparoscopy, with or without the use of intraoperative ultrasound. Where biopsy suggests malignancy neoadjuvant therapy, with pre and post-treatment CA19-9 , is recommended.(22) Tumours which respond to treatment are then resected. Postoperatively, patients who have no signs of recurrence or metastatic disease are given either chemoradiation, chemotherapy alone or considered for a clinical trial, taking into account any previous neoadjuvant therapy.(22) Chemotherapy regimens include various combinations of gemcitabine or 5-fluorouracil based chemotherapy.

Patients are then monitored every 3 to 6 months for 2 years and then every 6-12 months based on assessment of symptoms, CA19-9 levels and CT scan. Patients with recurrent disease are considered for chemoradiation or chemotherapy or treated palliatively, regardless of whether the recurrence is local or metastatic.

Patients deemed to have unresectable disease, either because it is locally advanced or metastatic, are treated palliatively. Self-expanding metal stents may be placed if the patient has jaundice and palliative chemotherapy is considered, based on performance status, defined as: ECOG 0-1 with good pain management, a patent biliary stent and adequate nutritional intake and patient preference.(22, 24) Chemotherapy regimens include treatment with gemcitabine and albumin-bound paclitaxel, FOLFIRINOX and other gemcitabine-based combination therapy, as well as treatment with other chemotherapeutic agents including capecitabine, fluoropyrimidine and oxaliplatin.(22)

Guidelines recommend that decisions and treatment, especially of surgical patients are carried out under a multidisciplinary team, at institutions performing a large number of pancreatic resections (approximately 15-20 resections per year) due to the rarity of the disease.(24)

1.10 Factors Influencing Survival After Resection

A number of factors have been associated with improved survival after resection of pancreatic cancer. Pre-operatively a lower level of tumour marker and absence of a biliary stent are associated with improved long term survival after resection.(29) Intraoperatively lack of bleeding and a reduced need for blood transfusion are also positively associated with survival.(29) In relation to the tumour and resection itself a smaller, well differentiated tumour with lower positive to negative lymph node ratio also improves long term survival.(29, 30)

Resection status, classified by margin involvement (defined as R0, R1 and R2 by the Royal College of Pathologists) is also thought to have an impact on survival, although there is some debate in the literature about this. This may be of particular importance as 76% of resections have an R1 (margin involvement within 1mm) margin status.(31)

A number of studies have found that no margin involvement (R0 resection status) improves overall survival after resection and is independently associated with improved survival.(29, 30, 32, 33) However, some more recent research has also suggested that microscopically positive R1 resections, do not affect survival.(31, 34, 35) It has been suggested that the margin may influence local recurrence but has no impact on overall survival.(36) Survival is thought to be more likely to be associated with a more aggressive tumour biology and factors associated with an increased likelihood of metastasis.(31, 34, 36) Therefore, it is thought that an R1 resection status is more likely to be a marker of more aggressive tumour biology therefore creating an association with poorer survival, but as the cause of this is related to the tumour biology achieving R0 resection status through revision of a surgical margin may not improve survival.(34) However, all of the studies agree that R0 resection status should be the surgical intention.

Chapter 2 - SPARC- Role and potential for use as a Biomarker for Pancreatic Cancer

Manuscript submitted for publication

Author Contributions:

Hawwa A. Bham: Substantial contributions to the conception of the work; **wrote first draft and** revised it critically for important intellectual content

George Sgourakis and Jemma G Kerns: Substantial contributions to the conception of the work; revised it critically for important intellectual content

SPARC – Role and potential for use as a biomarker for pancreatic cancer.

Hawwa A. Bham[1] George Sgourakis[2], Jemma G. Kerns[1]

1. Lancaster Medical School, Faculty of Health and Medicine, Lancaster University, LA1 4YG

2. University Hospitals of Morecambe Bay NHS Trust

HA Bham: MSc Student

G Sgourakis: Consultant General Surgeon

JG Kerns: Lecturer

Word count: 5875

Corresponding author:

Dr Jemma G Kerns

Lancaster Medical School

Furness College

Faculty of Health and Medicine

Lancaster University, LA1 4YG

Abstract

Pancreatic ductal adenocarcinoma (PDAC) presents an increasing mortality burden, with few of the recent developments in treatment having a significant impact on the poor survival rates. This is largely due to the insidious onset of the disease and difficulties in detection meaning most cancers are at an inoperable and so incurable stage at the time of diagnosis. Hence there is significant need for improvements in the diagnosis and screening of PDAC. Secreted protein acidic and rich in cysteine (SPARC) is a potential biomarker which appears to plays a role in the development of PDAC and has increased expression during the inflammatory stages preceding PDAC development and in the juxtatumoural fibroblasts and stellate cells in PDAC itself. There are a number of mechanisms identified by which SPARC appears to play both an anti-tumorigenic role but also influence the invasive and metastatic capacity of cells; features which extend to its role in PDAC. The controversial role played by SPARC has led to research into its role and potential as a prognostic marker and therapeutic target.

This review outlines the role and expression SPARC in the development of PDAC and its potential as a prognostic marker. It uses the current knowledge around this alongside more recent research into the detection of SPARC as a serum marker to understand the potential for SPARC to be used as a measurable biomarker and its clinical application in earlier diagnosis or screening for PDAC.

Introduction

Pancreatic cancer is the fourth most common cause of cancer related death in the developed world. With few specific symptoms and a lack of screening markers, diagnosis is often late making prognosis poor; it has an overall 5-year survival of only 3% in the advanced stages.(1, 2) Tumours with potential for resection are found in only 10-15% of patients meaning that for the majority of patients the diagnosis is terminal and treatment is palliative.(1) Amongst patients who do have resectable tumours, recurrence is a significant problem, with one study suggesting disease free survival at 8 months was only 50% (37) and 95% of recurrences occur within 2 years of resection.(38)

Symptoms for pancreatic cancer include loss of appetite, change in bowel habit and nausea, with jaundice being a later sign. The insidious onset of these relatively non-specific symptoms combined with the fact that pancreatic cancer is quite rare, means patients often present late. As well as this, investigations for pancreatic cancer include computer tomography (CT) imaging and endoscopy which are invasive and carry risks of high exposure to radiation. Hence, in accordance with NICE guidelines, doctors rarely refer patients for CT investigation until they present with painless jaundice, which is often indicative of an advanced tumour with little possibility of resection. Therefore, diagnosis of pancreatic cancer is often in the very late stages of the disease.

Risk factors for pancreatic cancer are also somewhat non-specific, with increasing age, obesity and high alcohol intake being the most common. Diabetes mellitus is also a major risk factor, associated with a 1.8-fold increased risk of pancreatic cancer.(1) Chronic pancreatitis is thought to be a potential precursor, however, even this condition is extremely rare and not present in a significant number of those diagnosed with pancreatic cancer. An estimated 4% of chronic pancreatitis sufferers will develop pancreatic cancer and 1.34% of pancreatic cancers are thought to be attributable to chronic pancreatitis.(1) The epidemiology of chronic pancreatitis is however unknown, as care is often in the community and the disease is associated

with high alcohol intake, creating a stigma which makes identifying and following patients up difficult.(23)

There has been some research on potential biomarkers for pancreatic cancer, with a number of recent reviews on the role and potential for various biomarkers to be used to predict prognosis.(39-42) Many of these reviews focus on the potential for these biomarkers to be used as a therapeutic target.

However, the delay in presentation, investigation and diagnosis of pancreatic cancer has led to a lack of knowledge about the pre-cancerous or early stages of the disease. There is therefore a need to consider how the current knowledge base could be used to consider avenues for research into the earlier detection of pancreatic cancer. This increased knowledge base, would be imperative in improving prognosis as resection is currently the only truly curative treatment.

Osteonectin or secreted protein acidic and rich in cysteine (SPARC) is a potential biomarker with extensive research into its role, ability to predict prognosis and potential as a therapeutic target.(39, 43) However, more recently there has been some work to suggest it may be present in early disease and its expression in various stages of pancreatic cancer and chronic pancreatitis has been investigated as well as its presence in bodily fluids. This newer area of research suggests potential avenues for SPARC to become a measurable biomarker with the possibility to lead to a role in earlier diagnosis.

Aim

This review outlines the role and expression of SPARC in the development of pancreatic ductal adenocarcinoma. It then considers its potential role in predicting prognosis of PDAC both in patients who have and have not received chemotherapy. It also examines the potential for SPARC to be measured as a serum marker, looking at potential clinical applications and limitations in detection methods, with a view to understanding the potential for SPARC to be used as a measurable biomarker in diagnosing or screening for PDAC.

Secreted Protein Acidic and Rich in Cysteine

SPARC is a calcium-binding, matricellular protein, which interacts with the extracellular matrix.(44) It is described as a non-structural or matricellular protein; a protein transiently secreted to control cell function and interactions between cells and the extracellular matrix. (45) In healthy tissue it is expressed in embryogenesis, bone and platelets, appearing to be a marker for activated fibroblasts (44) and has a role in cell migration, proliferation and invasion.(44, 46, 47) It is ordinarily rapidly degraded by various proteases, preventing its accumulation in the extracellular environment.(45) While its proteolysis can be initiated by matrix metalloproteinases (MMP), SPARC is also able to regulate MMP activity during inflammation and tissue remodelling.(45)

The SPARC gene is located on human chromosome 5q.(45) The protein structure is divided into 3 domains; the calcium binding N-terminus acidic domain and C-terminus extracellular domain which bind calcium with low and high affinity respectively and the follistatin-like domain, which is rigidly stabilized by five disulphide bonds and contains a β-hairpin subdomain.(45) Of these, the C-terminus domain is particularly important in SPARC's function in modulating angiogenesis, inhibiting vascular endothelial growth factor (VEGF), β-fibroblast growth factor (βFGF) and platelet derived growth factor (PDGF), in turn inhibiting endothelial cell stimulation and so angiogenesis. (45, 48)

Expression of SPARC in PDAC

Where it has been identified in PDAC, it is primarily expressed in the juxtatumoural fibroblasts(49) and pancreatic stellate cells and its presence here has been shown to suggest a poorer prognosis for these patients.(44, 50) There may also be some expression in the pancreatic cancer cells and surrounding endothelial cells although there remains some debate as to the expression of SPARC in the cancer cells lines in the primary tumour.(47, 49) However, in metastatic PDAC there is greater agreement that the expression is predominantly in the surrounding stroma.(47)

In a comparison of the roles of osteopontin and SPARC, osteopontin expression was increased in tumour cells and was also increased in tumour cells which had metastasised to the liver, suggesting it has a clear role in the promoting the growth of cancer cells in PDAC.(51) SPARC expression, however was more limited to the adjacent extracellular matrix as well as in the fibroblasts and endothelial cells and was thought to have an anti-tumorigenic effect on cancer cells expressing SPARC mRNA.(51)

The expression of SPARC in chronic pancreatitis, thought to be a precursor to PDAC, has also been investigated. This may give some insight into the early activity of SPARC and early changes which occur, including some of the precancerous changes. Interestingly, SPARC expression was found in 62% of chronic pancreatitis samples, but with little expression in malignant cells.(50) It was found that SPARC is transiently upregulated, with increased expression exhibited in the basal membrane of acinar cells, in acinar destruction and is only activated or synthesized during inflammation, in a rat model.(52) It is subsequently lost in the final stages of acinar destruction and during acinar to duct metaplasia, also an event known to preceed PanIN and PDAC, suggesting the SPARC expression is lost with the loss of acinar characteristics in a cell.(52) In the late stages of chronic pancreatitis, potentially immediately before or concurrent with the very early development of PDAC, there is some SPARC expression in stellate cells. (52) This corresponds with the observation that in PDAC, SPARC expression is primarily in the stellate cells of the stroma, with a lack of expression in the cancer cells.(50, 53) Hence, there may be potential for SPARC expression in these stellate cells to be used as a screening or diagnostic marker for early PDAC, especially in those with chronic pancreatitis.

In one study showing a lack of expression in pancreatic cancer cell lines, the aberrant methylation status of SPARC correlated with lack of expression, suggesting that DNA methylation is a mechanism for silencing of SPARC.(49) A further study showed this aberrant methylation to also interfere with tumour stromal interactions.(54) It was found to be a common feature of intraductal papillary mucinous neoplasms, thought

to be a non-invasive neoplastic precursor to PDAC, and to increase with histological grade.(54)

Methylation and Cell Cycle Mechanisms

More specifically hypermethylation peaks were found in the CpG sites 1 to 7 and CpG sites 8-12.(55) These appear to gradually increase from normal to chronic pancreatitis to the adjacent normal to pancreatic cancer tissues.(55) Of these, aberrant methylation of sites 8-12 in pancreatic cancer patients was significantly increased compared to the normal and an event thought to occur early in the development of pancreatic cancer tumours.(55) Furthermore, a larger tumour size was associated with, and shown to be a contributor to, an increase in methylation of sites 8-12.(55) Hence, hypermethylation of this region may be a potentially sensitive marker in high risk patients prior to the development of symptoms. While this supports the premise of SPARC as a tumour suppressor gene and adds to our knowledge of the role of SPARC in pancreatic cancer, a gap remains for there to be a more clinically applicable understanding. Much of the current research is conducted on pancreatic tissue and tumours themselves, while there is a need to detect a biomarker in a form that could be accessed and measured in a less invasive manner. To confirm hypermethylation as a change specific to pancreatic cancer, methylation in white blood cells in healthy volunteers was compared to that in pancreatic tissue.(55) However, it may be interesting to extend this to detecting hypermethylation of these CpG sites in the blood of patients with pancreatic cancer, as it would give further insight into its potential as a more clinically measurable marker of early PDAC.

While SPARC has previously been suggested to be a target for aberrant methylation and shown to have growth-suppressive activity, further work has been done on the mechanism of SPARC inhibiting the growth of human pancreatic cells. SPARC was shown to be highly expressed in the extra-cellular matrix components but rarely expressed in the cancer cells themselves.(56) Forced expression of SPARC was shown to inhibit cell proliferation in vitro whereas knockdown promoted growth and colony

formation, suggesting SPARC may be a tumour suppressor in pancreatic cancer.(56) Furthermore, this appeared to be associated with G0/G1 arrest, by inhibiting G1/S transition in the cell cycle but without inducing apoptosis,(56) as a result of the upregulation of both p53 and p27kip1, which are related to G1/S cell cycle arrest.(56) SPARC-mediated apoptosis has, however, been reported, by activating the extrinsic pathway via caspase 8.(48) Specifically, the N-terminus engages in this mechanism leading to apoptosis while inhibiting angiogenesis, whereas the other domains appear to have little activity. More importantly it was shown that the N-terminus increased chemosensitivity of the cells by augmenting apoptosis, through interfering with an interaction between caspase 8 and Bcl2, even in refractory cells.

Role of SPARC in Cancer

SPARC has been shown to play a controversial role in the context of cancer. Much of the literature suggests it has an anti-tumorigenic action on the cancer cells themselves. In a cell panel it was shown that cells expressing SPARC mRNA were unable to grow in vivo, possibly due to the increased expression of p21 in response to SPARC, leading to growth arrest.(51) This supports the premise of SPARC having anti-tumorigenic properties in the context of PDAC,(51) and corroborates an in vitro study showing exogenous SPARC supresses the growth of pancreatic cancer cells.(49) However, its expression and role in the extracellular matrix is one influencing invasion and metastasis of the cancer cells. In a number of cancers, SPARC has been shown to influence the invasive and metastatic capacity of cells in both human and mouse models, and this appears to extend to PDAC.(47) Tumours expressing SPARC have been suggested to be more advanced and likely to metastasise.(50)
Tumour protein 53 induced nuclear protein 1 (TP53INP1), a pro-apoptotic stress-induced p53 target gene has also been shown to modulate cell migration by regulating SPARC expression.(57) TP53INP1 is able to reduce SPARC expression in vitro.(57) A loss of TP53INP1 expression early in the formation of pancreatic tumours is thought to be in part responsible for the strong metastatic phenotype of pancreatic cancer.(57) Hence, a loss of TP53INP1, inducing expression of SPARC,

could lead to the increase in migration and metastatic capacity of pancreatic cancer cells.(57)

It has been suggested that SPARC and tumour growth factor-β participate in a feedback loop, where SPARC induces the expression of TGF-β and TGF-β reduces the expression of SPARC, with the two influencing each other's production.(47) However, the mechanism for this induction is currently unknown.

Furthermore, exogenous SPARC treatment has been shown to increase the invasive capacity of cells, in vitro, potentially due to the induction of expression of MMP-2 in PDAC.(47) It has been hypothesized that SPARC and MMP-2 may participate in a positive feedback loop, where SPARC stimulates MMP-2 and this then cleaves SPARC, increasing its affinity for collagen and localising it to the basement membrane.(47) This appears to be directly linked to the development of the desmoplastic reaction in PDAC,(47) which encourages tumour invasion, metastasis and chemoresistance.(58) As PDAC displays one of the most prominent desmoplastic stromal reactions of all carcinomas, (58, 59) and SPARC has been shown to play a significant role in the development of this reaction and is found highly expressed in the tumour stroma, further work looking at its expression in pancreatic juice or other bodily fluids may give some basis to consider it a measurable biomarker, bridging the link to clinical practice.

SPARC expression as PDAC progresses has also only recently been investigated. The normal pancreas has little normal stroma, however this forms as neoplastic lesions develop and extensive stroma formation is associated with invasive carcinoma.(53, 60, 61) It was observed that there is no SPARC expression in the normal pancreas but this expression arises in invasive PDAC and remains throughout metastasis, although in concordance with other studies it is restricted to the stroma of the tumour.(50, 53) It was further shown to be an independent prognostic factor in resectable pancreatic cancer.(53)

Prognostic Role of SPARC

The significance of the pancreatic tumour microenvironment; the role of the stroma as well as SPARC are considered to play an important role in tumour progression. The limited effectiveness of chemotherapeutic agents targeting cancer cells in PDAC has increased interest in the stroma as a potential therapeutic target.(59) The stroma is further thought of as a mechanical barrier, preventing drug penetration which may contribute to the often poor response to chemotherapy.(62) SPARC expression in the stroma of pancreatic tumours has been shown as a predictor of poor overall survival (50, 51) as well as being a potentially prognostic marker for the effectiveness of chemotherapy.(63)

The stroma itself was also initially associated with a poor prognosis,(60) although some more recent studies suggest the stroma may also have a protective role.(45, 59, 64) Hence, stroma depletion could be problematic where it occurs as a result of drug delivery, particularly where SPARC is the therapeutic target. As SPARC is antitumorigenic, depleting stroma, and so SPARC may cause an increase in proliferation of cancer cells. More so, where SPARC plays a role in delivering the drug to the cancer cells, depleting the stroma also depletes the carrier and so reduces drug delivery.

Tumour stromal interactions have been shown to promote invasion and metastasis.(60, 65) This occurs due to cancer cell derived MMPs releasing growth factors, which become isolated in the stroma. Further interaction of these growth factors with insulin and their correspondent receptors promotes cancer cell proliferation. Production of Cox-2 and VEGF-1 then encourages epithelial-mesenchymal interactions, making surrounding tissue more susceptible to invasion.(60)

However, recent experimental models have demonstrated that the tumour stroma may restrain tumour growth.(59) In the normal pancreas, stellate cells play a role in the repair of pancreatic injury, producing the extracellular matrix proteins. Whereas,

in chronic pancreatitis and pancreatic cancer prolonged activation of the stellate cells is a key player in pancreatic fibrosis and tumour desmoplasia.(65) Some reports have suggested that this fibrosis could play a role in restricting tumour growth. (59, 64) It could therefore be hypothesised that stroma production may be defensive mechanism in response to the proliferation of cancer cells, in order to reduce their rate of growth. While it may be somewhat successful in doing this, it also appears to have an impact on the surrounding healthy tissue, making it more susceptible to invasion. Therefore, although there may be some inhibitory effect on the rate of growth of the tumour, this is counteracted by a simultaneous increase in susceptibility to invasion. Hence, the stroma may have a protective role, but still be associated with a poor prognosis. Where there is greater proliferation of cancer cells, there is a dependent increase in stroma production, and so a greater resultant impact on the surrounding tissue.

Moffitt et al classified stroma as 'normal' and 'activated', with the activated type expressing a more diverse set of genes associated with macrophages and proteins including SPARC, suggesting a more complex model of stroma in PDAC.(66) It was hypothesized that only activated stroma may be responsible for disease progression.(66) Furthermore, two-tumour specific subtypes of PDAC were classified, with basal like subtypes conferring a poorer prognosis than the classical subtype.(66) It was further shown that while SPARC expression is higher in the intratumoural stroma of PDAC, and this expression has been associated with reduced overall survival, the presence of cancer associated fibroblasts themselves was not associated with a poor prognosis.(59) It was shown that cancer associated fibroblasts are a heterogeneous population, with distinct functions, although the variety in this population and these functions are not yet clearly understood. (59) It is therefore possible that an increase in certain fibroblasts with the population, expressing certain proteins, for example SPARC, may show different survival patterns and this may warrant further investigation. Another recent study found there was no significant negative association between increased stromal SPARC expression and overall survival.(67) The exact function and interaction of each of the stromal components is not yet completely understood and clinical trials for stromal depletion

in PDAC have failed, making it difficult to draw clear conclusions on the role of the stroma.(67)

SPARC expression in the stroma has previously been shown to be a predictor of poor prognosis,(44, 50, 53, 61, 65, 68), independent of any adjuvant treatment.(53) In particular, greater expression of SPARC in the more distal stromal cells correlates with poorer overall survival and more nodal metastases.(65) One very recent study, using 73 patients suggested this expression may also have a potential role as a marker in predicting lymph node metastasis and has been suggested to be more sensitive and specific for this than CA19-9.(61) However, further work is needed to determine the validity of the results, both due to the retrospective nature of the study and use of immunohistochemical staining which the authors believe is insensitive for protein detection.

SPARC expression has further been investigated to understand its value in predicting the efficacy of chemotherapy. Its impact on overall survival and prognosis with different regimens of chemotherapy is conflicted in the literature. Combination treatment of gemcitabine with nab-paclitaxel has recently been approved for the treatment of metastatic pancreatic cancer. Nab-paclitaxel is a nanoparticle sized albumin-bound taxane.(62) It is thought that through an albumin-SPARC interaction, stromal SPARC facilitates the accumulation of albumin in the tumour.(62, 69) Hence, SPARC is thought to have a potential role as a predictive marker for the combination treatment, partly as it increases the delivery of the chemotherapeutic agents to the tumour cells as well as having its own anti-tumorigenic mechanisms.(70)

However, a phase III metastatic pancreatic adenocarcinoma clinical trial (MPACT) comparing nab-paclitaxel plus gemcitabine vs gemcitabine alone suggested that SPARC is not an independent predictor of overall survival or of nab-paclitaxel efficacy.(71) The MPACT trial used tissue samples from metastatic lesions or samples of unidentified origin, with only 11% of samples as confirmed pancreatic lesions, (71) whereas previous trials were conducted on resected primary PDAC tumours. A further study, observed that the kind of tissue origin (primary vs metastatic) may

have a significant impact on the value of the biomarker and this may be an important consideration in the design of future trials.(67)

For treatment with adjuvant gemcitabine alone after resection it has been shown to be a negative predictive marker for response to chemotherapy with gemcitabine.(67, 70) This is despite the fact that in vitro studies have shown that overexpression of SPARC enhances the inhibition of cancer cell proliferation, by enhancing the impact of gemcitabine though an increase of apoptotic signals and the induction of G0/G1 arrest causing apoptosis.(72) It is hypothesized that this may be because an increased stromal SPARC expression may be due to a more dense stroma and this denser stroma could present a more significant treatment barrier.(67) Therefore, although SPARC may enhance gemcitabine induced apoptosis, the stromal components producing SPARC may prevent the drug from effectively penetrating the tumour to exert these effects.

While SPARC expression as a predictive marker for chemotherapy as well as its potential as a therapeutic target is well described in the literature, at present the impact of chemotherapy in PDAC is limited largely by the fact that most patients present with very advanced disease. Chemotherapy with gemcitabine alone increases median overall survival to 6.6 months and the addition of nab-paclitaxel in metastatic disease further increases this to 8.7 months.(62) Although this is a great improvement in comparison to no treatment, the prognosis for most patients is still poor and chemotherapy is largely considered to be palliative. In addition, the majority of patients present with advanced tumours which are non-resectable, which further limits the efficacy of chemotherapy and prevents any treatment from being curative. Hence, the need for a method of early detection, or a screening marker, of pancreatic cancer is paramount, to allow the cancer to be detected at a stage where there may be potential for a cure and so significantly improving prognosis.

Early detection

There is limited literature on a potential marker that could be used for screening for PDAC. There are however, some small studies on the detection of SPARC in the serum of patients with PDAC, although there is little concordance in their findings.(47, 49, 73, 74)

Of the four studies that have attempted to measure SPARC as a serum marker, Sato et al found no significant difference in the mean SPARC level in the serum of patients with PDAC against controls.(49) Guweidhi et al, on the other hand found lower serum SPARC in patients with PDAC against controls,(47) whereas most recently Papapanagiotou et al found higher serum SPARC in patients with PDAC. Furthermore, the latter found an association between tumour size and the serum SPARC level, within PDAC patients, although there was no comparison between the amount of SPARC measured in the tumour and serum.(74)

There were some differences in the methodology of the studies, which may account for some of the differences in results. Whereas Guweidhi et al looked for a correlation between SPARC mRNA levels in tissue and serum SPARC levels, and found no correlation, the correlation in Papapanagiotou et al's study was found between tumour size and serum SPARC levels. Differences in matching patients and comparison groups, with only Papapanagiotou at el's study matching according to confounding variables, may also account for some of the differences in the results of the 3 studies.(74)

Sato et al's study showed no differences in serum SPARC levels between patients with and without PDAC, although this may be because samples of tissue and serum samples were not taken from the same patient.(49) Therefore, although there is a comparison made between disease types, any correlation between tissue and serum SPARC levels can't be measured. Furthermore, neither intrapatient nor interpatient variability have been accounted for.

However, the results of Papapanagiotou et al's study may also need to be interpreted cautiously due to the small sample size, especially when considering the correlation between tumour size and SPARC levels; 15 patients had a diagnosis of PDAC and these patients were categorised according to tumour size, meaning there were very few patients in each of the tumour stage classes, although the results were statistically significant.(74)

Another recent study showed that, in the healthy individuals, BMI correlated with systemic levels of SPARC, associated with higher number of bone marrow-derived stem cells in peripheral blood, which are known to be involved in the pathogenesis of obesity-associated cancers, of which PDAC is one.(73) However, it was found that mean plasma levels of SPARC were significantly lower in patients with PDAC compared with healthy controls, in line with Guweidhi et al's findings, as was the SPARC/osteopontin ratio, (73) although only SPARC/osteopontin ratio correlated with BMI and this is thought to contribute to the systemic spread of the tumour. It is hypothesized that the lack of association between levels of SPARC and BMI may be due to the increased production of SPARC by fibroblasts in the extracellular matrix. (73) Overall this provides a basis for further clinical studies looking at plasma levels of SPARC in patients with PDAC as well as further work looking at the influence of the desmoplastic fibrotic environment and metabolic activity of stromal cells on SPARC levels in patients with PDAC.

In line with these studies, it could be hypothesized that as SPARC expression appears to be closely linked with prognosis and expression appears to arise with the development of PDAC, there is potential for SPARC to be used as a screening marker, although the serum levels of SPARC that may be significant and any correlation with tumour grading has yet to be determined. Furthermore, SPARC is expressed in 62% of chronic pancreatitis samples,(50) thought to be greatest risk factor and a potential precursor for the development of PDAC.(75) Therefore, if there is a continuum from chronic pancreatitis to the development of PDAC, the expression of SPARC may correlate and this could be used to identify a clinically significant value as a potential marker. However, difficulties in detecting SPARC at low quantities remains an

obstacle and improving methods of detection may go some way to developing a screening method.

Papapanagiotou et al's study suggested enzyme linked immunosorbent assay (ELISA) could be used as a method of detecting SPARC, with a detection range of 0.78ng/ml to 50ng/ml with a minimum detection concentration of 0.195ng/ml.(74) It is the first paper to propose a potentially clinically relevant cut-off point, suggesting serum values higher than 100.18ng could be used to predict pancreatic cancer. However, the difference between T1/T2 tumour groups and the control group was only marginally significant, which might suggest using this cut-off value might not be sufficiently sensitive in detecting early stage cancer.(74) On the other hand the authors suggest that a larger study, with more participants may be helpful in establishing this difference.(74)

Some studies have also shown potential for urine to be a source of possible biomarkers for pancreatic cancer, although the studies are very small and the literature is limited.(76-78) Urine biomarkers have shown potential in being able to differentiate chronic pancreatitis from pancreatic cancer,(76-78) which could be clinically useful in diagnosis and screening. This suggests urine could be a potential source of a biomarker for diagnosis or screening in pancreatic cancer, and further work to detect expression of SPARC in the urine may be of value. Although high SPARC expression has been detected in PDAC there is currently no literature about how it may be excreted.

A key difficulty in early detection however, may be that the exact cell type that gives rise to PDAC is unknown.(60) There is some evidence to suggest that intraepithelial neoplasms(60) and intraductal papillary mucinous neoplasms(54) may be non-invasive precursor lesions but identifying the initial cell type undergoing metaplasia would be imperative in allowing for further work in identifying a screening or diagnostic marker. The lack of information about SPARC expression in these precursor lesions, especially in those studies attempting to measure SPARC as a serum marker, where no patients with such precursor lesions were used is a further

limitation to all of these studies. The lack of knowledge regarding initial cell type creates a difficulty in research in looking for an early biomarker and further knowledge in this area may be a basis to investigate SPARC expression in pre-invasive neoplastic lesions.

The value of early screening may also be questionable due to the high rate of recurrence even amongst patients who have resection. However, at present resection, where possible, offers the best prognosis; where the overall 5-year survival is less than 5%, this can be up to 30% in those who have surgical resection with adjuvant chemotherapy.(76) As recurrence is a significant problem in long term prognosis,(37, 79) identifying any association between SPARC expression and the likelihood of recurrence after resection would also be of value, alongside further work into the potential for SPARC to be used in early detection, possibly as a serum marker.

Risk factors and links to SPARC

A further difficulty in screening may be that PDAC is so rare with an estimated lifetime risk of 1 in 70. (2) (Cancer Research UK). While there has been an increase in incidence of 15% since 1990, potentially due to the increase in the ageing population, it accounts for 3% of the all cancer diagnoses in the UK.(1, 2) Therefore, even where a highly specific and sensitive biomarker for pancreatic cancer could be found, screening the general population may not be practical or cost effective. Risk factors for pancreatic cancer are also broad, with age being the greatest risk factor, making it difficult to determine who a screening marker should be aimed at. Hence, where a potential screening marker or test could be found, further determining who to screen for the disease would be a clinically important consideration and potential avenue for research.

Having a sensitive and specific biomarker could, however, be useful in aiding diagnosis as even the gold standard CT imaging at present can misdiagnose benign lesions as malignant ones leading to some patients undergoing unnecessary surgery.

Moreover, the current guidelines suggest that a negative biopsy is not necessarily a reason to delay resection, where clinical suspicion of PDAC is high. Therefore, a marker for pancreatic cancer, would be valuable in both identifying the disease earlier and reducing misdiagnosis.

Research suggests there may be some links between levels of SPARC and risk factors for PDAC, including obesity and diabetes. As the knowledge base around these links increases, subgroups within these risk factors may form potential screening criteria, especially when using SPARC as a biomarker. As well as this the link between these risk factors, SPARC expression and PDAC may give new insight into the role of SPARC and these risk factors in the pathogenesis of PDAC.

Obesity is also considered to be a significant risk factor for PDAC and there is some literature to suggest a link between SPARC expression and obesity. SPARC expression in adipose tissue is increased by high levels of insulin and leptin, and weight loss was shown to reduce SPARC levels.(80, 81) It seems likely that SPARC has a role in the development of obesity related complications although its contribution to the association between obesity and cancer has yet to be understood.(81)

In diabetes, it is proposed that SPARC is secreted by stromal cells and regulates B cell response to growth factors.(80) Stromal SPARC expression in the pancreas could be regulated by the metabolic parameters and so be induced in type 2 diabetes, potentially contributing to the risk of pancreatic cancer.(80)

Conclusion

SPARC is a matricellular protein involved in cell migration, proliferation and invasion. As such it plays a role in the development of a number of cancers. In PDAC its expression has been described primarily in the tumour stroma, where it is thought to have an anti-tumorigenic impact on cancer cells. Expression is upregulated during inflammation, which is thought to be part of the aetiology of PDAC. It is then downregulated during metaplasia of cells. Hence, SPARC is expressed in and plays some role in the development of PDAC.

Aberrant DNA methylation appears to be a mechanism for this downregulation and interference in tumour stromal interaction. A number of cell cycle mechanisms have been suggested as methods by which SPARC inhibits cell proliferation including by inducing G1/S transition and induction of apoptosis.

Despite having an antitumorigenic role, SPARC has also been shown to be linked to the desmoplastic reaction in PDAC, due to interactions with TGF-β and MMP2. It is possible that stroma and SPARC production is a defence mechanism to cancer cell proliferation, but counter-productive as it simultaneously increases tumour invasion as a result of its impact on surrounding tissue. The relationship between SPARC and PDAC is clearly complex and further work may be needed to understand interactions between components of the stroma, SPARC and the surrounding tissue, to determine the extent to which these make healthy tissue vulnerable to invasion compared to their potential ability to reduce the rate of tumour growth.

While SPARC has been widely researched as a therapeutic target, literature is still undecided on how useful a predictive marker it is for the efficacy of chemotherapy. However, given so many patients only receive chemotherapy as palliation, understanding SPARC's role and expression with a view to determining its potential as a detectable diagnostic or screening marker, may be more clinically beneficial. The literature on this is however much more limited and conflicted.

The recent work around detecting SPARC as a serum marker and its associations with risk factors for PDAC suggest that it may have the potential to be used as a biomarker. Further work understanding these associations may also be helpful in developing a clinical aid for deciding in which patients SPARC would have greatest utility as a screening marker and how results could be interpreted in the context of other clinical factors. This further and more clinically applicable work will give potential to find a biomarker for PDAC, which will play a significant role in improving diagnosis, screening and ultimately improving the survival rate of PDAC.

Chapter 3 - Emerging Methods in Detection and Diagnosis

3.1 Raman Spectroscopy

Raman spectroscopy is a technique used to understand the chemical fingerprint of a substance by analysing the scattered light emitted due to molecular vibrations. This is similar to infrared spectroscopy, however a change in molecular polarisability is required for the Raman effect. Hence, some vibrations can be measured using Raman spectroscopy, which are undetectable in the infrared spectrum and vice versa.

When light, usually from a monochromatic laser, is directed at a substance the majority is either absorbed, reflected or unchanged in energy, known as Rayleigh scattering. However, a small amount of light changes in frequency when absorbed then emitted, as it interacts with molecular bonds, which vibrate due to the energy given to the sample, as photons exchange part of their energy with the molecular bonds in the substance.(82, 83) This is known as Raman scattering, which occurs in less than 1% of photons that interact with the molecules.(83)

As each molecular bond has a unique vibration the resultant scattering process is unique to the bond.(82) Thus, by understanding the vibration of each bond and measuring the energy change in the Raman scattered light it is possible to understand the chemical composition of a substance. The wavelength at which the Raman scattering occurs can be affected by the strength and configuration of the bond, giving information about the overall compound. The measurements are depicted on a graph as Raman spectra, with the intensity of the scattered light on the y-axis and each wavenumber on the x-axis.

The spectrum gives information about the chemical composition of the material through the location of the Raman bands. Stresses in the sample, variation in crystallinity or the amount of the material, relative to a band shifting, narrowing or broadening or variation in intensity respectively, can be detected.

3.2 Surface Enhanced Raman Spectroscopy

As Raman scattering is an inefficient process, mostly because the Raman signal is significantly less powerful than the fluorescence signal, it can be useful to enhance the scattering intensity to provide greater sensitivity. The surface enhanced Raman spectroscopy (SERS) technique can be applied for this purpose. SERS uses nanoparticles of noble metals, silver, gold or copper, to enhance the signal at the surface, giving a sensitivity 6-10 orders in magnitude greater than conventional Raman spectroscopy.(82, 83) Nanoparticles of noble metals are most suited for use in biological samples due to their chemical inactivity and optical properties, allowing amplification of the Raman signal when introduced into cells, without changing their chemical composition.(82, 84)

The amplification of the Raman signal is achieved by two mechanisms; the interaction of electromagnetic waves with nanoparticles with dimensions smaller than the wavelength and the chemical interaction between the molecule and nanostructures surface. The electromagnetic mechanism is the excitation of a propagating surface plasmon polariton mode, occurring at the interface between a metallic waveguide and a dielectric. (84) For this enhancement to occur, the molecule needs to located close to the metallic surface at hotspots.(84) The chemical enhancement occurs when there is the formation of a charge-transfer state between the nanoparticle and molecule, which can be resonantly excited leading to a resonance Raman enhancement. (84)

SERS can be employed using two methodologies in biological application. Label free detection enhances the intensity of the overall intrinsic chemical fingerprint, through the analysis of the direct interaction between the samples and nanoparticles.(84) Indirect detection can also be used, allowing single molecule detection, through the use of SERS tags labelled with Raman reporter molecules with distinct signals.(84)

3.3 Advantages and Disadvantages

Raman spectroscopy is a useful technique allowing for analysis of a wide range of materials. As a non-destructive technique that does not face interference from water molecules it is particularly useful in biological applications and means little sample preparation is required.(83, 85) Hence results are more representative of in vivo conditions and Raman spectroscopy has been widely explored for its potential in biomedical exploration.(85, 86) The technique also has the potential to be used safely in vivo, allowing for future use as a potential diagnostic or intraoperative technique.(83) In the context of pancreatic cancer this could be particularly useful in guiding surgical margins during resection and in diagnosis acting as an adjunct or substitute for the current practice of analysing a frozen section. Moreover, variations in the technology have been developed allowing for diverse application. This includes spatially offset Raman spectroscopy (SORS), which allows Raman spectra to be taken at a point offset from the point of the laser, allowing for, for example, subcutaneous detection.(83) Clinically this provides opportunity for Raman spectroscopy to be used as an aid to endoscopic or laparoscopic techniques which could be used in detecting changes in an organ that is otherwise anatomically difficult to reach, such as the pancreas.

The data collected gives a highly specific chemical fingerprint of the material. In biological samples, it is capable of detecting cellular changes.(85) However, the Raman signature of some substances can supress other signals. The Raman effect is also very weak requiring a highly sensitive instrument and can sometimes be masked by background photoluminesence.(85) This can mean that background noise can be a problem in analysing samples. Although there are statistical methods of removing this background noise, it remains a problem and processing of data once acquired can be subjective.

Although Raman is a non-destructive technique, overheating of samples can occur, causing the sample to burn, especially with very thin or dry samples. This can often

be avoided by reducing the power of the laser, however, this may mean spectra with a lower signal to noise ratio (S/N) are acquired.

3.4 Computational Analysis

3.4.1 Pre-processing

Pre-processing techniques are necessary to allow analysis of the data by retaining pertinent information but removing noise, accounting for sloping baseline effects and differences in thickness and concentration of the samples. Steps such as cosmic ray removal can be selected in the WiRE software, which uses a combination of acquisitions to identify and remove cosmic rays to prevent these influencing the spectra.

Baseline correction removes fluorescence from the data. This can be done by a number of methods, the most common of which fits a convex polynomial line along the baseline of the spectra and removes anything beneath this, thus removing background fluorescence.(83) A second differentiation method, where the spectra are differentiated twice, can also be used, however this can cause the spectrum to lose its shape and can then only be normalised by vector normalisation.(83)

Normalisation techniques are usually subsequently employed to account for differences due to thickness or concentration of the sample. Two commonly used techniques are min-max normalisation or vector normalisation. Min-max normalisation requires a consistent, stable peak in all of the spectra,(83) often phenylalanine, Amide I or Amide III. For this method, the highest intensity of the chosen peak is converted to 1 and the intensity of a nearby peak, with minimal intensity, converted to 0. All other peaks are then scaled accordingly. Vector normalisation does not rely on a single peak, instead dividing the entire spectrum by is Euclidean norm.(83)

3.4.2 Processing

3.4.2.1 Multivariate Analysis

An analysis is described as multivariate when looking at the joint behaviour of multiple independent variables, as opposed to univariate analysis, where there is a single dependent variable. In spectroscopy, this is useful as each wavelength, of which there are hundreds, is an independent variable.

3.4.2.2 Principle component analysis

Principle component analysis (PCA) is a multivariate technique commonly used in vibrational spectroscopy to identify variation in the data. It is able to transform a large number of variables, wavenumbers in the example of spectroscopy, to a smaller number of uncorrelated variables.(87) In spectroscopy, there often hundreds of wavenumbers, making it impossible to visualise all of the data and identify subtle differences. PCA minimises data by producing linear combinations of the variables and ranking them based on variance.(87) Thus, a large data set is converted to a smaller one, still containing most of the variance in the data. The first 3 principle components are frequently used as they contain up to 99% of variance in the data.(83)

Principle components are visualised with each spectrum converted to a point on a scores plot and principle components as the axis of the plot. The further apart these points on the scores plot, the greater the spectral and therefore biochemical difference.(83) Principle component 1 is the line of greatest variance within this data.(87) Subsequent principle components are orthogonal to each other, each displaying succeeding degrees of variance, independent from one another.(83) As principle components are eigenvectors, with the correspondent eigenvalues as PCA factors, of the original covariance matrix of the data, PCA allows us to understand the data from an angle of greatest variance, without changing the data.(87) A greater PCA factor suggests greater variance in the data, and so greater biochemical difference.(83) However, as an unsupervised technique it is not given information about categories in the data and so PCA is unable to distinguish intracategory

variance from intercategory variance, unless this is the greatest natural variance in the data.(83, 87) This can be a limitation with biological samples as there is often significant biochemical difference within categories.(83) However, where variance is found, its detection is unbiased as the technique is unsupervised.

The data can also be viewed as loadings curves, showing the contribution of each wavenumber to the variance for a given principle component. In this plot the wavenumbers are viewed on the X axis and variance coefficient on the Y axis; wavenumbers with a greater variance between spectra have a greater coefficient and so a larger peak.(83) This peak can be either positive or negative and both are of equal value where the magnitude of the peak is the same. As loadings plots can distinguish important wavenumbers which create greatest variance in the data, this can then be worked backwards to identify the corresponding biochemical and so be helpful in identifying potential novel biomarkers.

3.4.2.3 Principle Component Analysis – Linear Discriminant Analysis (PCA-LDA)

Linear discriminant analysis (LDA) is a supervised technique, which draws out differences in the data dependent on pre-categorised classes.(88) It holds the advantage of being able to prioritise variation between classes over variation within classes, although this can mean that LDA analysis can 'overfit' the data and impose a bias when processing, dependent on preconceived classification of the data.(83, 88)

Following LDA transformation, the Euclidean distance within the LDA transformed space is equivalent to the Mahalanobis distance between any point and the centre of the class.(83) Hence, the Mahalanobis distance and LDA transformation can both account for the ellipsoidal clustering of the data.(83, 89) LDA can be particularly useful in that, with enough spectra and samples, sensitivity and specificity values for the contribution of wavenumbers to the variation in the data can be calculated.(90) This is particularly helpful with a view to clinical application as these values are needed for translation to clinical practice, to allow patients and practitioners to be adequately informed when such information is being used to aid diagnosis. However,

at a research stage, utilising LDA analysis is dependent on having enough samples and spectra to carry out this method of processing, which can be difficult with rare diseases.(89)

PCA-LDA is the application of LDA analysis on factors derived from an initial PCA of the data.(83) It has the advantage of requiring a smaller data set than LDA. In this case using 10 PCA factors provides enough information to give an adequate analysis of the data, without so much information that LDA overfitting occurs or information coming from background noise obscures the interpretation of loadings plots.(83)

3.5 Use of Raman Spectroscopy in Pancreatic Cancer Research

While Raman spectroscopy has been widely used in the detection of a number of cancers, including breast, skin and gynaecological cancers amongst others, as well as in cancer surgery guidance, suggesting potential for its use, very little research has been done on the potential use of Raman spectroscopy in pancreatic cancer.(84, 91)

Much of the current literature has focussed on developing detection markers, utilising SERS to identify and detect known and emerging biomarkers, thereby improving the detection limits of these proteins which are found in low quantities in serum.(28, 92-94)

The MUC4 and CA19-9 biomarkers have previously been detected, using a SERS based sandwich immunoassay, with a limit of detection of 1ng/ml and 27ng/ml respectively.(94) More recently a SERS based immunoassay has been developed using gold nanoparticles, to detect CA19-9, MUC4 and MMP7 in serum, with the potential to detect under $2ng/ml^{-1}$ concentration of each of the biomarkers and ability to detect the biomarkers simultaneously.(28) The authors conclude that such a sensitivity should be sufficient to detect these biomarkers and differentiate between normal and diseased patients, particularly using simultaneous detection of all 3 biomarkers.(28) These studies have shown potential use of Raman spectroscopy and in particular SERS, where more conventional methods such as enzyme-linked

immunosorbent assay and radio immunoassay have failed to provide adequate sensitivity in detecting and utilising new biomarkers.

The development of the potential use of SERS aims to provide a solution to the lack of detection limits of current clinical blood assays. It has been suggested that, at present, biomarkers being shed by a developing tumour burden could be undetectable in blood samples for more than 10 years(93). Therefore, use and development of SERS based immunoassays is currently a popular area of research with a number of recent developments, focussing on improving the performance of nanoparticles to identify ways by which the sensitivity can be improved and the Raman signal stabilised, to provide reproducible and easily interpreted results.(28, 93, 95) The use of multiplex detection for pancreatic cancer, to improve specificity as well as sensitivity of biomarkers has been of particular focus, to provide a solution to the significant problem of lack of specificity of CA19-9.(28, 92) There is general agreement in the literature that SERS is able to provide at least similar degree of accuracy to ELISA, but has the advantage of needing a smaller sample size and a lower limit of detection.(92-94)

Raman spectroscopy has also been shown to be able to differentiate between healthy pancreatic β cells and insulinoma cells in rat model.(95) There is therefore the potential for a similar methodology to be extrapolated to differentiate between pancreatic cancer in the exocrine pancreas and normal pancreatic tissue and so identify differences which could aid with the diagnosis and surgical resection of pancreatic cancer.

Another study on a mouse model, attempted to use injected surface enhanced resonance Raman spectroscopy (SERRS) nanostars to detect tumour margins at resections.(96) This found multiple sub-millimetre foci could be identified using a Raman spectral fingerprint of SERRS, where no residual tumour was seen with white light imaging.(96) Histological examination demonstrated that SERRS nanostars accumulated in the tumour stroma and within epithelial tumour cells and were also found in and able to identify PanIN lesions.(96) Importantly this method showed high

specificity for malignant regions as the SERRS nanostar is non-existent in biological tissue and so the Raman signal can only be detected in malignant tissue, where there has been uptake of the reporter molecule.(96) However, the mechanism by which SERRS-nanostars are taken up by malignant tissue is unknown, although it is hypothesised that macropincytosis could be the underlying mechanism, caused by malignant mutation.(96) This mechanism could however, vary been between different mouse models and human patients and so the specificity of the method could also vary. Therefore the work with injected SERRS nanostars would require significant further work for translation to humans.

While the use of Raman spectroscopy in pancreatic cancer is beginning to show potential, this is a very new area of research, with very little literature. Notably, Raman spectroscopy on human pancreas tissue is not described in the current literature nor is there any work differentiating healthy pancreas from malignancy of the exocrine pancreas using Raman spectroscopy, which are significant limitations to the potential translation of the technique to clinical practice.

3.6 ELISA

Enzyme-linked immunosorbent assay is a plate-based technique used to detect and quantify peptides, protein, antibodies and hormones. The technique is dependent on an immobilised antigen and highly specific antibody-antigen interaction with the antibody linked to an enzyme. Assessing the enzyme activity, by incubating with a substrate, allows for detection and quantification of the antigen.(97)

The antigen of interest needs to be immobilised to a solid surface, either directly adsorbed to the assay plate or by using a capture antibody that is attached to the plate. Detection can be direct, the antigen is linked to a primary antibody linked to an enzyme, or an indirect method, where the primary antibody is linked to a secondary antibody.

The most common and sensitive method is a 'sandwich' assay, which captures the antigen between two primary antibodies.(98) An antibody is attached to th plate, to which the antigen is linked and second primary antibody attaches to the antigen. A secondary antibody is linked to the primary detection antibody and this links to the enzyme, the activity of which is measured to allow for detection. As the primary antibody has several epitopes to which the secondary antibody can bind, the signal can be amplified, increasing sensitivity.(97) In this method, it is important that the secondary antibody is specific to the primary detection antibody and not the capture antibody to ensure the assay is specific to the antigen. This is often achieved by using a capture antibody from a different species to the detection antibody.

While the direct detection method is often faster and eliminates any potential affinity between the detection antibody and capture antibody, ensuring good specificity to the antigen, it is less sensitive as the signal cannot be amplified.

3.7 Immunohistochemistry

Immunocytochemical techniques are techniques developed over the past 60 years, which utilise antibodies to give information where the morphology and clinical data alone cannot confirm a diagnosis. In the context of cancer, these techniques are particularly useful as antibodies which bind to cytokeratin, the epithelial cytoskeleton, are specific to the diagnosis of most cancers.(99)

While immunofluorescence staining enables the visualisation of such antigens, it has the disadvantages of needing a fluorescence microscope and limited detail of the morphology of labelled cells. Immunohistochemical techniques overcome this by counter staining with haematoxylin. In addition, samples prepared for immunohistochemical staining can be stored for longer periods of time as unlike the fluorescence dyes, the staining intensity does not diminish with time.(99)

For samples fixed in formalin and paraffin, which enable the samples to be sectioned, many epitopes are masked or destroyed during the fixing and processing steps.(99) Hence, it is necessary to first retrieve antigens from the samples before staining. This can be done using a number of methods including, proteolytic enzyme digestion, microwave antigen retrieval, pressure cooker antigen retrieval and steam.(99) Of these, microwave antigen retrieval is the most suited to a laboratory, both because of speed and safety.

A number of methods for immunohistochemical staining have been developed. These can be split into a direct or indirect method. The direct method uses a primary antibody directly conjugated to a label. While this is a simpler method, requiring a single application of antibody it has a lower sensitivity than the indirect method.(99) The indirect method requires the application of a primary antibody, followed by a secondary labelled antibody directed against the first. Horseradish peroxidase is the most commonly used label for this method, with an appropriate chromogen substrate.(99)

Hypothesis

It is hypothesised that Raman spectroscopy is able to differentiate between healthy and cancerous tissue in the exocrine pancreas. It is thought that these differences will be seen in peaks related to DNA and protein which will identify and provide further information about genotypic and phenotypic changes to the cells involved in the development of pancreatic cancer. These changes are expected to be identified in a way that enables the potential use and translation of the technology into clinical practice. It is further hypothesised that the matricellular protein SPARC plays a role in the development of pancreatic cancer and its production by PSCs is dependent on the interaction between cancer cells and PSCs.

Aim

This study aims to identify the differences between cancerous and healthy pancreatic tumour resection tissue using Raman spectroscopy. It aims to utilise Raman spectroscopy to analyse the patients' blood and resections to identify potential novel biomarkers which could be used in the screening, diagnosis and detection of tumour margins in pancreatic cancer.

A primary objective is to use cocultures of HPAF-II and PSCs, aiming to understand the interactions between these cell types and their role in both the production of SPARC and development of pancreatic cancer. This is hoped to be achieved by using ELISA and Raman spectroscopy to provide information and analyse the interactions between cells. This ultimately aims to create a 2D cell line model, which is able to be characterised using Raman spectroscopy, which could be used in further research.

Overall, this study aims to demonstrate the potential utility of Raman spectroscopy in identifying the development of pancreatic cancer and differences between healthy and cancerous pancreatic tissue and providing information as to why these changes may occur. It aims to be able provide a basis for further research allowing translation of the technology to clinical practice.

Chapter 4 – Methods and Materials

4.1 Sample Preparation

4.1.1 Human Tissue

Tissue from human pancreatic cancer tumour resections were taken, with ethical approval from Greece (St Savvas Cancer Hospital and Red Cross Hospital in Athens) and the UK (REC approval: 17/YH/0283), after surgery from patients diagnosed with PDAC (Table 2). The tissue was frozen at -80°C for transportation and storage. It was defrosted, cut and placed fresh on calcium fluoride (CaF_2) slides to be scanned using the Raman spectrometer. Samples with a gross tissue margin were cut in line with the margin, giving a sample with healthy tissue, a tissue margin and cancerous tissue (Figure 2).

Once scanned fresh, the samples were fixed and stored in 10% neutral buffered formalin and scanned again, using the same settings, to identify any differences in spectra between fresh and fixed tissue. Formalin fixation was used as it causes less protein degradation and tissue shrinkage than fixing using ethanol.(100)

4.1.2 Preparation of Blood samples for Raman spectroscopy and SERS

Blood samples from each patient were also received frozen, for patients 1, 2 and 3, and stored at -80°C. The blood sample from patient 1 was received as serum and samples from patients 2 and 3 were received as whole blood. Samples were transferred to a quartz well plate for scanning. For SERS measurements blood was mixed with an equal volume of 60nm gold nanoparticles (BBI Solutions, UK), and incubated at 4°C for 2 hours.(101, 102) The gold nanoparticles were citrate capped, suspended in water with no preservative at a concentration of $2.6x10^{10}$ per ml.

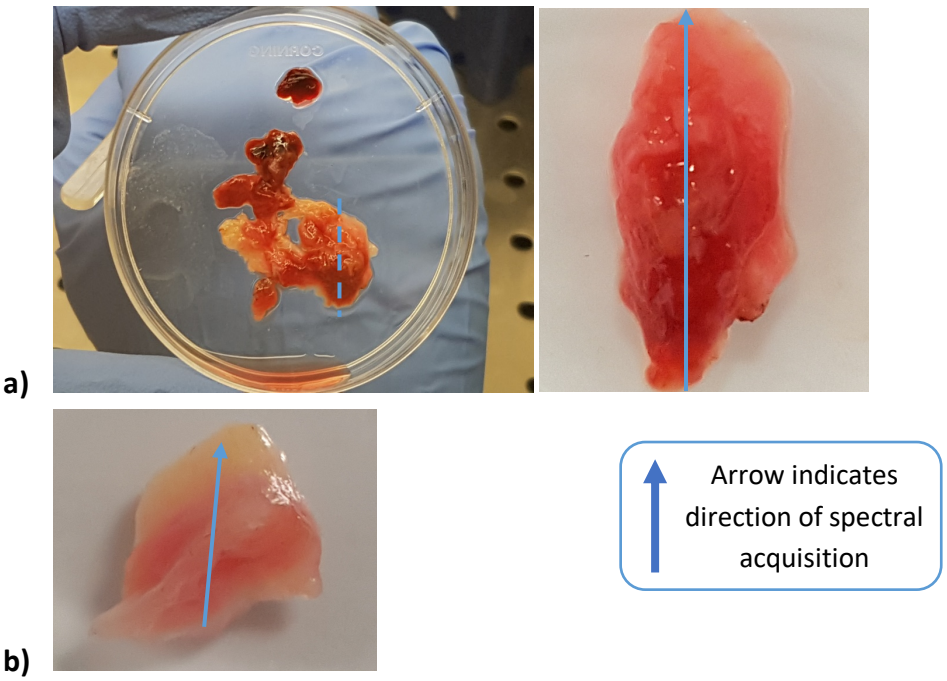

Figure 2: a) resection patient 2, dashed line shows where tissue was cut before spectra were taken, b) resection patient 3, arrow indicates direction of spectral acquisition

Pancreatic tumour resections – Patient Characteristics

Patient	Sex	Age	Site	Histological Type	Differentiation	Pathological staging	Resection status	Blood sample received	Tumour margin visible
1	M	75	Head/uncinate	Undifferentiated (anaplastic or sarcomatoid) carcinoma		Stage IIA: T3, N0, M0	Incomplete	Y	N
2	F	60	Head/uncinate	Undifferentiated carcinoma with osteoclast-like giant cells	Moderate	Stage IIA: T3, N0, M0	Complete	Y	Y
3	M	73	Body/neck	Ductal Adenocarcinoma	Moderate	Stage IIA: T3, N0, M0	Incomplete	Y	Y
4	M	73	Head	Ductal Adenocarcinoma	Moderate	Stage IIB: T2, N1, M0	Complete	N	N

Table 2:Patient characteristics for study samples

4.1.3 Cell Lines

A human pancreatic cancer cell line, HPAF-II (ATCC, LGC standards, UK), and human pancreatic stellate cells (PSC) (iXCell Biotechnologies, San Diego, CA, USA) were initially cultured in Dulbecco's modified eagles culture medium, supplemented with 10% foetal bovine serum (FBS), 1% penicillin and 1% streptomycin. Confluent cells were split by removing media and washing with 5ml of phosphate buffer solution, before adding 5ml trypsin, both warmed to 37°C and incubating for 5 to 10 min at 37°C and 5% CO_2, to allow the cells to detach. The trypsin was then neutralised with 5ml of media and then centrifuged at 400rpm for 5 min. The supernatant was removed and the cells suspended in 15ml of media in a 75mm^2 flask to allow to grow.

Experiments were conducted with confluent cells, ensuring all cells were at the same stage in the cell cycle, allowing for comparable results. For Raman experiments the cells were transferred to CaF_2 slides in petri dishes and allowed to grow. HPAF-II cells were grown on CaF_2 slides for varying lengths of time to identify a timepoint which would mean cells were suitably attached to the slide to be able to acquire spectra. The optimal method was to deposit cells on the slide and incubate at 37°C and 5% CO_2 for a minimum of 3 hours, allowing cells to rest and attach for before adding 10ml warmed media to the petri dish, to ensure cells were attached to the CaF_2 slides and did not wash into the petri dish. Cells were then allowed to grow for 7 days, which enabled enough growth and attachment for spectral acquisition.

4.1.3.1 Coculture

For co-culture experiments, HPAF-II cancer cell line was grown with and without human pancreatic stellate cells to identify if a model for tumour stroma could be produced for future research. The cell line was initially grown alone for tests, then alongside combinations with fibroblasts at ratios of 1:1, 1:3 and 3:1 (cell line:PSC). Ratios were calculated based on number of cells and each combination had Raman spectra acquired from live cells, after being allowed to grow for 7 days. Cells were counted after centrifuging, by resuspending the pellet in 1ml media and depositing

0.1ml onto a haemocytometer for counting. The average figure was then multiplied by 10,000 to estimate the number of cells in 1ml.

Cells were co-cultured both on a slide, where they could directly interact, and in an insert in a wells plate, where cells types grew without direct contact with one another but sharing media, and therefore growth factors and other secreted products. Media was changed to media without FBS at day 5, to allow this media to be conditioned before ELISA testing.(103) This growth medium, in each case, was tested to identify SPARC production and secretion using quantitative ELISA.

4.1.3.2 Preparation of Cells for SERS measurements

Surface enhanced Raman spectroscopy (SERS) was subsequently employed on fresh cells, using 60nm gold particles (BBI Solutions, UK), to enhance any signal that may have been specific to a potential biomarker. The gold nanoparticles were citrate capped, suspended in water with no preservative at a concentration of $2.6x10^{10}$ per ml. Cells were grown in co-culture using the same method previously described and were incubated with the SERS substrate at a volume ratio of 2:1 (media:nanoparticles) for 7 days at 37°c and 5% CO_2, before scanning with the Raman microspectrometer.(86)

4.2 Raman Spectroscopy

4.2.1 Calibration

An inVia Raman microspectrometer (Renishaw plc, Gloucestershire, UK) with a 785nm laser was used to acquire spectra from the samples. The instrument was initially allowed to stabilise for 30 minutes after being switched on, to ensure constancy of the laser and charged coupled device. The instrument was calibrated daily, first ensuring the laser was correctly aligned and in focus. Secondly, a measurement taken of silicon, with an expected peak at $520.5cm^{-1}$ and the absolute intensity of this peak was recorded. Calibration was needed daily to ensure the laser began at the same starting point before taking measurements, ensuring measurements were accurate and comparable. Silicon was used for this purpose as it

has a very clear single peak at 520.5cm^{-1}. Where the peak had shifted the instrument was optimised to ensure a measurement at 520.5cm^{-1}. A further calibration measurement was taken using polystyrene, as this has peaks in the biochemical fingerprint. The intensity of the two largest peaks, wavelengths 1001 cm^{-1} and 1031 cm^{-1}, was recorded with the intensity of the 1001 cm^{-1} peak expected to be four times that of the peak at 1031 cm^{-1}.

4.2.2 Optimisation

Optimisation of Raman setting was needed to identify a power setting which would give maximal Raman signal without damaging the sample and a time and acquisition setting which was both time effective and gave good signal to noise ratio, allowing identification of important peaks. Initial optimisation was done using a sample of HPAF-II cells grown for 24 hours on calcium fluoride (CaF_2) slides, as these have no Raman signal, and bought into focus under the microscope. A range of 593cm^{-1} to 1705cm^{-1} was selected as this range includes peaks in the biological spectrum. Spectra were then taken to identify the most appropriate power of the laser, which would not cause damage to the samples.

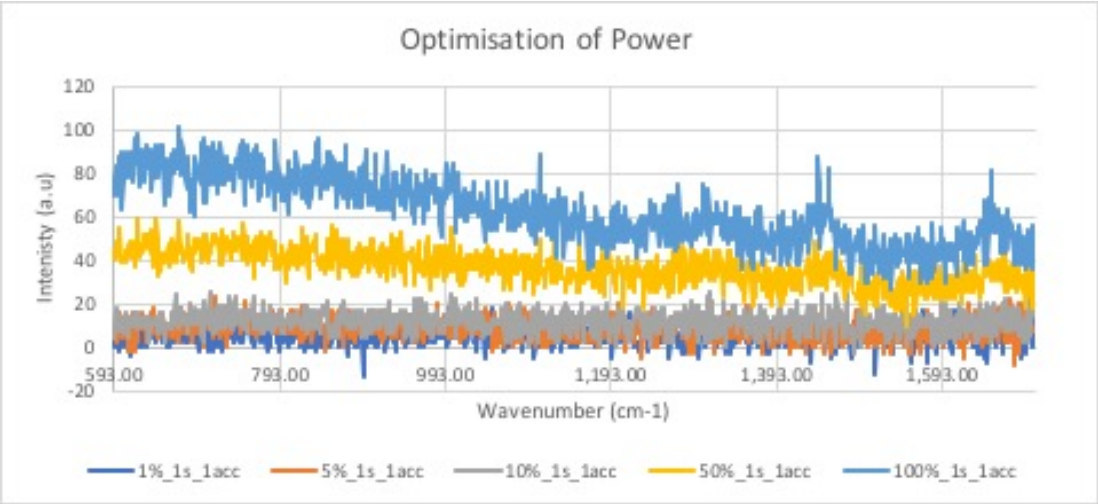

Figure 3:Optimisation of laser power settings for Raman spectroscopy. A final setting of 100% was chosen as this gave maximal Raman signal and did not damage the samples.

Initially spectra were taken with the laser varying in power, to identify the maximal power that could be used without causing damage to samples as this would give the maximal Raman signal and information. The optimal laser power was 100%; this gave the greatest intensity of the laser and did not damage the samples (Figure 3).

a)

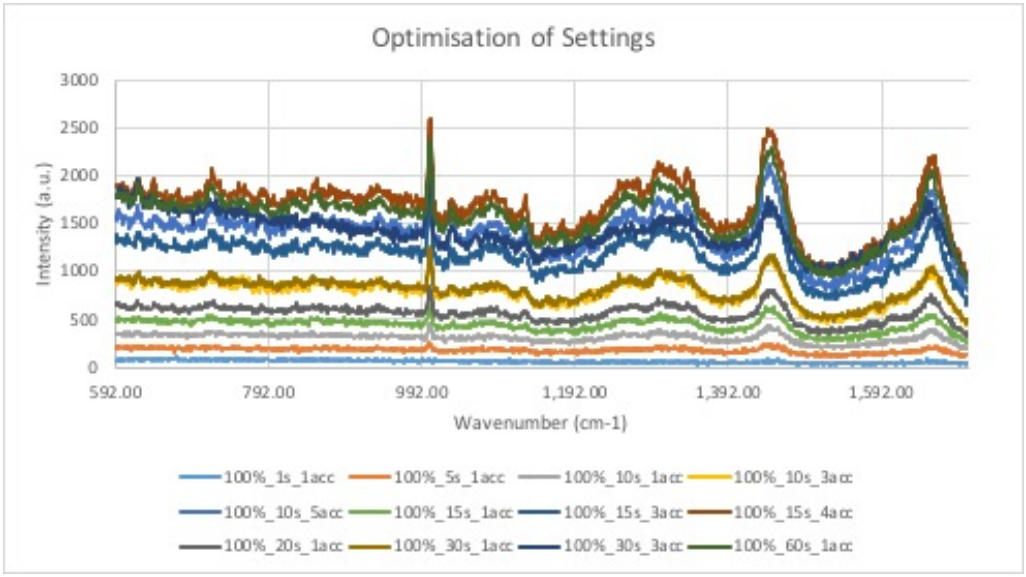

b)

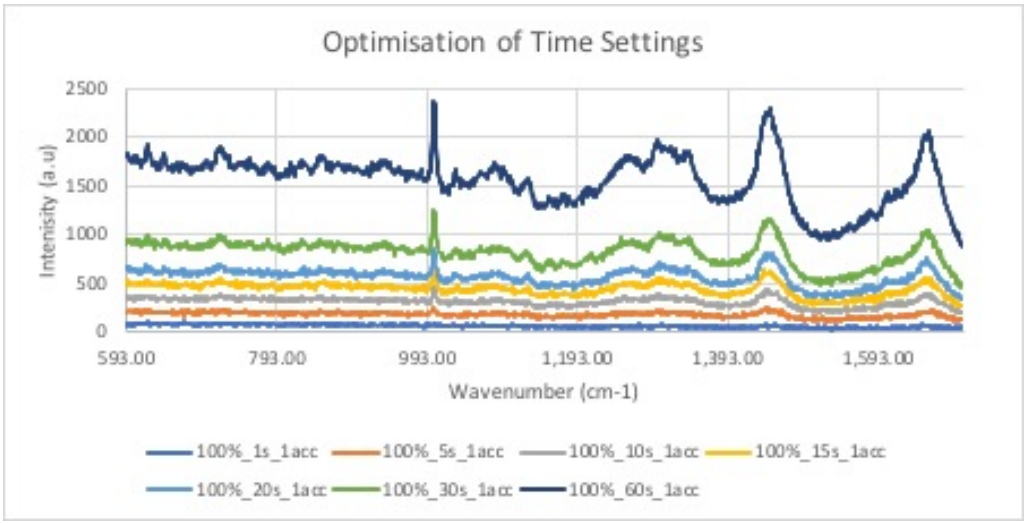

c)

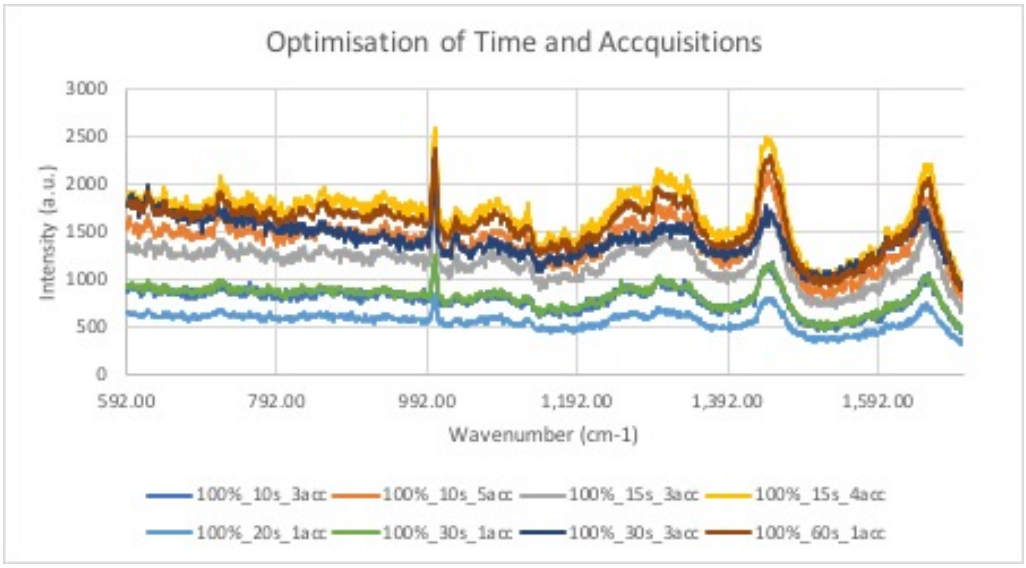

Figure 4:Graphs showing rationale for optimisation of settings a) overall optimisation of settings, b)optimisation of time setting using 1 acquisition, c) optimisation of combined time and acquisition setting

The combination of time the laser focussed on the sample and the number of acquisitions was tested next to identify a setting giving a spectrum with the optimum signal to noise ratio, allowing identification of biological peaks (Figure 5a).
To do this, spectra were initially taken at differing time settings, using only 1 acquisition (Figure 5b). Spectra were then taken combining time with numbers of acquisitions, to identify which combination both gave the optimal signal to noise ratio and so allowed for the best identification of potential peaks in the spectra and was most time effective (Figure 5c). A final setting of 15s by 4acc was used to take measurements.

4.3 Spectral Acquisition

4.3.1 Tissue

Spectra were taken using a 785nm laser and x50 long working distance objective. Settings for scanning with the Raman spectrometer were optimised. (Figure 5) A final setting used laser power of 100% and 15s and 4 acquisitions; these were the same settings as used for cell lines, making spectra comparable to cell line spectra. Spectra were taken in a line, with a minimum distance of 250μm between spectra, to ensure independent measurements (Figure 2). Spectra were taken either moving from tissue which appeared healthy to that which appeared cancerous or vice versa, to ensure results were due to changes in the samples and not degradation of the laser over the course of the day. The number of spectra taken varied dependent on the length of the resection, with a minimum of 15 spectra acquired per sample.

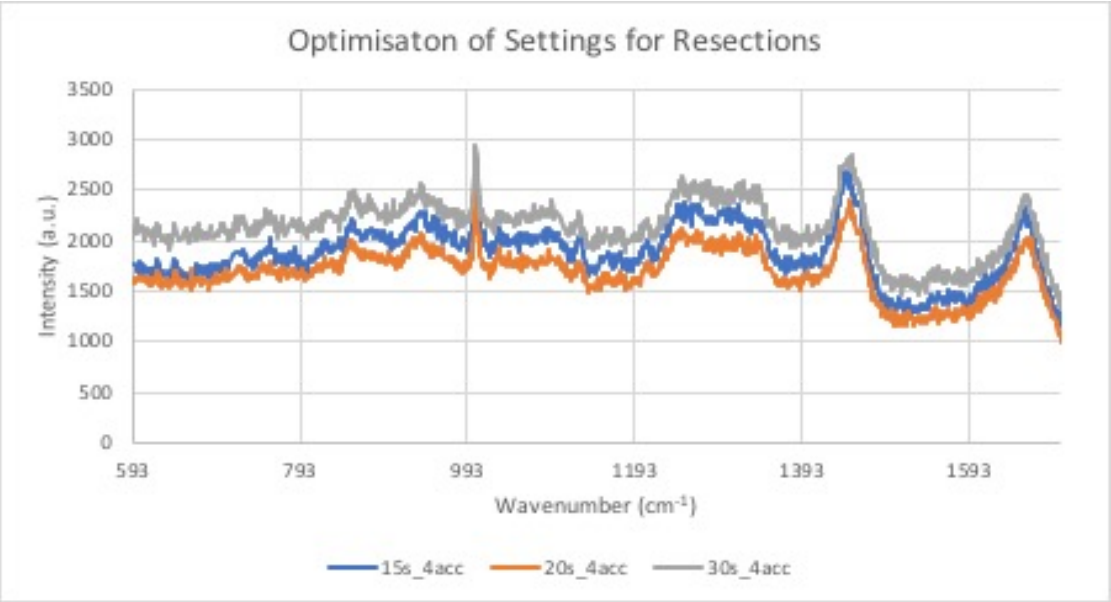

Figure 5:Graph showing spectra for optimisation of time and acquisition setting for tumour resections. Spectra taken from patient 1 tumour sample. Final settings were optimised to 15s by 4 acquisitions.

4.3.2 Blood

Blood samples were transferred to a quartz well plate for scanning. Spectra were taken, using a 785nm laser and x15 long working distance objective, from both fresh blood as well as SERS measurements to enhance signal.

The depth at which the measurement was taken was optimised for each sample. The rationale for depth optimisation is demonstrated, using spectra from patient 1's blood sample, in Figure 6. The same method was used for all blood samples. The depth was optimised by initially setting the z axis to 0 at the top of the wells plate and then taking a single 10s measurement every 400μm beginning from the bottom of the wells plate, to the top (Figure 6a). A second depth optimisation measurement was taken, with spectra taken every 100μm in the region identified as the optimum based on the initial measurements (Figure 6b). This gave the optimum depth from which to acquire spectra. Raman settings were optimised to 15s by 40 acquisitions (Figure 7) and SERS settings to 60s by 3 acquisitions (Figure 8). A laser power of 100% was used as the sample was liquid and so could not be damaged, by this laser.

a)

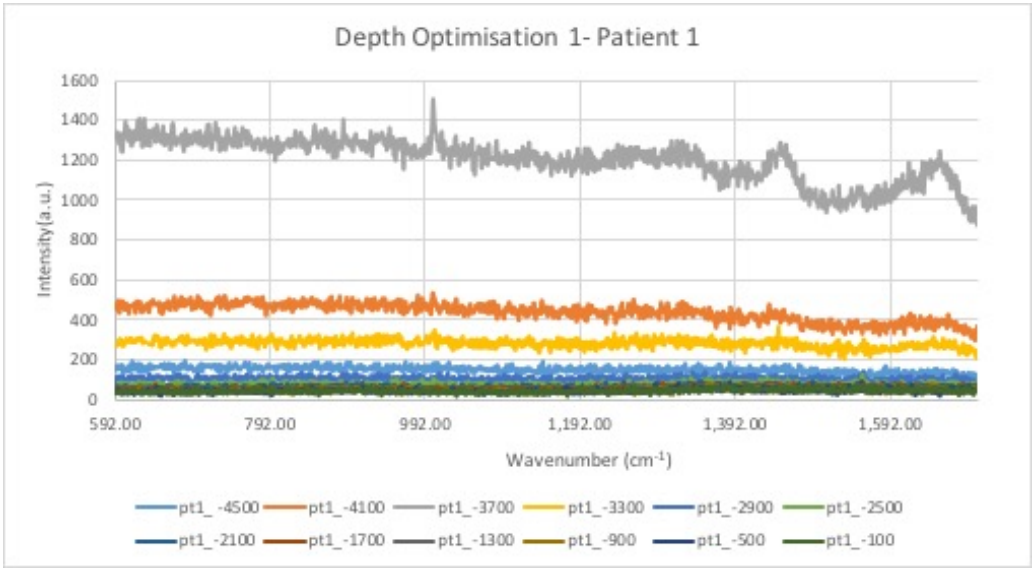

b)

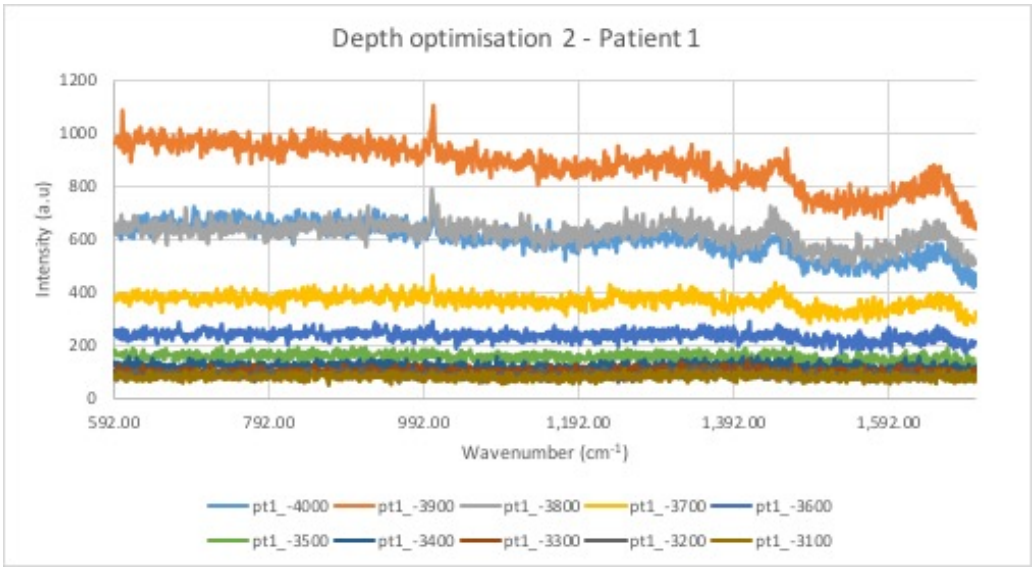

Figure 6:Spectra demonstrating rationale and method of depth optimisation using patient 1's blood sample a) first depth optimisation with spectra taken every 400μm moving down from the top of the well plate, the spectrum at -3700μm on the z axis can be seen as the clearest spectrum for this sample b) second depth optimisation with spectra taken every 100μm from -3000 to -4000μm. The clearest spectrum was seen at -3900μm and all other spectra were taken from this point for this sample.

a)

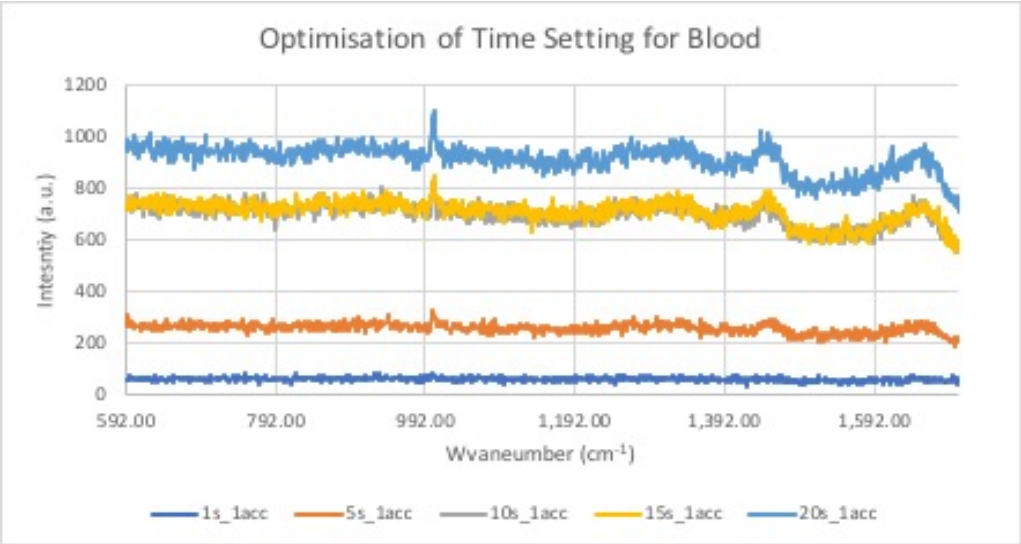

b)

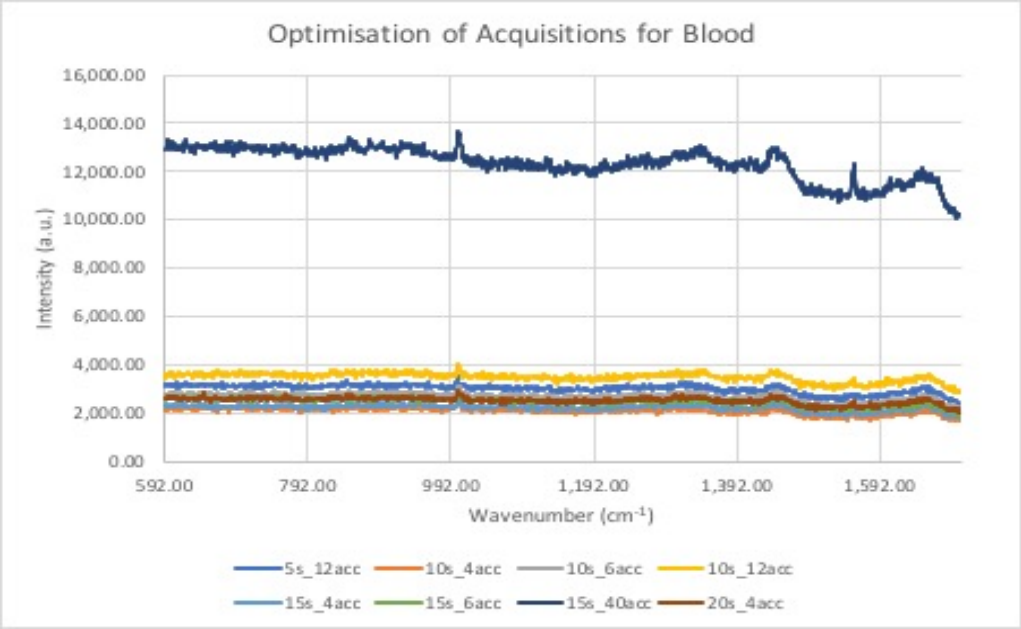

c)

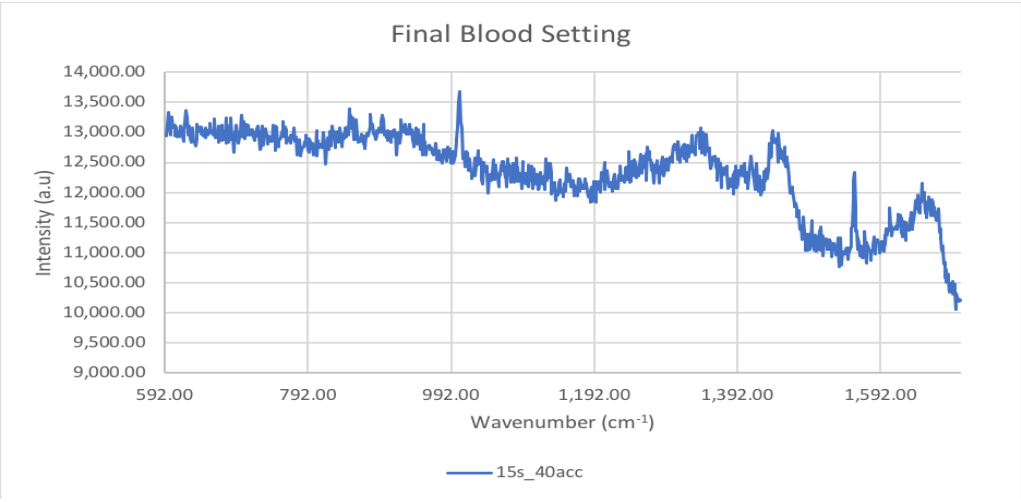

Figure 7:Graphs showing spectra for optimisation of time and acquisition setting for tumour resections. Spectra taken from patient 1 blood sample, a)optimisation of time settings with using 1 acquisition b)optimisation of time and acquisition settings, c) raw spectrum for final setting of 15s by 40 acquisitions

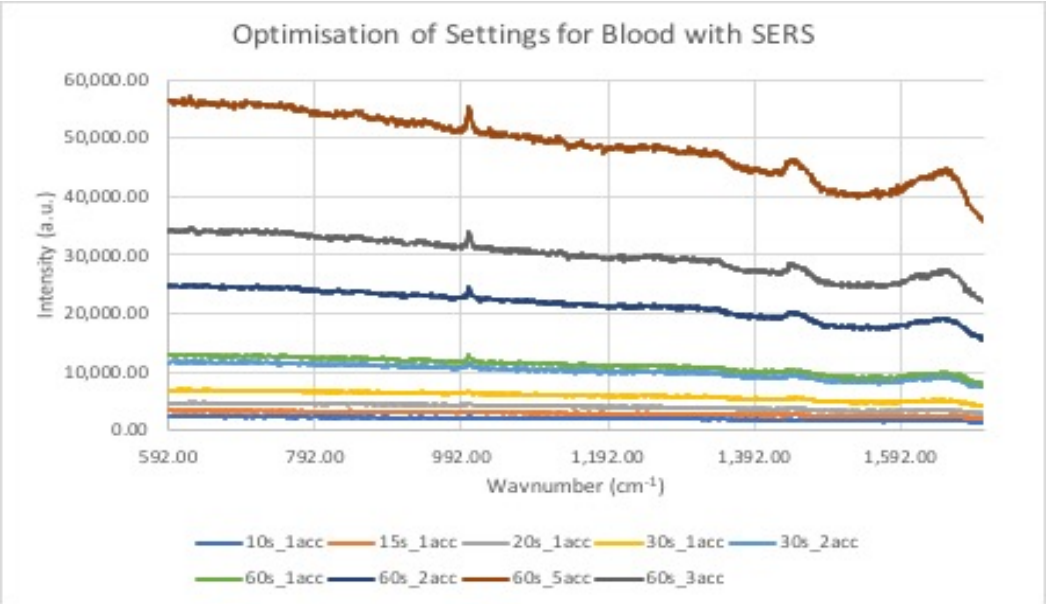

Figure 8:Graph showing spectra for the optimisation of settings for blood samples with SERS. Final settings were optimised to 60s by 3 acquisitions

4.3.3 Cell Lines

Spectra were taken using an x60 immersion objective to acquire spectra, with cells still in media.(85) Spectral acquisition was limited to 1 hour after cells were removed from the incubator to ensure spectra were taken from live cells. The settings for acquiring spectra were optimised using the described method. The spectra were taken at a laser power of 100%, using a setting of 15s and 4 acquisitions (Figure 4). 15 independent spectra were taken per sample.

Cells were then fixed in 10% neutral buffered formalin for 30 minutes and scanned again however this gave a noisy spectrum and with no identifiable peaks. Fixed cells were stored in 10% neutral buffered formalin at 4°C before immunohistochemistry, to identify SPARC, was attempted on the fixed cells.

4.3.3.1 SERS on Cells

Surface enhanced Raman spectroscopy (SERS) was subsequently employed on fresh cells, using 60nm gold particles (BBI Solutions, UK), to enhance any signal that may have been specific to a potential biomarker. The gold nanoparticles were citrate capped, suspended in water with no preservative at a concentration of $2.6x10^{10}$ per ml. Cells were grown in co-culture using the same method previously described and were incubated with the SERS substrate at a volume ratio of 2:1 (media:nanoparticles) for 7 days at 37°C and 5% CO_2, before scanning with the Raman microspectrometer.(86) SERS settings were optimised to 100% power, using a setting of 1s by 3 acquisitions, to allow cosmic ray removal (Figure 9a). Spectra were taken using a mapping setting, as there were significant differences between different areas of cell and due to the distribution of nanoparticles (Figure 9b). Approximately 200 spectra were taken from 2 locations on every slide, giving a total of approximately 400 spectra per slide.

a)

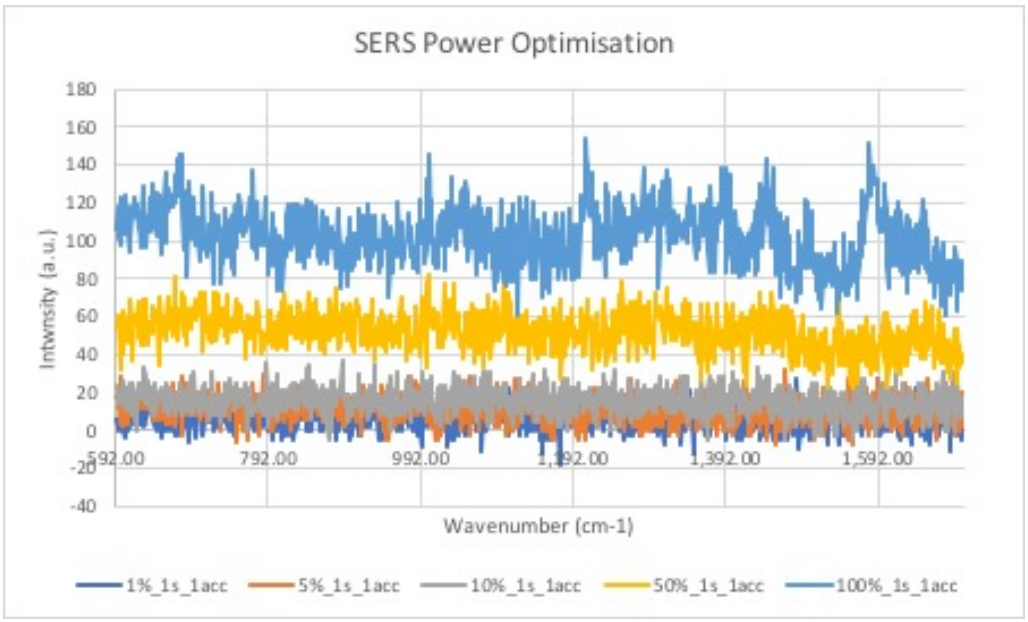

b)

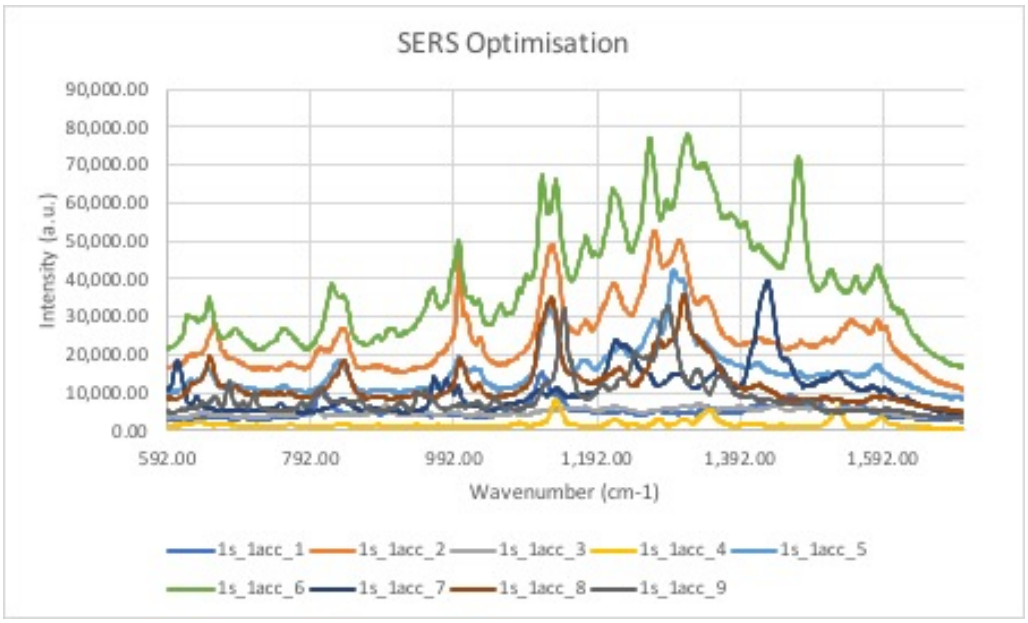

Figure 9:Graph showing spectra for the optimisation of settings for cell cocultures with SERS. a) Optimisation of power setting for cells with AuNP. 100% power was suitable and did not damage the samples. b) Optimisation of time and acquisition settings. 1s and 1 acquisition gives a clear spectrum but the quality and configuration of spectra vary dependent on the location from which they are taken.

4.4. Raman Data Analysis

4.4.1 Pre-processing

Data was analysed using an in-house written Matlab (The Mathworks Inc, MA, USA) script.(104) All spectra were baseline corrected using a polynomial order of 6, to remove fluorescence. This polynomial order was chosen to sufficiently remove background noise and fluorescence with minimal loss of Raman signal intensity and change to the configuration of the peaks (Figure 10). Vector normalisation and min-max normalisation using both the phenylalanine and amide III peaks were then tested on the baseline corrected data. Vector normalisation was chosen as the normalisation technique for the data as this gave a representation of the chemical peaks after scaling for volume, allowing for comparison, as differences caused by focussing depth and thickness across the samples were removed. While both vector and min-max normalisation were suitable techniques for achieving this, vector normalisation caused minimal change to the original data (Figure 11). All data was pre-processed using the same settings to allow spectra to be comparable.

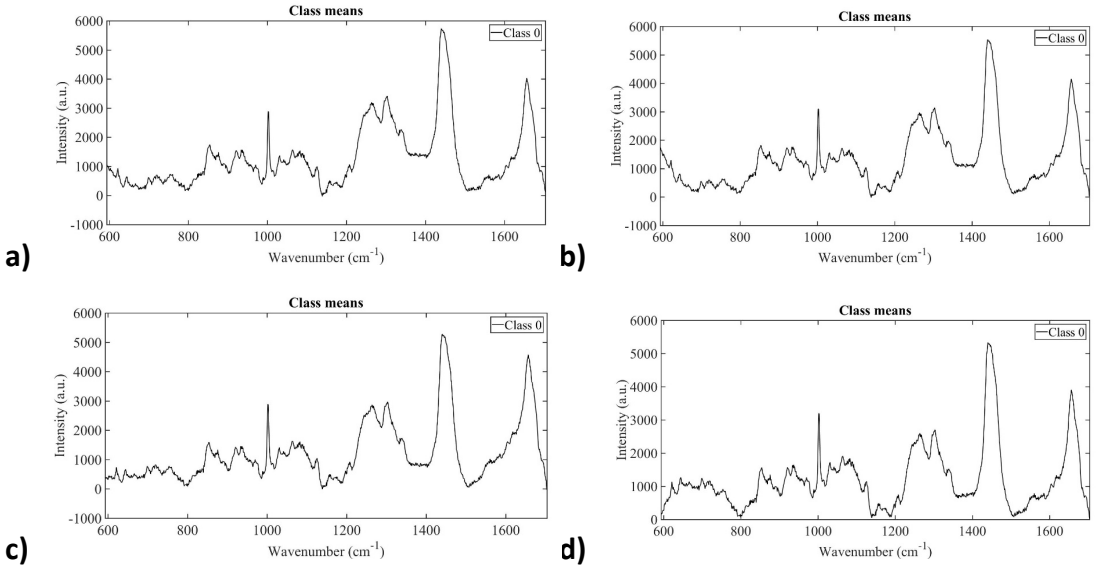

Figure 10:Baseline corrected data, a) polynomial order 4, b) polynomial order 5, c) polynomial order 6, d)polynomial order 7

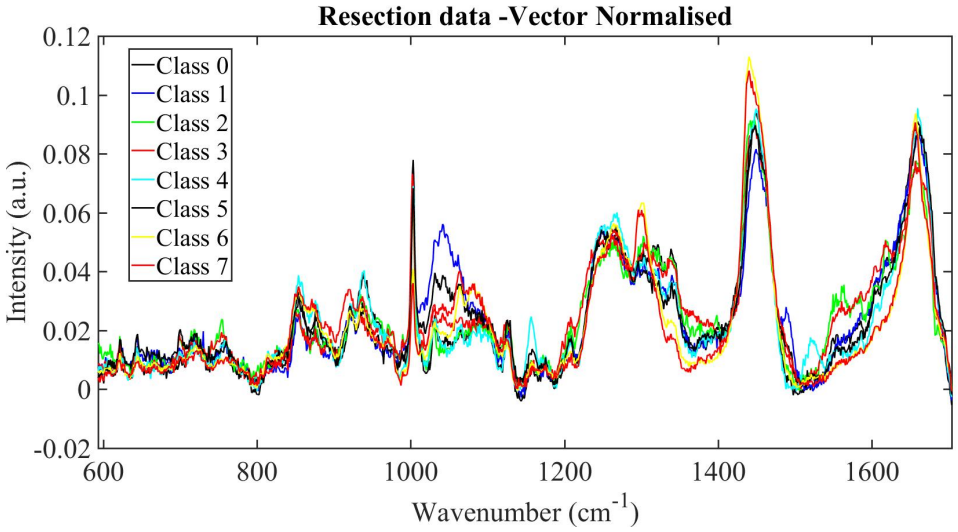

a)

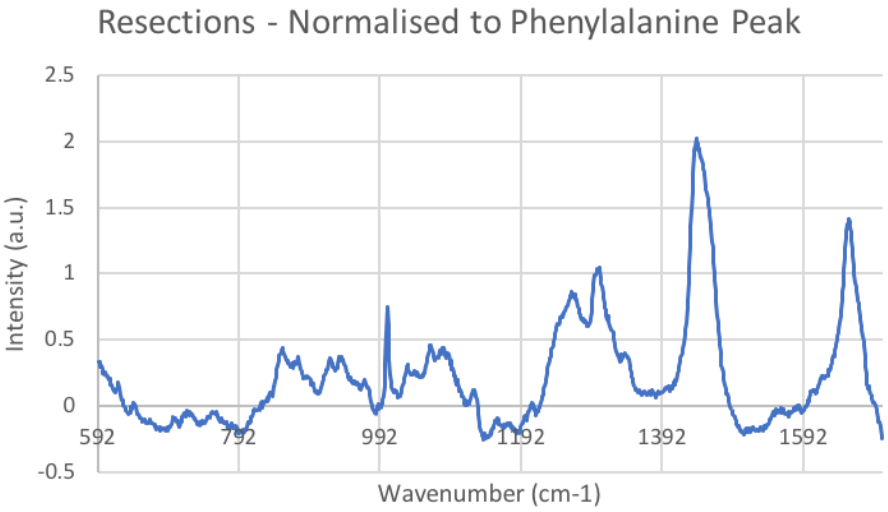

b)

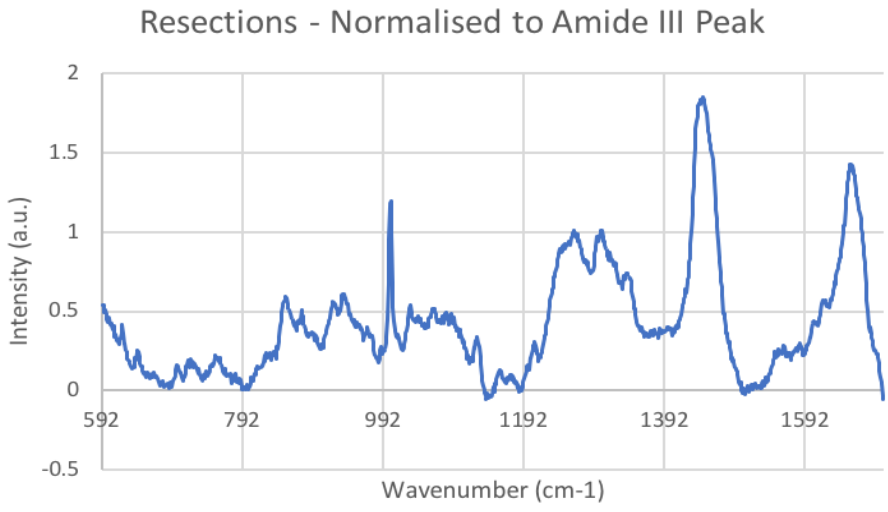

c)

Figure 11:a) Resection data baseline corrected, polynomial order 6, vector normalised; Class 0&1 – patient 1 fresh and fixed, Class 2&3 – patient 2 fresh and fixed, Class 4&5 – patient 3 fresh and fixed, Class 6&7 – patient 4 fresh and fixed b) Mean spectrum of all resection data baseline corrected, min-max normalised to phenylalanine peak, c) Mean spectrum of all resection data baseline corrected, min-max normalised to amide III peak

4.4.2 Processing

Data was processed using PCA and PCA-LDA analysis, using an inhouse Matlab script, which calculated 10 PCs before scores and loadings plots were reviewed. For resection data, an initial PCA-LDA scores plot was done to determine whether it was possible to separate data based on if they were acquired from fresh or fixed tissue. LDA alone was not used as there were not enough spectra within each class to ensure the analysis would not overfit the data.

Maps acquired from cells using SERS were reviewed and shaded using signal to baseline analysis for wavenumbers 600-800cm and 1325-1345cm, which are both regions which identify changes to DNA. The data was pre-processed in WiRE 4.2 using mean centring and vector normalisation, to keep pre-processing steps as similar as possible to that of the cell data without SERS. An intensity range of 5-95% was selected to give clearer visual representation of the location of the SERS peaks as spectra with the lowest intensity, which were unlikely to be SERS spectra and those with the highest intensity where the receiver had been saturated was minimalised in the shading, They were also shaded by PCA, using the full range of intensity and calculating 10 PCs before shading to PC1 and PC2 to identify variation within cell maps.

4.5 ELISA

Quantitative ELISA for SPARC was done on media from cells co-cultured both in direct contact and in indirect contact, using an insert in a wells plate. A human SPARC ELISA kit (Abcam, Cambridge, UK) was used and relevant company protocol followed. Briefly, samples of conditioned FBS free media from cocultures and serum from patient 1 were defrosted to room temperature and prepared by centrifuging, to remove any remaining cell matter. Standards were then prepared to allow for comparison of concentrations. Samples and standards were distributed to appropriate wells and an antibody cocktail added. This was followed by a 1 hour incubation period at room temperature on a plate shaker. Each well was washed 3 times with a wash buffer, before a tetramethylbenzidine (TMB) substrate was added

and samples incubated for 10 minutes. A stop solution was then added and the plate was read at 450nm.

4.6 Histology

A protocol for immunohistochemical staining developed from Bancroft's Theory and Practice of Histological Techniques was used to prepare and stain both slides of cocultured fixed cells and fixed tissue resections.(99)

Formalin fixed tissue samples were embedded in wax, by transferring from formalin to ethanol (70% then 90%) to xylene and incubating for 30 minutes at each stage, before embedding in paraffin. Samples were embedded by incubating for 30 minutes in hot paraffin wax twice, to allow the wax to permeate the samples before moving to a wax block. Embedded samples were sliced as a cross-section to 4μm using a microtome and dried overnight before staining.

4.6.1 Haematoxylin and Eosin staining

Paraffin embedded tissue sections were transferred through xylene to ethanol (absolute and 90%) to water, standing for 5 minutes at each stage, to allow for staining with water based dyes. They were then stained with Harris Haematoxylin, followed by Eosin Y, washing for 5 minutes under running tap water after the application of each dye to allow the stain to develop. They were then transferred back through ethanol to xylene before being mounted using a xylene based mounting agent.

4.6.2 Immunohistochemical staining

The samples were initially prepared by deparaffinising and endogenous peroxidase activity was blocked by incubating in 0.5% hydrogen peroxide in methanol for 10 minutes. Samples were then rehydrated and washed before transferring to tris buffered solution (TBS). The microwave antigen retrieval method was used, heating samples placed in a citrate buffer for 10 minutes in a 750W microwave at full power.

The samples were stained using horseradish peroxidase (HRP) as a conjugate. Slides were washed in TBS plus 0.025% TritonX-100 for 5 minutes, twice, with gentle agitation. Antigens were blocked with 1% Bovine serum albumin (BSA) in TBS incubating at room temperature for 2 hours, before adding the SPARC mouse monoclonal IgG_{2B} primary antibody (Santa Cruz biotechnology, Texas USA, SC:398419, Lot #A2618) diluted 1:50 in TBS with 1% BSA. After incubating overnight at 4°C slides were rinsed twice in TBS plus 0.025% Triton X-100 for 5 minutes with gentle agitation. They were then incubated in 0.3% hydrogen peroxide in TBS for 15 minutes, before the IgG-HRP-conjugated goat anti-mouse secondary antibody (Santa Cruz biotechnology, Texas USA, SC: 2031, Lot #G1715), diluted 1 in 500 in TBS with 1% BSA, was added to the slide and incubated at room temperature for 1 hour.

The stain was developed with diaminobenzidine (DAB) for 10 minutes at room temperature.

Chapter 5 – Results and Discussion - Resections and Blood

Pancreatic cancer presents an increasing mortality burden, arising from late diagnosis and a high rate of recurrence of disease.(1) An insidious onset of non-specific symptoms as well as the invasive nature of current diagnostic methods means many patients present late, with a cancer which is non-resectable.(1) Current diagnostic and pathological methods also show limited in accuracy in the detection and diagnosis of pancreatic cancer.(105) While surgical resection can be curative, even after resection many cancers recur, potentially because the tumour margin is difficult to identify.(1, 37, 38) This presents the need for the application of a new method which is both able to differentiate healthy and cancerous tissue more accurately and could be used in a clinical setting.

Raman spectroscopy has been shown to be able to identify a number of cancers, although its application to pancreatic cancer is very limited.(91) The current literature differentiating healthy pancreas from that which is diseased, using Raman spectroscopy, does so using animal models and there is no literature showing differences between healthy and cancerous tissue in the exocrine pancreas.(95, 96)

This chapter displays the results of the use of Raman spectroscopy on human tissue resections, to identify differences between healthy and cancerous tissue. It further shows the results of Raman spectroscopy on blood samples from patients with pancreatic cancer and the differences identified in these samples. These results aim to demonstrate the utility of Raman spectroscopy to analyse both fresh and fixed human pancreatic tissue, in a way which, with further research, could be used in the screening, diagnosis and detection of tumour margins in pancreatic cancer.

In line with the hypothesis for this study, these results show Raman spectroscopy is able to differentiate healthy and cancerous human tissue in the exocrine pancreas as well as identify variation between blood samples from patients with different types of pancreatic cancer. This provides the basis for further research which could promote the application of Raman spectroscopy to clinical practice.

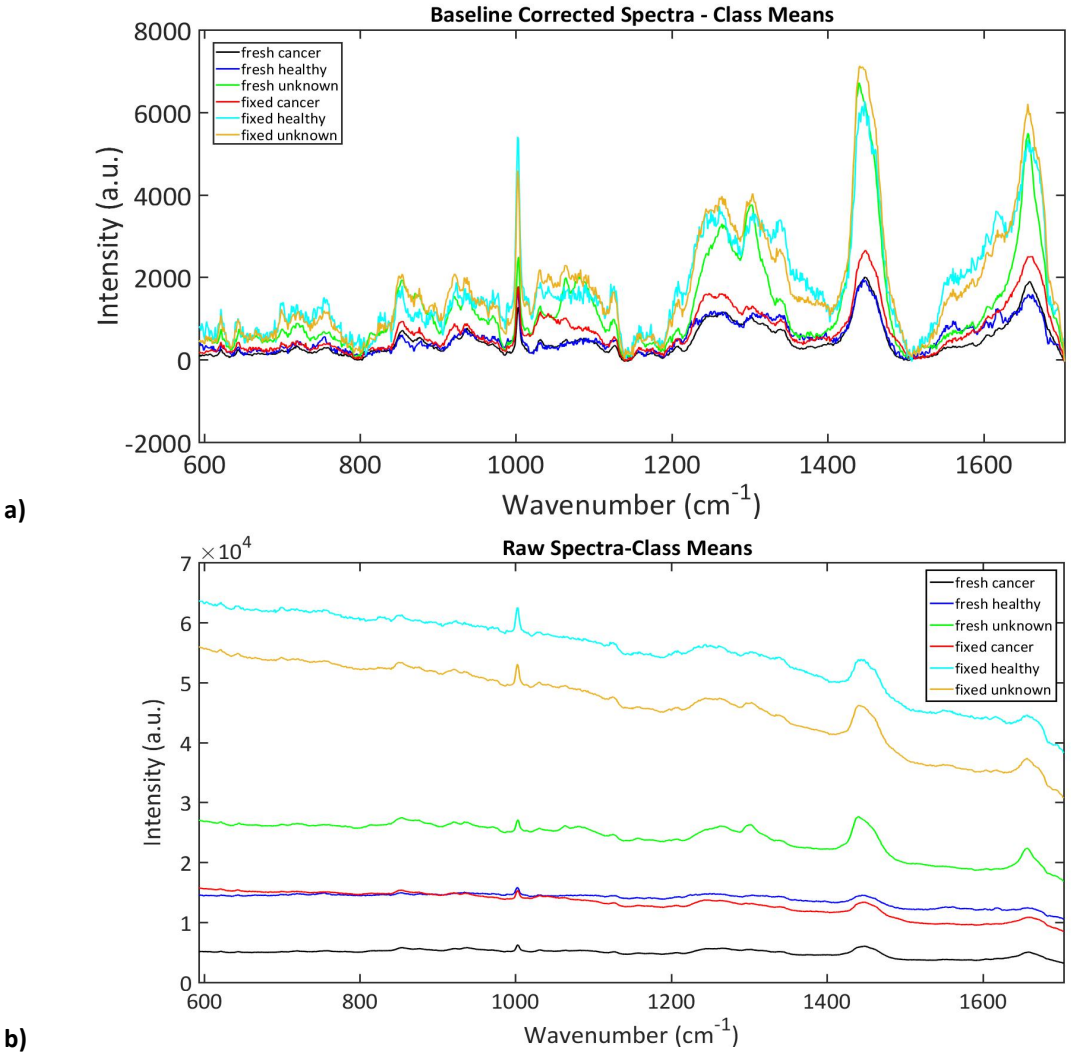

Figure 12:Spectra for resections from all patients classed by methods of sample preparation (fresh and fixed) and cancer status (cancer, healthy, unknown) a) Raw spectra b) Baseline corrected spectra (polynomial order 6)

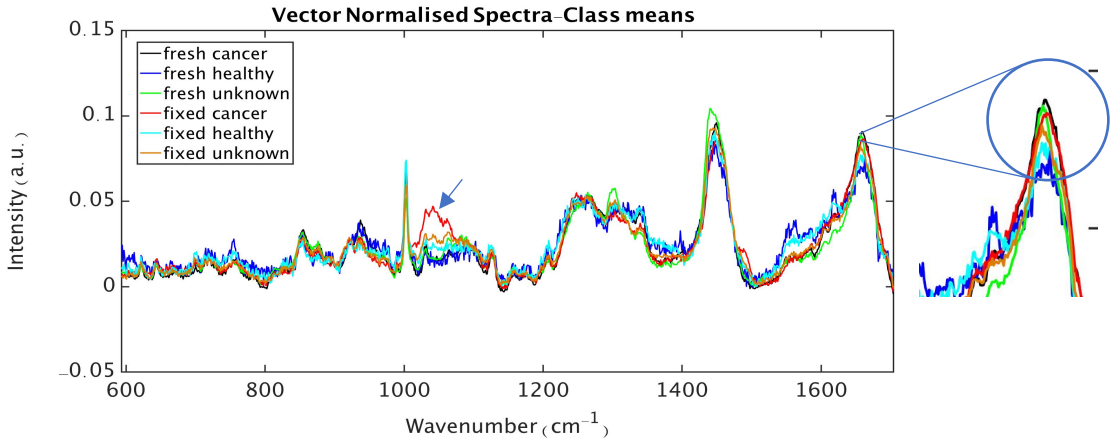

Figure 13: Vector normalised average spectra (polynomial order 6) data for resections from all patients classed as by method of sample preparation (fresh and fixed) and cancer status (cancer, healthy, unknown). The peak at 1662cm^{-1} is visibly higher in fresh cancerous tissue, than in healthy or unknown tissue. Arrow shows collagen peaks which is higher in fixed cancerous tissue than healthy or unknown tissue.

Initial observation of spectra suggests a significant difference in fluorescence between cancerous and non-cancerous tissue, with fresh tissue less fluorescent than fixed tissue, and the greatest fluorescence seen in the tumour margin and normal tissue (Figure 12a). This is to some degree surprising as cancer tissue contains collagen I, which is naturally fluorescent, whereas the data shows normal tissue to be more fluorescent than the cancer tissue. Although this is not a result of the Raman signal and can be removed though baseline correction, the very clear differences in fluorescence suggest that fluorescence may also be a useful way of differentiating cancer from normal tissue.

After both baseline correction and vector normalising there are still visible differences in the peaks between classes, suggesting Raman may also give important information about differences between cancer and normal tissue. (Figure 13)

5.1 Cancer Differences

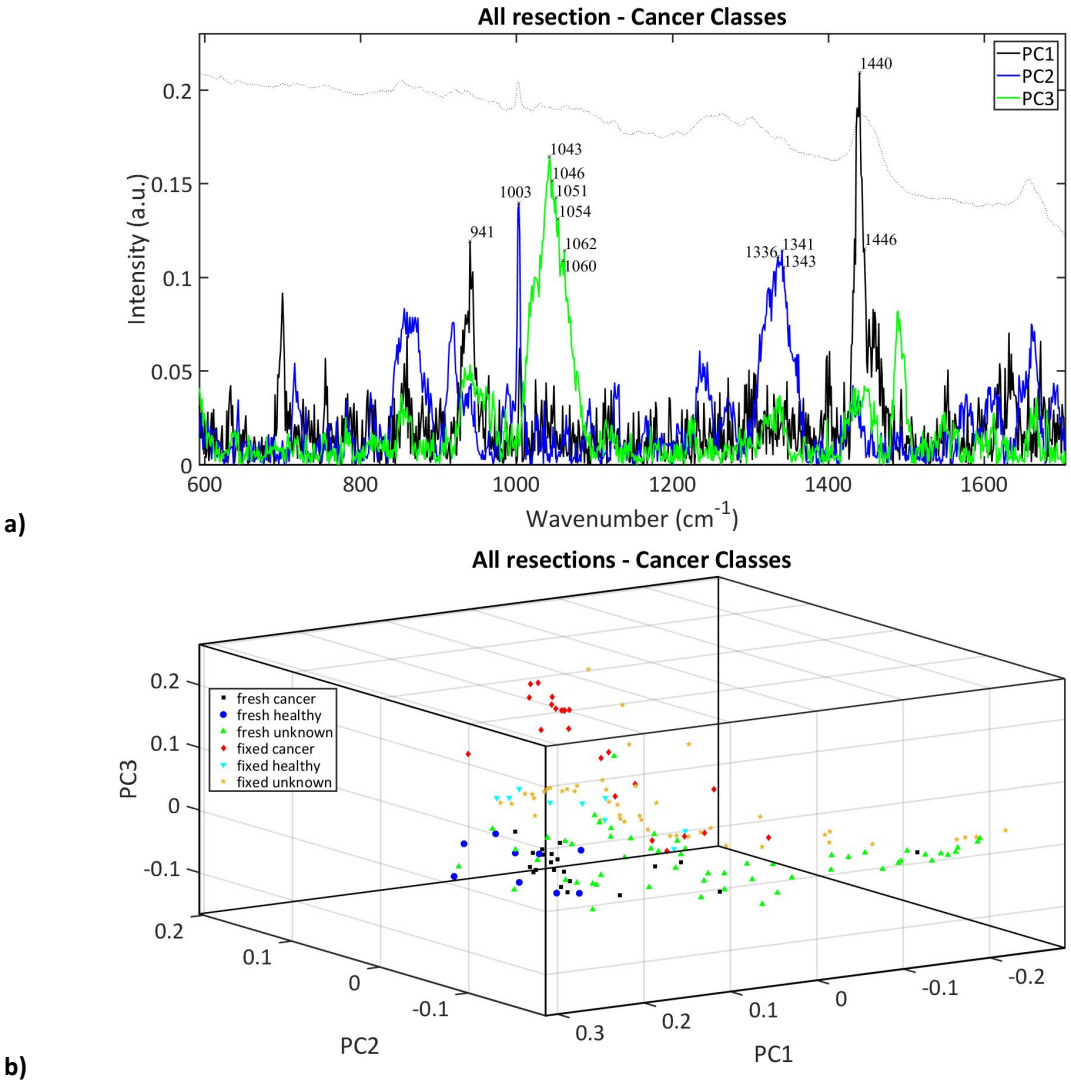

Figure 14:PCA of all resection spectra, classed by visible presence of cancer a) PCA loadings plot for all resections, b) PCA scores plot for all resections

Along PC1 there is a cluster of cancer spectra, suggesting PCA is able to differentiate based on malignancy of tissue, regardless of whether tissue is fixed (Figure 14b). It is worth noting that there was variation in cancer types between patients, both in the location of the tumour and histological cancer type, which may account for some of the heterogeneity in cancer and normal tissue classes. There is separation between fresh and fixed tissue along PC3, showing variation, as expected, in the collagen region of peaks (Figure 14). After separating fresh and fixed tissue, and classing by the presence of cancer, differences between cancerous and normal tissue were clearer. It is also difficult to attribute peaks and causes of variation to the presence of cancer or

to the method of sample preparation without first identifying the impact of fixing the tissue.

5.2 Fresh vs Fixed

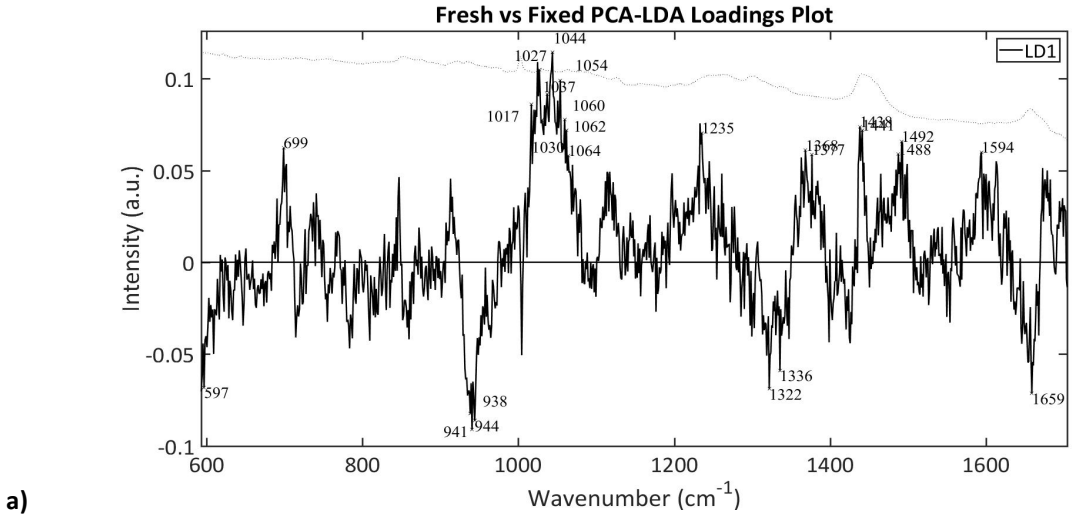

a)

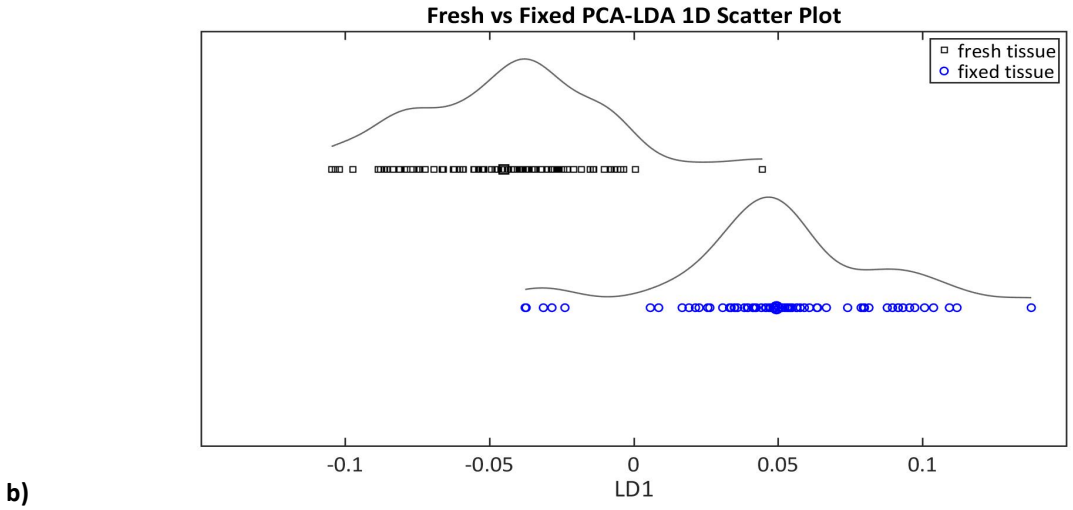

b)

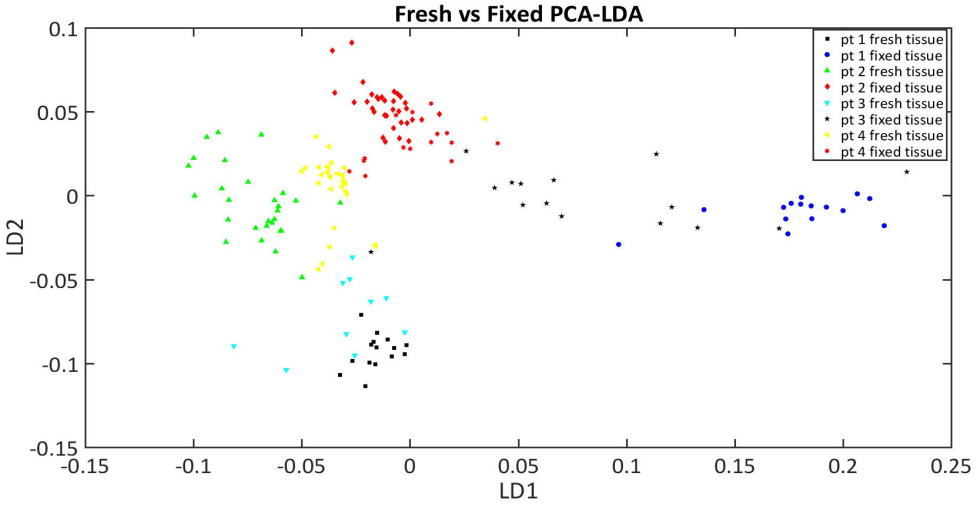

c)

Figure 15:PCA-LDA showing differences between fresh and fixed tissue a) PCA-LDA loadings plot, b) PCA-LDA Scatter plot, fresh versus fixed tissue, c) PCA-LDA scores plot

PCA-LDA analysis shows differences between fresh and fixed tissue (Figure 15). The most significant of the differences are in the collagen peaks, with particular changes to phenylalanine of collagen (1030cm^{-1}) proline (1044cm^{-1}) C-O or C-N stretching in protein (1054cm^{-1}) and skeletal C-C stretching (1060cm^{-1}, 1064cm^{-1}) (Figure 15a).(106) This is expected as formalin fixes tissue by inducing covalent bonds causing cross-linking of proteins,(100) and suggests that the fixing process alters these proteins to the greatest degree. As such significant differences can be seen due to methods of sample preparation, all further analysis was done with fresh and fixed tissue separately.

While clusters of spectra taken from individual patients are well defined and largely distinct, there is spread of the data both between classes and within them, suggesting Raman spectroscopy can identify differences both between patients and within patients. The latter could suggest identification of differences due to cancer type or grading, as some samples contained spectra from both healthy tissue and cancer tissue.

5.3 Patient Differences

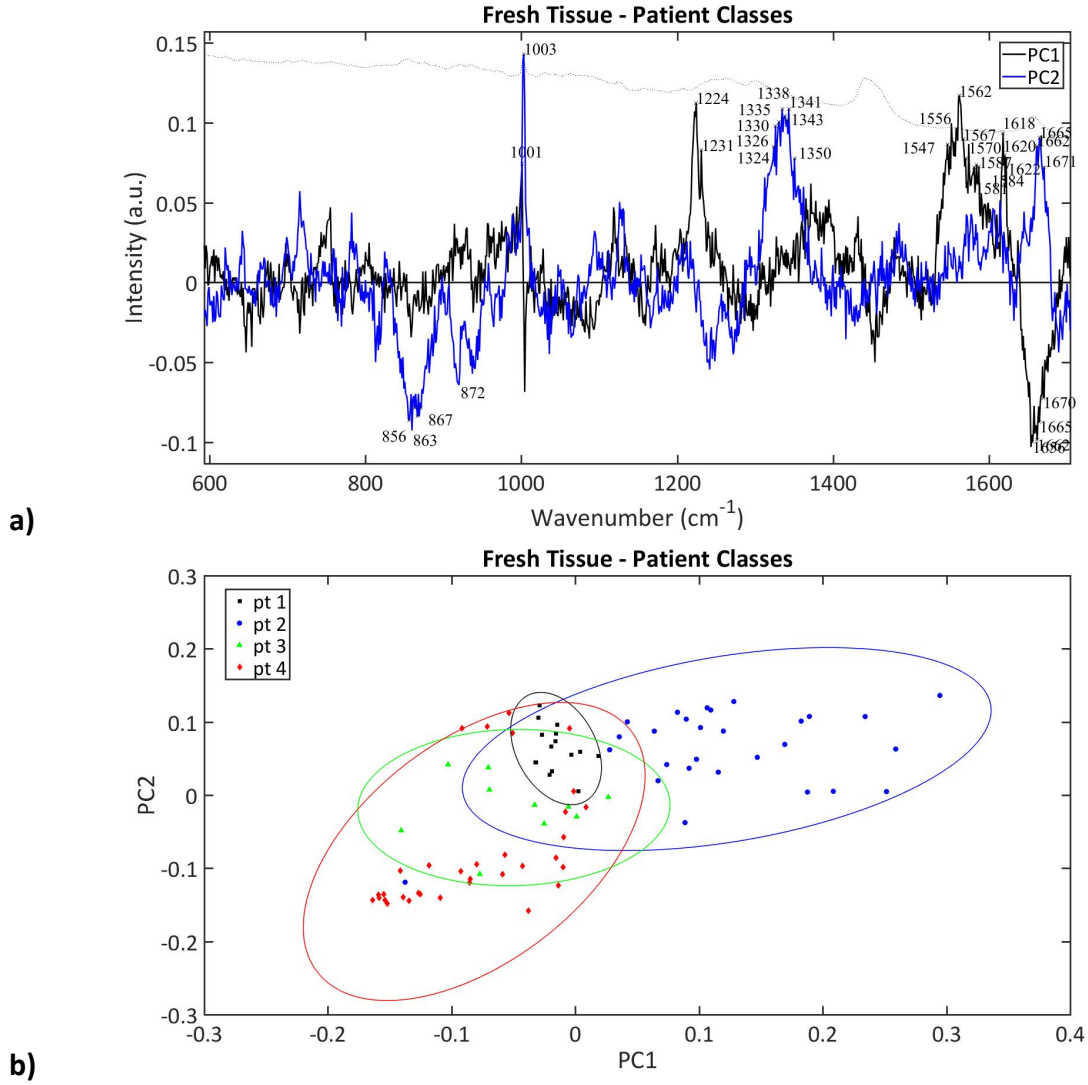

Figure 16:PCA of fresh tissue; 'pt' indicates 'patient number' a) PCA loadings plot for fresh resection tissue, b) PCA 2D scores plot for fixed tissue, with 95% confidence ellipses.

PCA shows Raman spectra can be used to identify clear variation between patients. Confidence intervals (95%) suggest the homogeneity of cancer tissue (Figure 16b); patient 1's sample was only cancer tissue, with no tumour margin in the sample. This can also be identified as the spectra for Patient 1 are much more tightly clustered, with the smallest confidence ellipse of all samples. Patients 2 and 3 show the greatest variation within the patients; these also had the largest grossly visible tumour margin of the received samples (Figure 16b), suggesting there is also likely to be variation along the tumour margin, due to differences in the tissue type itself.

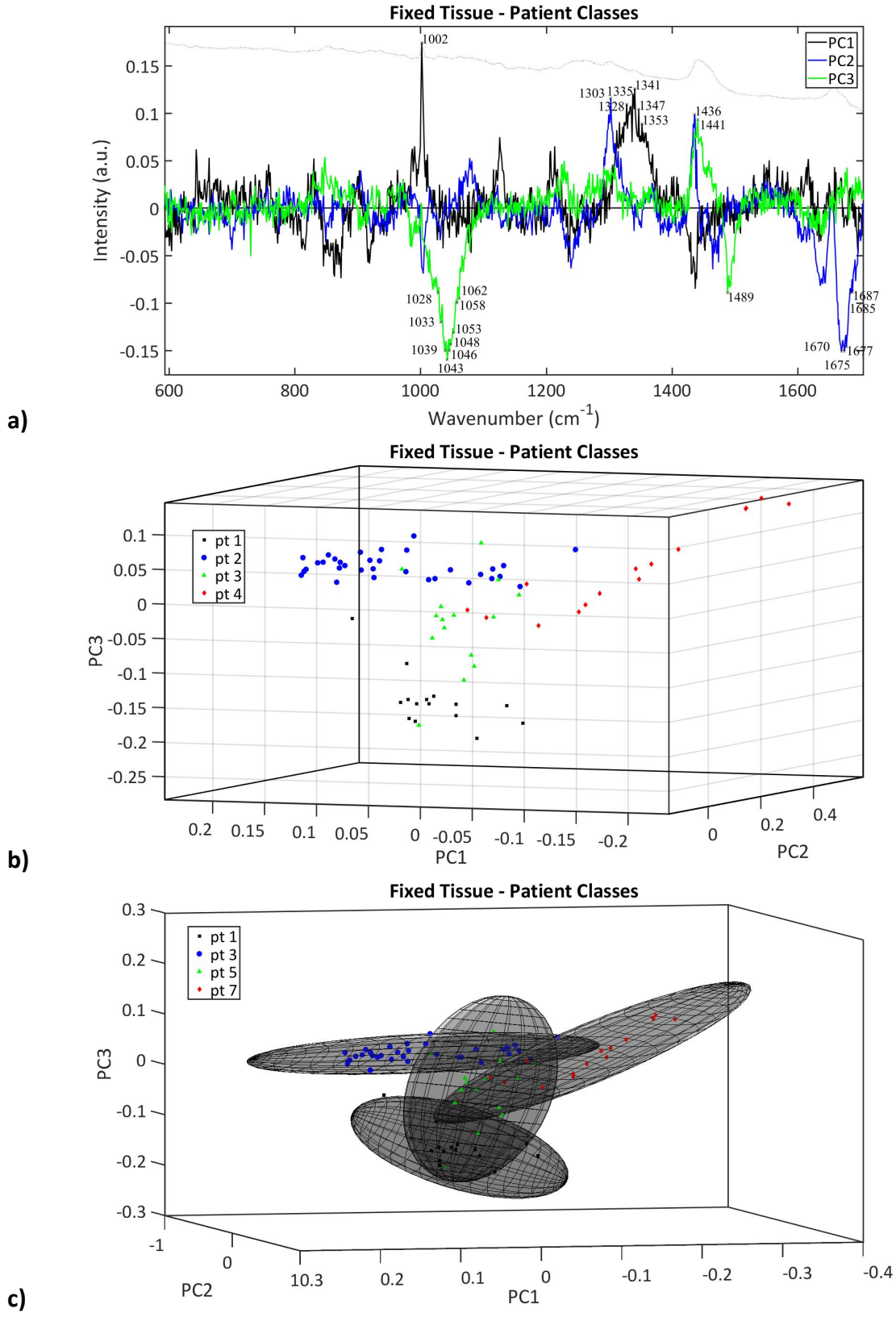

Figure 17:PCA of fixed tissue; 'pt' indicates 'patient number' a) PCA loadings plot for fixed resection tissue, b) PCA 3D scores plot for fixed tissue, c) PCA 3D scores plot for fixed tissue with 95% confidence ellipses.

Interpatient variability can be identified more clearly in fixed tissue than fresh tissue. When viewed with 95% confidence ellipses, patients, 1,2 and 4 appear as distinct groups, showing PCA analysis to able to clearly differentiate between these patients (Figure 17c). There is clear separation between patients 2 and 4 along PC1, and between patient 1 and 4 along PC2 (Figure 17b). Patient 3 has greatest overlap with other patients; anatomically this was the only body/neck tumour (Figure 17c). The greater degree of overlap between patient 3 and 4, compared to the overlap between patient 3 and patients 1 and 2, may be a result of both patients 3 and 4 having ductal adenocarcinomas, whereas patients 1 and 2 had undifferentiated tumours.

Patients 1, 2 and 3 also separate most clearly along PC3, showing differences in the 1028-1062cm^{-1} range of peaks, attributed to mostly to variations in collagen including, collagen content, (1033cm^{-1}) and proline (collagen assignment) as well as (1043cm^{-1}), C-O or C-N stretching in proteins (1053cm^{-1}) (Figure 17a). This may be due to the differences in cancer type, or the fact that patient 1's tissue was only cancer tissue, whereas patients 2 and 3 had the greatest amount of healthy tissue and tumour margin. There is also less separation between patient 1 and 3, both of whom had incomplete resections and so no completely healthy tissue, suggesting there is potential for Raman spectroscopy to identify differences between healthy and cancerous tissue. Patients 1, 2 and 3 also had different cancer types, which could suggest that Raman spectroscopy may also have the potential to differentiate between cancer types in pancreatic cancer, as well as between healthy and cancerous tissue. However, along PC3 there is greater similarity between spectra taken from patient 4 and patient 2 than between patient 3 and 4 (Figure 17b). This is despite the fact that both patient 3 and 4 had a ductal adenocarcinoma, whereas patient 2 had an undifferentiated carcinoma with osteoclast-like giant cells, suggesting the variation along PC3 may be contributing more to the differentiation between cancerous and normal tissue than histological type of cancer. The fact that spectra from patients 2 and 4 were most similar and these were only 2 patients with complete resections adds weight to this theory, as the similarity may be a result of the presence of healthy tissue, which was only present in patients 2 and 4.

There is also a glycogen (1048cm^{-1}) peak, contributing to PC3, which is surprising as the pancreas does not ordinarily store glycogen (Figure 17c). This may therefore be a marker of malfunction or a characteristic of the types of malignant cells. Alternatively, it may be related to the fact that patients are fasted preoperatively and so related to the pancreas' role in releasing glucagon to convert glycogen to glucose, when blood sugar levels are low.

The differences between patients, particularly between patients 2 and 4, based on PC1 are due to variations in 1335cm^{-1} showing differences in the CH_3CH_2 wagging in collagen and nucleic acid and 1341cm^{-1} showing the presence of an A or G in the DNA (Figure 17a).(10) While these differences may be due to differences in the patients themselves, as the patients had differing tumour types some of the difference could also be attributed to cancer type; it is likely that both factors contribute to some degree but it is difficult to assess the degree of contribution of each factor with such a small sample.

5.4 Cancer Differences

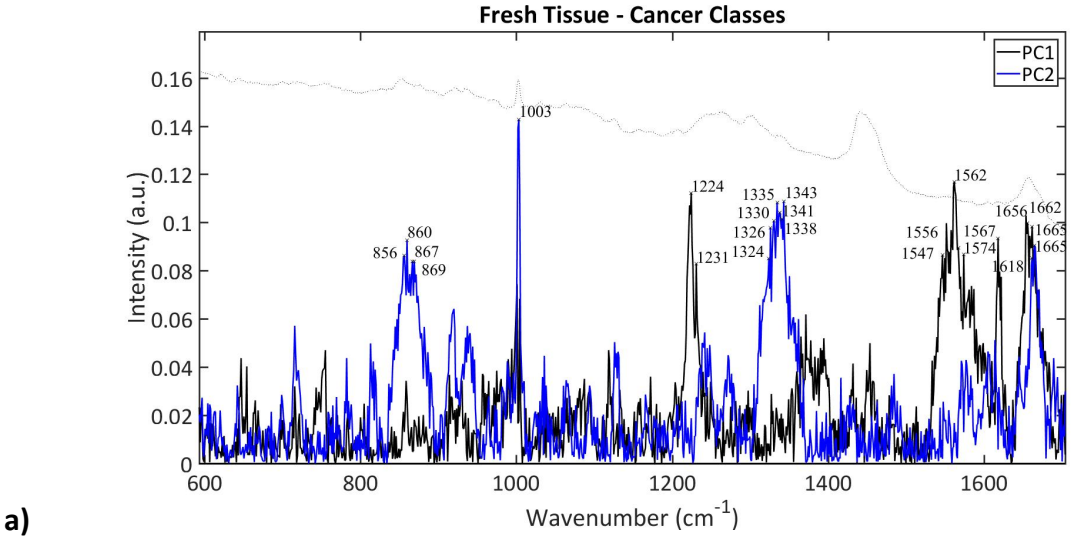

a)

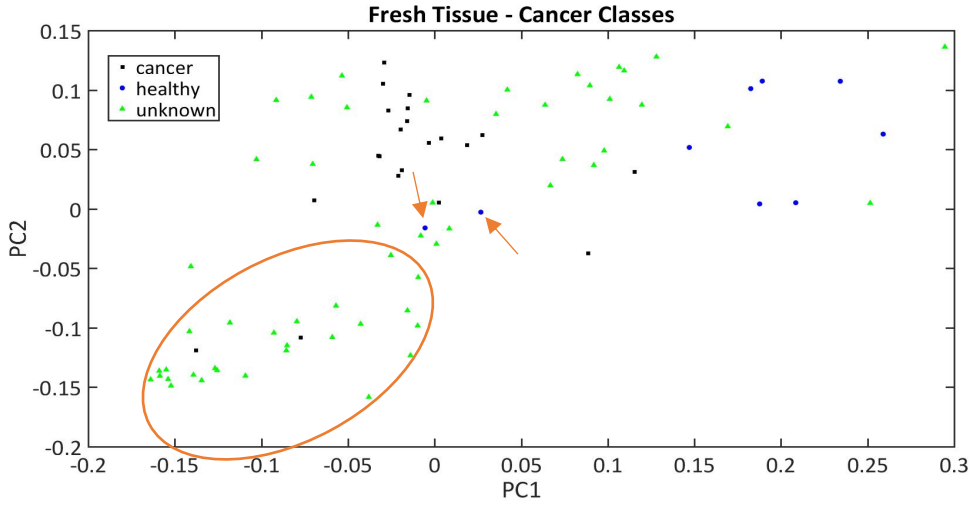

b)

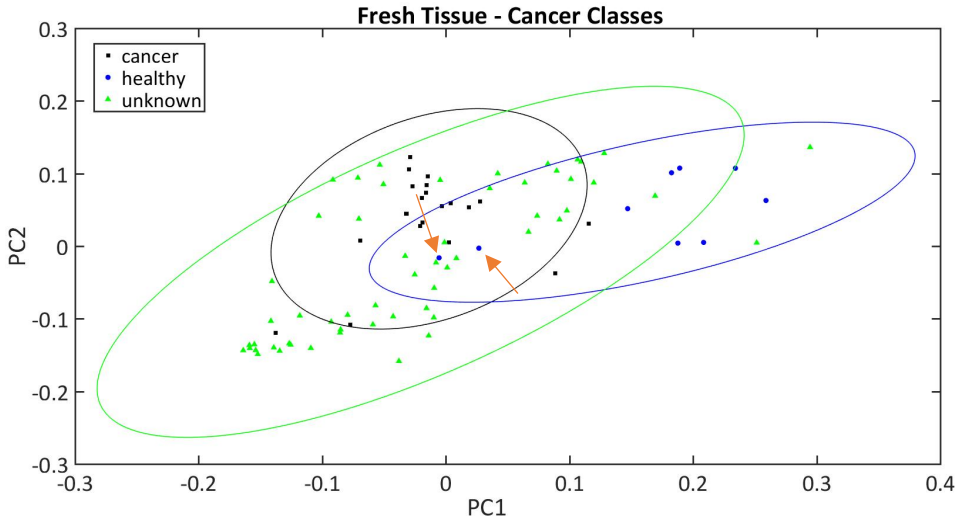

c)

Figure 18:PCA of fresh tissue classed by visible presence of cancer a) PCA loadings plot b) PCA 2D scores plot for fresh tissue, Circled – cluster of spectra, separating on PC1 and PC2, which could be a class in its own right c) PCA 2D scores plot with 95% confidence ellipses. Arrows show 2 spectra from normal tissue which overlap with cancerous tissue.

For fresh tissue, there is clear clustering of cancerous and normal tissue, with the greatest variation in the tumour margin. Despite the overlap of the 95% confidence intervals, there is clear separation of the normal and cancerous tissue, except 2 spectra (arrows in Figure 18b and 18c). There is also overlap between areas of unknown tissue and cancer tissue and similarly between areas of normal and unknown tissue, which suggests using Raman enables us to identify where tissue is malignant, which cannot be identified by observation of the gross features, by eye, of pancreatic cancer alone. Similarly, the 2 spectra from normal tissue which overlap with the cancerous tissue could be malignant but without an obviously gross appearance of malignancy.

As the classes were separated by eye, based simply on the appearance of cancer being whiter and more sclerotic than normal tissue, and the resection samples were small, there could be differences in opinion on which areas were definitely cancer and which were not, based on operator experience. While histological examination may give a more specific inclination of the tumour margin and which areas are cancer and normal, there is always some inter-operator variability and opinions are, to some degree, subjective. Raman spectroscopy may also be a much faster method of achieving a similarly specific classification as it requires minimal sample preparation, unlike histological techniques. The greater degree of variation in the tumour margin/unknown tissue, is expected as this area of tissue is likely to be the most heterogeneous, with some areas at a more advanced premalignant stage than others.

Along PC1 there is clear separation of cancer and normal tissue with a cluster of tumour margin spectra in between (Figure 18b). This suggests that there is separation of cancerous and normal tissue due to differences in the proline and COO^- bonds (Figure 18a). The peak at 1556cm^{-1} may also suggest some differences in tryptophan and various regions of amide II, although these are usually assigned to a peak at 1554cm^{-1} or 1558cm^{-1} (Figure 18a).(107) Similarly, the peak at 1574cm^{-1} may suggest variation due to the presence of guanine or adenine, ordinarily seen at 1573cm^{-1}, or ring breathing modes in the DNA bases, previously seen at peak 1575cm^{-1} (Figure 18a).(107) The peak at 1662cm^{-1} is associated with nucleic acid modes, thought to

indicate the presence of nucleic acid content in tissues (Figure 18a).(107) The raw spectra after pre-processing show a greater intensity of this peak in cancerous tissue than in healthy tissue (Figure 13).

However, there also appears to be a cluster on the far left of the graph (circled Figure 18b) which separates on both PC1 and PC2, which could be a class in its own right. The tumour margin spectra, along PC2 could be seen as 2 separate clusters, suggesting within the tumour margin there may differences based on premalignant changes which can be identified using Raman spectroscopy.

For this cluster (circled in Figure 18b) the separation on PC2 appears to be due differences in the phenylalanine peak and peaks associated with changes in the collagen and nucleic acid regions (Figure 18a). Changes in the 1325 – 1330cm^{-1} region and at 1335cm^{-1} and 1343cm^{-1} are associated with the purine bases of nucleic acids and twisting or wagging of CH_3CH_2 in collagen, with the 1335cm^{-1} peak more specific to the protein assignment of collagen.(107) The peak at 1341cm^{-1} suggests the presence of an A or G of DNA and the peak at 1665cm^{-1}, seen as contributing to the variation both along PC1 and PC2, is due to the presence of amide I, often in collagen. (107) These differences would be in line with the premalignant changes or indicative of a more advanced tumour that could be expected in pancreatic cancer as it is known that the cancer stroma contains collagen and malignant changes cause change to the protein and DNA structures in cells.

There was minimal separation of fresh tissue along PC3 (PCA scores and loadings plots not shown). The loadings plot however, shows variation along PC3 to be based on changes in the nucleotide conformation region, 600-800cm^{-1}, of peaks.(107) Although this variation is minimal on the scores plot, it may be of great importance as identifying changes to the DNA could be imperative in gaining a better understanding of the development of PDAC and also identifying the changes in DNA before phenotypic changes arise. This could allow for earlier detection and give more information about tumour margins during and after surgical resection.

The other peaks along PC3, at 596cm^{-1}, 609cm^{-1} and 614cm^{-1} suggests the presence of phosphatidylinositol, a family of lipids in the class of phosphatidylglycerides, and cholesterol.(107) Peaks at 662cm^{-1} and 665cm^{-1} suggest C-S stretching mode of cysteine in collagen type I and at 700cm^{-1} the presence of the amino acid methionine, (107) which may again be important changes. Despite there being minimal spread of data along PC3, the importance of these peaks could be identified more easily and associated more strongly with differences due to cancerous changes or differences between patients, with a bigger sample size.

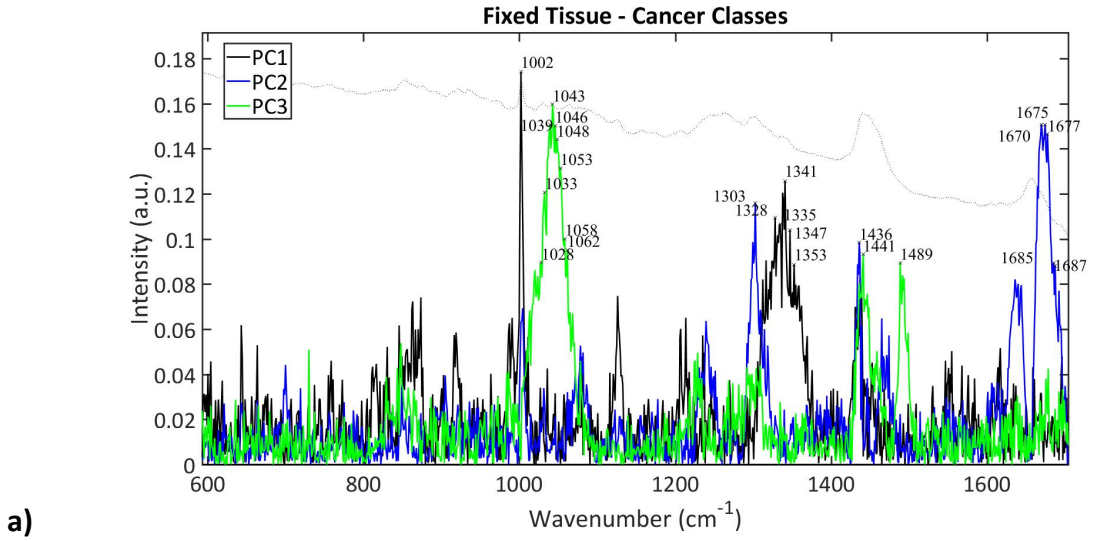

a)

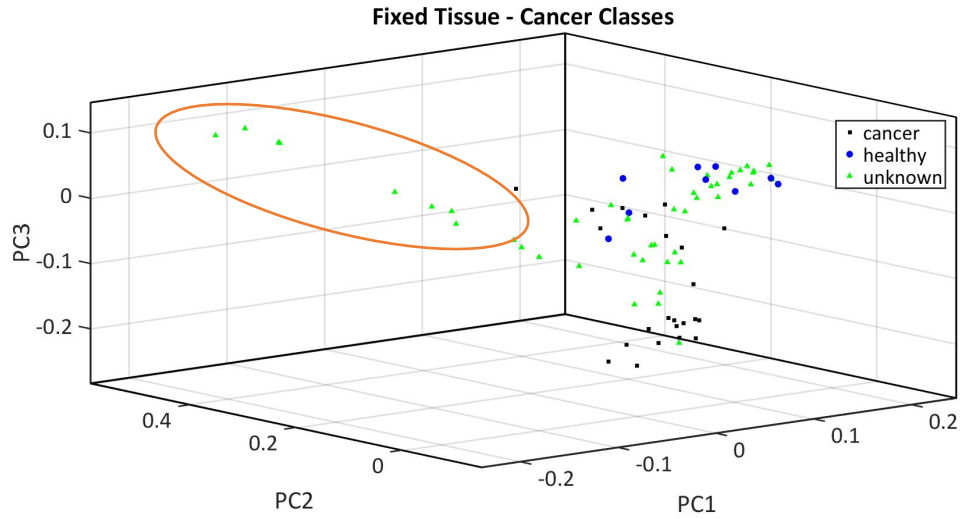

b)

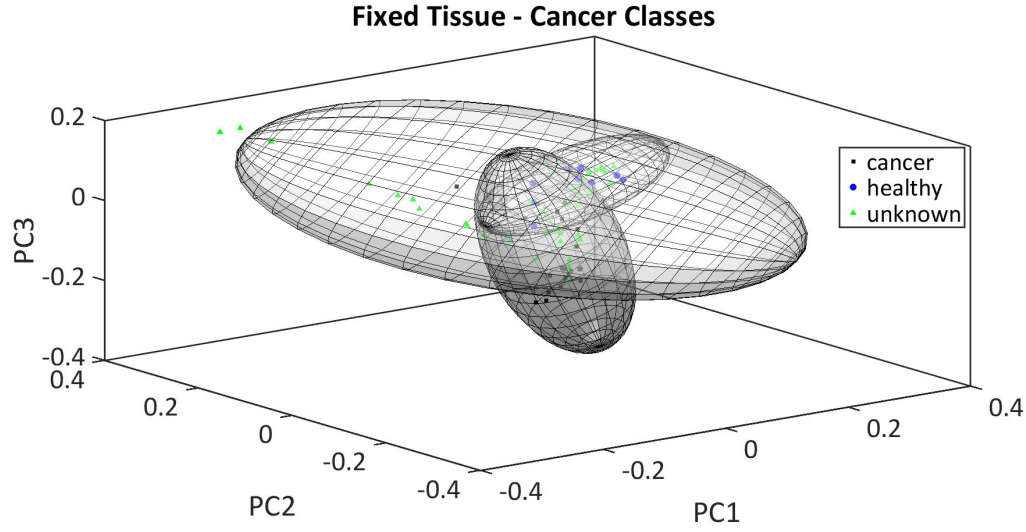

c)

Figure 19: PCA of fixed tissue classed by visible presence of cancer a) PCA loadings plot b) PCA 3D scores plot for fixed tissue, Circled – separation of unknown spectra along PC2 c) PCA 2D scores plot with 95% confidence ellipses.

Differences between cancer and normal tissue separate most clearly along PC3, (Figure 19) with differences due to collagen; a variation which may be enhanced by fixation due to the increased presence of collagen in cancer tissue. The peak at 1053cm^{-1} also suggests variation in the C-O and C-N stretching in proteins (Figure 19a).(107)

There is no identifiable clustering in the variation along PC1, when the tissue classed by the presence of cancer. However, the fixed tissue identifies differences between patients along PC1, with confidence intervals showing little overlap, when the tumours were classed based on the patients (Figure 17). There is some separation of some of the unknown spectra along PC2 (circled Figure 19b) and this appears to be due to differences in the CH_3CH_2 twisting in the collagen shown by the peak at 1303cm^{-1} and in the purine bases of nucleic acids shown at the peak at 1328cm^{-1} (Figure 19a).(107) Some of the differences along PC2 are also due to differences in the amide I and lipid regions. A comparison to the classes in Figure 17 shows that these spectra were taken from patient 4. This area of clustering therefore, may be because patient 4 was the only patient with a stage IIb cancer; tumour >20mm and limited to the pancreas (T2) tumour but also involving local lymph nodes (Table 2). All other patients had larger (T3) tumours, with invasion of local tissues but not involving local lymph nodes (Table 2), which suggests Raman spectroscopy was able to identify and differentiate a tumour which had spread to lymph nodes from those which had invaded local tissues.

5.5 Blood

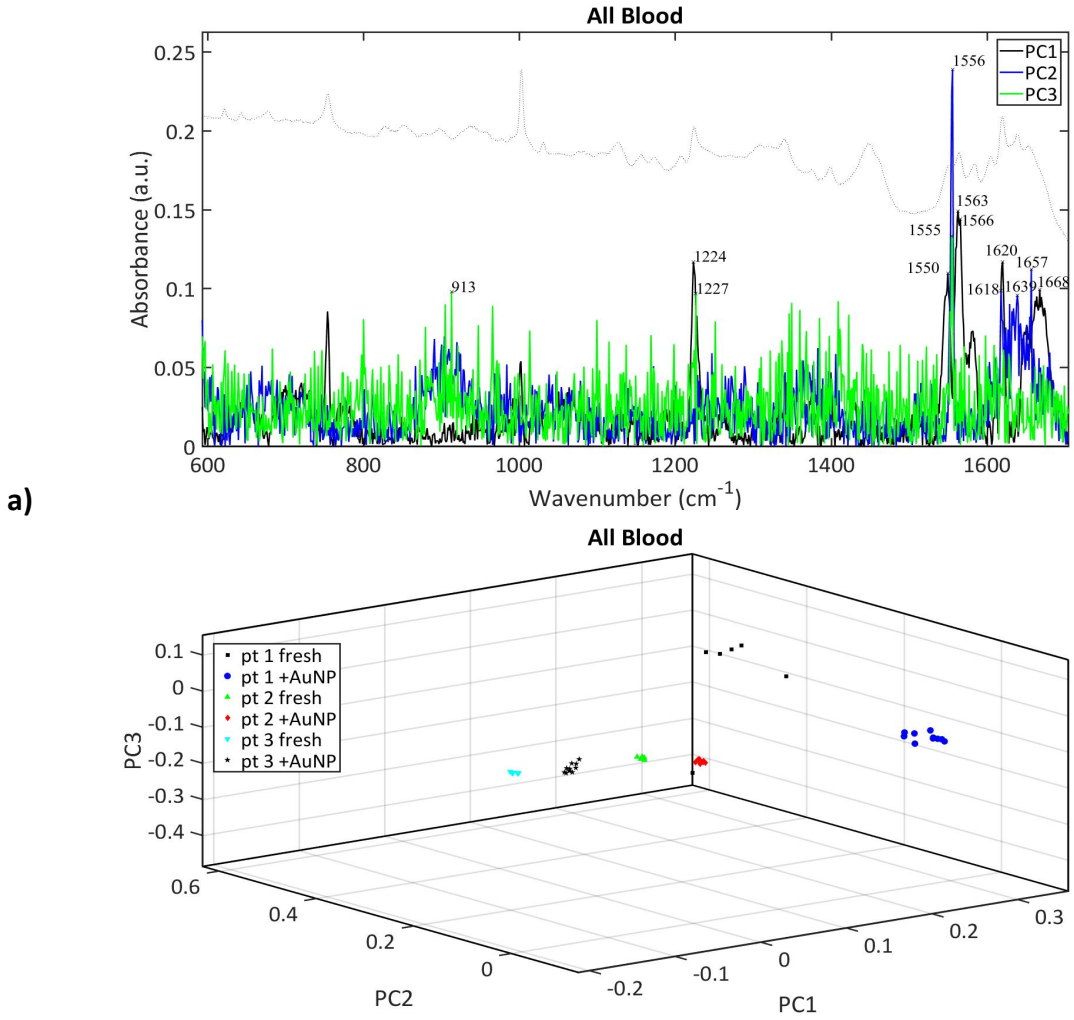

Figure 20: PCA of blood sample, classed by patient (pt) and the addition of 60nm gold nanoparticles (+AuNP) for SERS measurements, a) PCA loadings plot, b) PCA 3D scores plot

PCA analysis shows separation on PC1 which appear to be dependent on patient characteristics and separation on PC2 dependent of the addition of AuNP (Figure 20b). The addition of AuNP creates differences in the tryptophan or amide II range of peaks (Figure 20a).(107) Peaks at 1556cm^{-1} and 1563cm^{-1}, showing the greatest contribution to PC2 on the loadings plot, don't have a definite assignment to a chemical bond (Figure 20a). Interestingly, the greatest variation within a single patient occurs in patient 1, after the addition of AuNP (Figure 20b). This blood sample was the only sample of serum as opposed to whole blood, suggesting the addition of AuNP may have a greater impact in highlighting differences in serum due to sample preparation, potentially because of the colour and optical properties of serum.

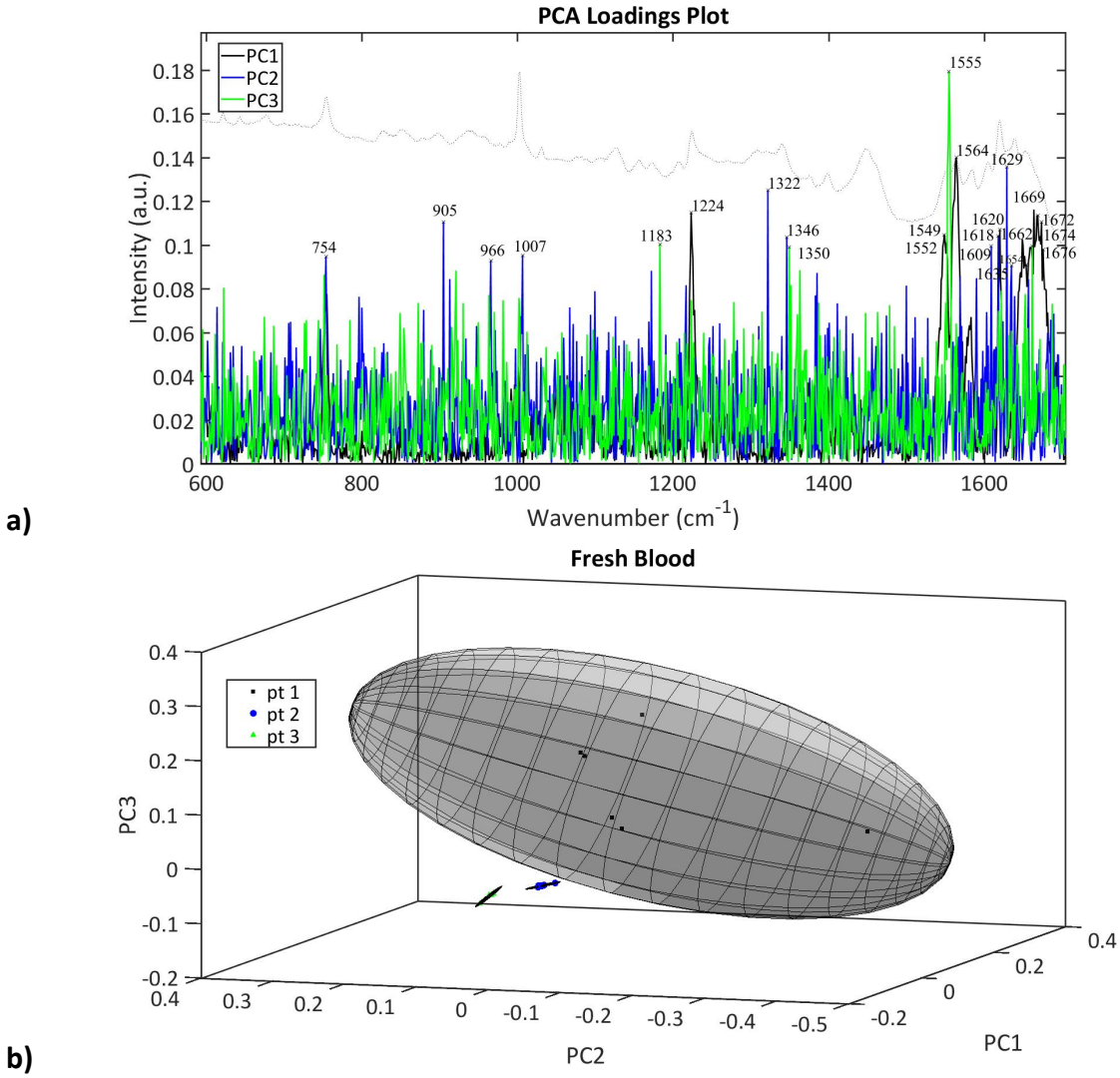

Figure 21:PCA of fresh patient (pt) blood. A) PCA loadings plot b) PCA 3D scores plot with 95% confidence ellipses

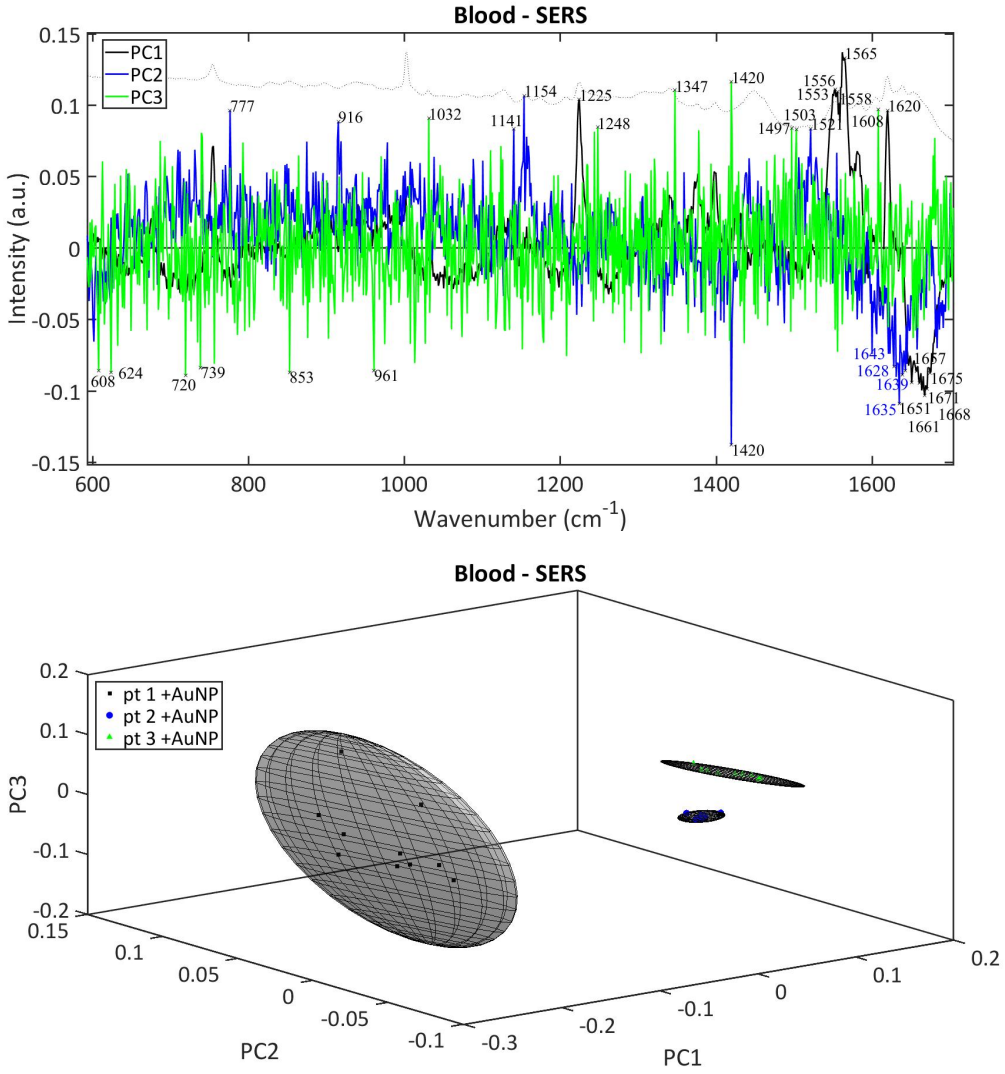

Figure 22:PCA of patient (pt) blood with 60nm gold nanoparticles added for SERS measurements (+AuNP). A) PCA loadings plot b) PCA 3D scores plot with 95% confidence ellipses

Comparison of the scores plots shows that the general trends in the data are the same with and without the addition of AuNP; differences between patients are separated along PC1 and the heterogeneity in patient 1's serum sample is separated along PC2 and PC3 (Figure 21b, Figure 22b). The addition of AuNP brings out a degree of separation between patients 2 and 3 along PC3 (Figure 22b). The average spectrum for blood samples with nanoparticles shows fewer clear peaks and a marginally lower intensity than blood samples without the addition of AuNP. This is surprising as the addition of nanoparticles ordinarily increases the Raman signal by creating hotspots. Patient differences are clearly evident from PCA of blood samples.

Differences between patients' blood samples could be identified with and without the addition of nanoparticles.

Spectra taken from a serum sample from patient 1, show more heterogeneity within the sample, both with and without the addition of AuNP (Figure 21b, Figure 22b). This could be due to the fact that it was the only serum sample whereas patients 2 and 3 were whole blood samples. Equally, clinically, patient 1 was the only patient with a histologically undifferentiated (anaplastic or sarcomatoid) carcinoma, and so this clinical difference in tumour type may be reflected in the chemical properties of the patient's blood, as a result of secretion or excretion of a tumour related compound into the patient's blood. However, patient 2's sample shows less heterogeneity than patient 3 and this was an undifferentiated carcinoma with osteoclast-like giant cells, whereas patient 3 had a ductal adenocarcinoma (Table 2). Histologically, both were moderately differentiated (grade 2), whereas the grade of differentiation is unknown for patient 1 (Table 2). While a conclusion cannot be drawn from a single result, this would present an interesting opportunity with a much larger sample size to see if Raman spectroscopy could be used to predict or identify cancer types using serum samples, which could be pivotal in aiding and changing the diagnosis of pancreatic cancer, with the potential use of a much less invasive method.

The use of both Raman and SERS shows differences between patients most clearly along PC1 (Figure 21b, Figure 22b). This variation appears to be associated with the same peaks regardless of the use of SERS. These differences appear to be due to peaks at 1552cm^{-1} and 1558cm^{-1}, associated with tryptophan and at 1224cm^{-1}/1225cm^{-1} due to the β sheet structure of amide III (Figure 21a, Figure 22a).(107) The difference due to peaks at 1662cm^{-1} to 1676cm^{-1} are associated with differences in nucleic acid modes, cholesterol ester and C=C stretching or an amide I band (Figure 21a, Figure 22a).(107) There is also peak at 1564cm^{-1}/1565cm^{-1} which does not have a designated association.

A comparison of loadings plots for fresh blood (figure 21a) and blood with AuNP (Figure 22a) shows where differences by patient type are identified differently based

on the addition of the nanoparticles; some peaks are enhanced by the addition of the nanoparticles, particularly along PC2 and PC3 (Figure 22a). The contribution of intensity of peaks to the variation is similar in samples with and without AuNP, but the PCA identifies and attributes the variation to different wavenumbers dependent on the use of SERS.

In particular, the use of SERS highlights difference in peaks in the nucleotide conformation, cholesterol and DNA peaks along PC3 (Figure 22a).(107) The peak with greatest contribution along PC3, without the use of SERS, is at 1555cm^{-1}, which is likely to be associated with variation within patient 1's sample due to the presence of amide II. As there is separation between patient 2 and 3 along PC3, when using SERS, (Figure 22b) this could suggest the differences in interpatient differences in DNA and nucleotides are highlighted with the addition of AuNP. There is, however, also a spread of spectra, all taken from patient 1's sample, along PC3 (Figure 22b). As these spectra have all been taken from the same patient, it is unlikely that the essential DNA in the sample is varied, but subtle variations between components of the blood or cells, may have been identified. The utility of these variations could be of limited importance, if the information simply identifies between blood components and cells types. However, if this was the case it could be expected that there would be greater spread of patient 2 and 3 spectra along PC3, as these samples were whole blood, which include red blood cells as well as serum components, and so the extra components should show greater heterogeneity of these samples than the serum sample. As this heterogeneity was not seen with the whole blood samples it could be inferred that the differences along PC3 are not simply due to differences in blood components. Therefore, as patients 1, 2 and 3 all had different types of cancer, understanding whether the variation in nucleotides and DNA is due to differences between the patients, or differences between their cancer types, could be of great potential significance.

The spread of spectra along PC2, in both the fresh blood samples and those with AuNP, shows a spread within patients (Figure 21b, Figure 22b). The addition of AuNP was expected to give clearer spectra and acquire many different spectra, showing

where different components have been enhanced dependent on the presence of the nanoparticles. In the fresh blood, the variation within patient samples, appears to be due to differences in the symmetric breathing of tryptophan, shown on the PCA loadings plot at peak 754cm^{-1}, 966cm^{-1}, phenylalanine thought to be at peak 1007cm^{-1} and peak 1322cm^{-1} suggesting CH_3CH_2 deforming modes of collagen and the presence of nucleic acids (Figure 21a).(107) Further differences are shown due to peaks at 1609cm^{-1} thought to be associated with the presence of cytosine (NH_2), 1618cm^{-1} due to tryptophan and 1654cm^{-1} seen with a change in amide I (Figure 21a).(107)

The addition of SERS identifies variation due to different peaks, at wavenumbers 777cm^{-1}, 916cm^{-1}, 1032cm^{-1}, 1141cm^{-1} and 1154cm^{-1} and 1420cm^{-1} potentially attributed to phosphotidylinosotol, ribose vibration, CH_3CH_2 bending modes of collagen or the phenylalanine or proline of collagen, β carotenes and G,A in DNA/RNA or deoxyribose respectively (Figure 22a).(107) Peaks at 1635cm^{-1} (thought to be due to differences in collagen content), 1639cm^{-1}, and 1643cm^{-1} are also identified, with the addition of AuNP (Figure 22a). There is also some overlap between wavenumbers thought to attribute to the variation identified in the fresh blood samples and those using SERS, at peak 1628/1629cm^{-1}, associated with either C=C stretching or amide C=O stretching absorption in the β-form polypeptide films (Figure 21a, Figure 22a).(107)

These differences, along PC2, are likely to be differences in the blood components themselves, as there is a similar spread within each class, irrespective of the addition of AuNP. This is understandable as components such as β carotene (vitamin A), lipids, and proteins are components of blood which could be expected to vary dependent on the location in the sample from which the spectrum was taken.

5.6 Blood Vs resection

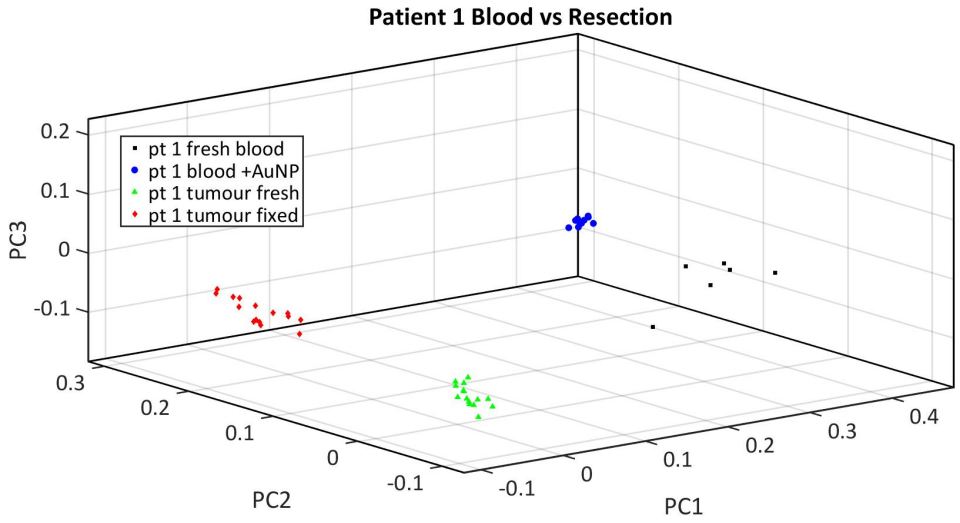

Figure 23: PCA of blood and resection samples from patient 1

Using PCA there was clear separation of blood spectra from resection spectra, with no overlap. This variation is expected as there are significant differences in the 2 tissue types. Finding correlations between components of the tumour and blood, which might suggest secretion or excretion of a tumour component into the blood might make interesting further work. However, these correlations cannot be identified using PCA and may require alternative data analysis.

5.7 Histology

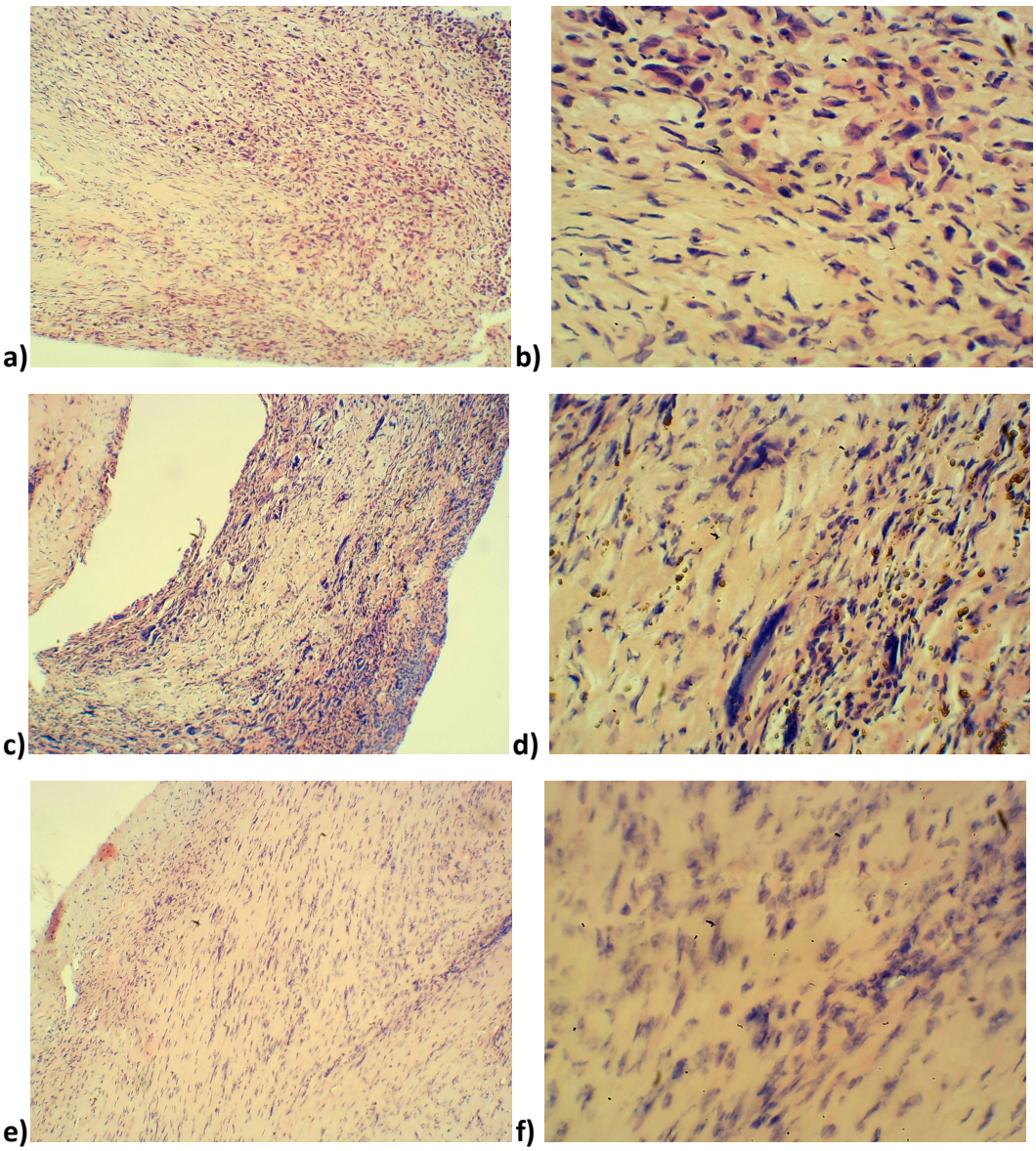

Figure 24:Histology images of cancerous resection tissue stained with haematoxylin and eosin a) patient 1 x10, b) patient 1 x40 c) patient 2 x10 d)patient 2 x 40 e)patient 3 x10 f)patient 3 x40

Haematoxylin and eosin staining shows the presence of stroma and morphology of cells in the tissue resections (Figure 24). The stroma is abundant in all resections. There is the visible presence of rounded cells with a large nucleus which are likely to be cancer cells as well as cells with a fibroblastic appearance, which are likely to be PSCs. There are no visible glands, which would also indicate the presence of cancer,

nor the presence of clear healthy pancreatic tissue, however the tissue was small and was unable to be sectioned to include both healthy and cancerous tissue.

Immunohistochemical staining was also performed on the tissue, however this did not show the presence of any SPARC antigen (Appendix, Figure 40). However, it is likely that this was due to faults in the technique as opposed to the lack of SPARC in the tissue itself. Therefore, it would be necessary to optimise the immunohistochemistry technique for these samples, including altering antigen retrieval time and optimising the dilution of the antibodies.

Chapter 6 – Results and Discussion – Cell Lines

The development of pancreatic cancer is an area which remains incompletely understood. Using 2D coculture models of HPAF-II and PSCs in varying proportions, Raman spectroscopy and ELISA are used to understand interactions between cancer cells and PSCs, identify changes to the cells and the quantify production of SPARC. Spectra taken from cocultured cell lines show potential to use Raman spectroscopy to identify differences between cell types as well as demonstrate changes which may occur due to the coculture environment.

Cocultures of HPAF-II and PSCs were set up with cells in direct and in indirect contact, at proportions of HPAF:PSC 25:75, 50:50 and 75:25 (Figure 25). Those in indirect contact were grown in a wells plate using a permeable insert, meaning cells could share media but there was no direct contact between cells. Spectra were taken from cells grown on CaF_2 slides and were pre-processed using baseline correction (polynomial order 6) and vector normalisation, before being analysed using PCA.

These results analyse interactions and relationships between cell types in different environments and at different proportions. The data suggests biochemical changes are occurring in cells dependent on their coculture environment and interactions, giving further insight into the development of pancreatic cancer and suggesting pathways which might stimulate or inhibit these changes. It aims to identify what some of these biochemical changes might be using Raman spectroscopy and creates a model and basis for further research into pancreatic carcinogenesis and progression.

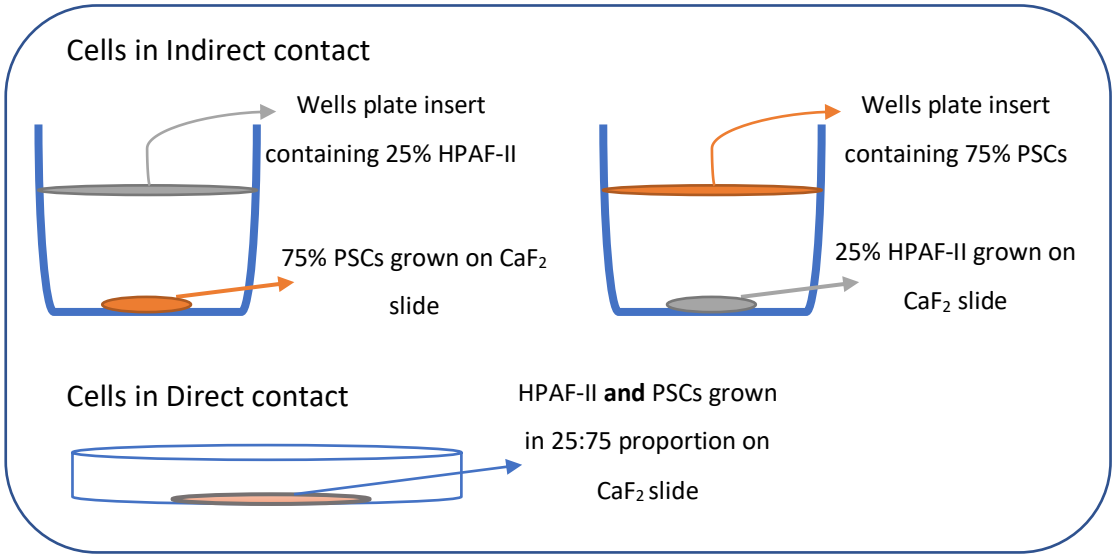

Figure 25:Diagram showing set up of coculture HPAF-II:PSC 25:75 in direct and in indirect contact. The same set up was used for HPAF:PSC 50:50 and 75:25 proportions. Spectra were taken from cells on CaF2 slides.

6.1 Cell Cocultures

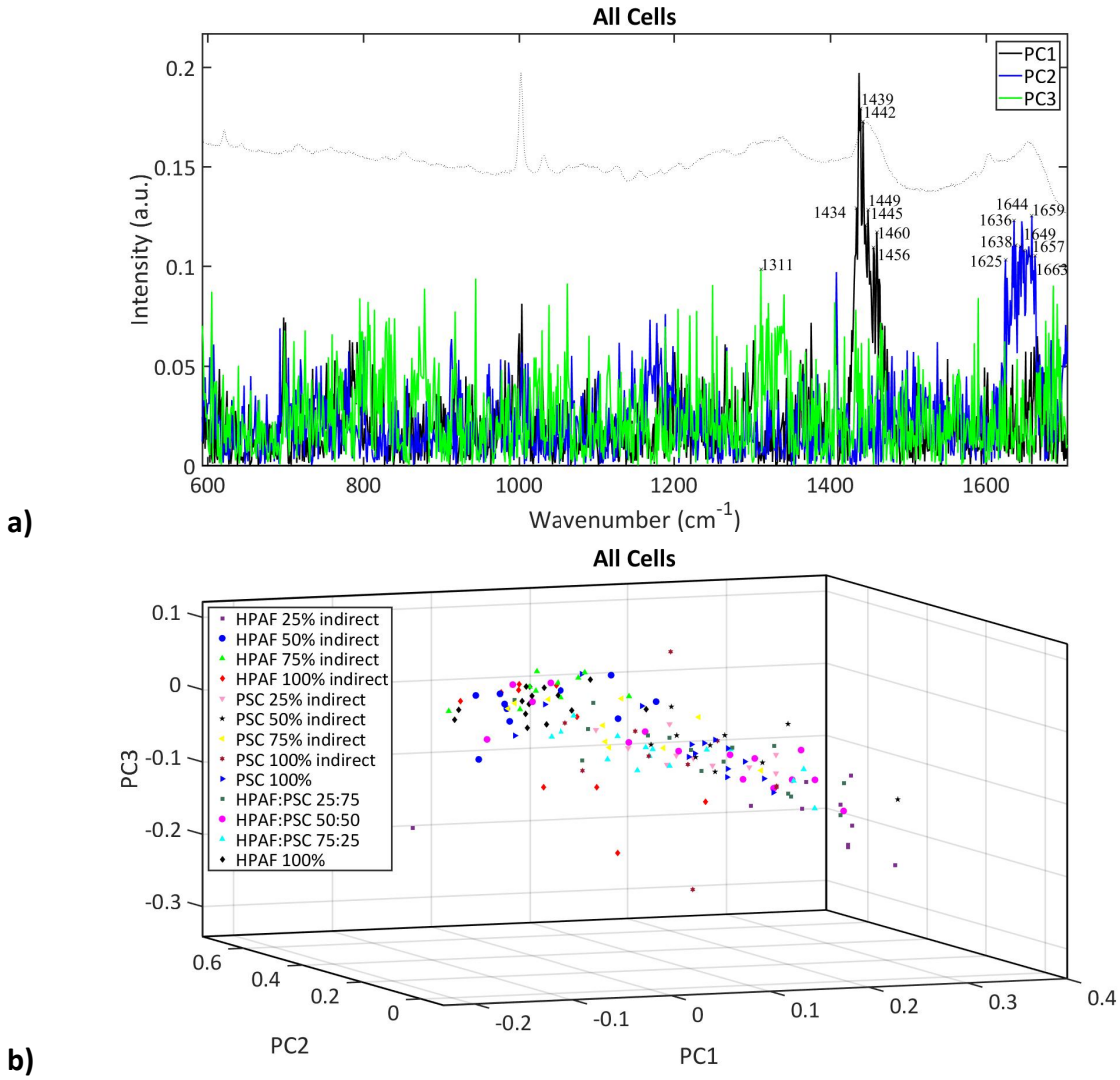

Figure 26:PCA analysis of all cells. a) PCA loadings plot, b) PCA 3D scores plot. 'Indirect'' indicates cells grown in coculture in a wells plate, with cells sharing media but no contact between the cells.

PCA of all cell cocultures, those grown in direct and indirect contact at all proportions, shows substantial overlap of groups. There is a similar pattern of variation along both PC1 and PC3, showing separation between groups of cells(Figure 26b). Separation along PC2 is less pronounced and shows heterogeneity within HPAF-II grown in a 25:75 (HPAF:PSC) coculture in a wells plate and within one group of 100% HPAF-II cells (Figure 26b). The relationship between the cell types appears to have some impact as the greatest separation along both PC1 and PC3 is between the HPAF-II grown alone and those grown in a 25:75 (HPAF:PSC) coculture in a wells

plate, with no contact between cells. HPAF-II and PSCs grown in 75:25 (HPAF:PSC) coculture in contact on a slide, show the greatest separation within their own group and greatest overlap with all other cells groups(Figure 26b).

Separation is seen mostly along PC1 and PC3, and attributed to differences in peaks associated with changes to a CH_2 bond (1439cm^{-1},1442cm^{-1}, 1445cm^{-1}, 1449cm^{-1}) as well as a C-H vibration in either proteins or lipids (1449cm^{-1}) and CH_2/CH_3 deformation of lipids and collagen or deoxyribose (1460cm^{-1}) (Figure 26a).(107) It is, however, difficult to identify the degree to which this separation is due to inherent differences between PSCs and HPAF-II cells because they are different cell types or an impact of the coculture.

6.2 HPAF-II versus Pancreatic Stellate Cells

Comparison of slides containing either 100% HPAF-II or 100% PSC, shows the innate differences between the 2 cell types. On initial PCA analysis, PSCs show greater heterogeneity than HPAF-II cells, although there is some overlap between 4 HPAF-II spectra and the general cluster of PSCs (circled Figure 27b). The cell types vary along PC1 with greatest difference in the symmetric ring breathing mode of phenylalanine (1001cm^{-1}) and CH_2CH_3 deformation or collagen (1448cm^{-1}) (Figure 27a).(107) There is also separation along PC2 of stellate cells when grown as part of the wells plate experiment as opposed to the slides, but also within the group grown on the wells plate, which shows greater differences of spectra within a single class than any other group of cells (Figure 27b). The heterogeneity highlighted by PC2 is due to phenylalanine (peak 1001cm^{-1}) and some contribution from peaks in the range 1631cm^{-1} to 1654cm^{-1}, associated with collagen content (1635cm^{-1}), and amide I (1643cm^{-1}, 1646cm^{-1}, 1654cm^{-1}) (Figure 27a).(107)This is surprising as both slides contained only PSC, grown in the same conditions, with no other external influencing factors. The only difference between the 2 sets of PSC was the passage at which the experiment was conducted, which could be a contributing factor as the PSC are a primary cell line and so may be sensitive to biochemical changes, if not morphological ones, with a greater passage.

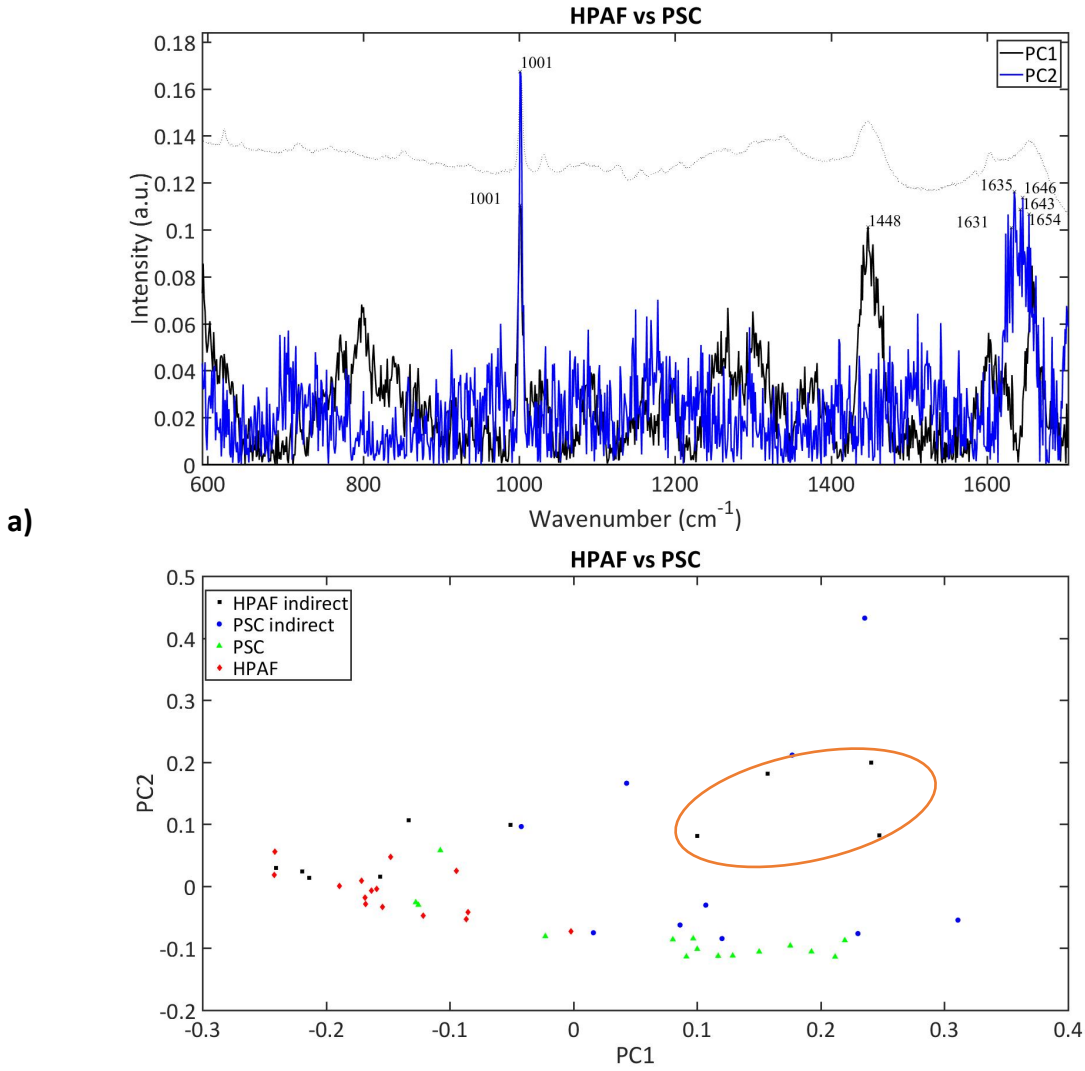

Figure 27:PCA analysis of 100% HPAF and 100% pancreatic stellate cells. a) PCA loadings plot b) PCA 2D scores plot. Overlap between 4 HPAF-II spectra and the general cluster of PSC is circled. 'Indirect'' indicates cells grown in coculture in a wells plate, with cells sharing media but no contact between the cells.

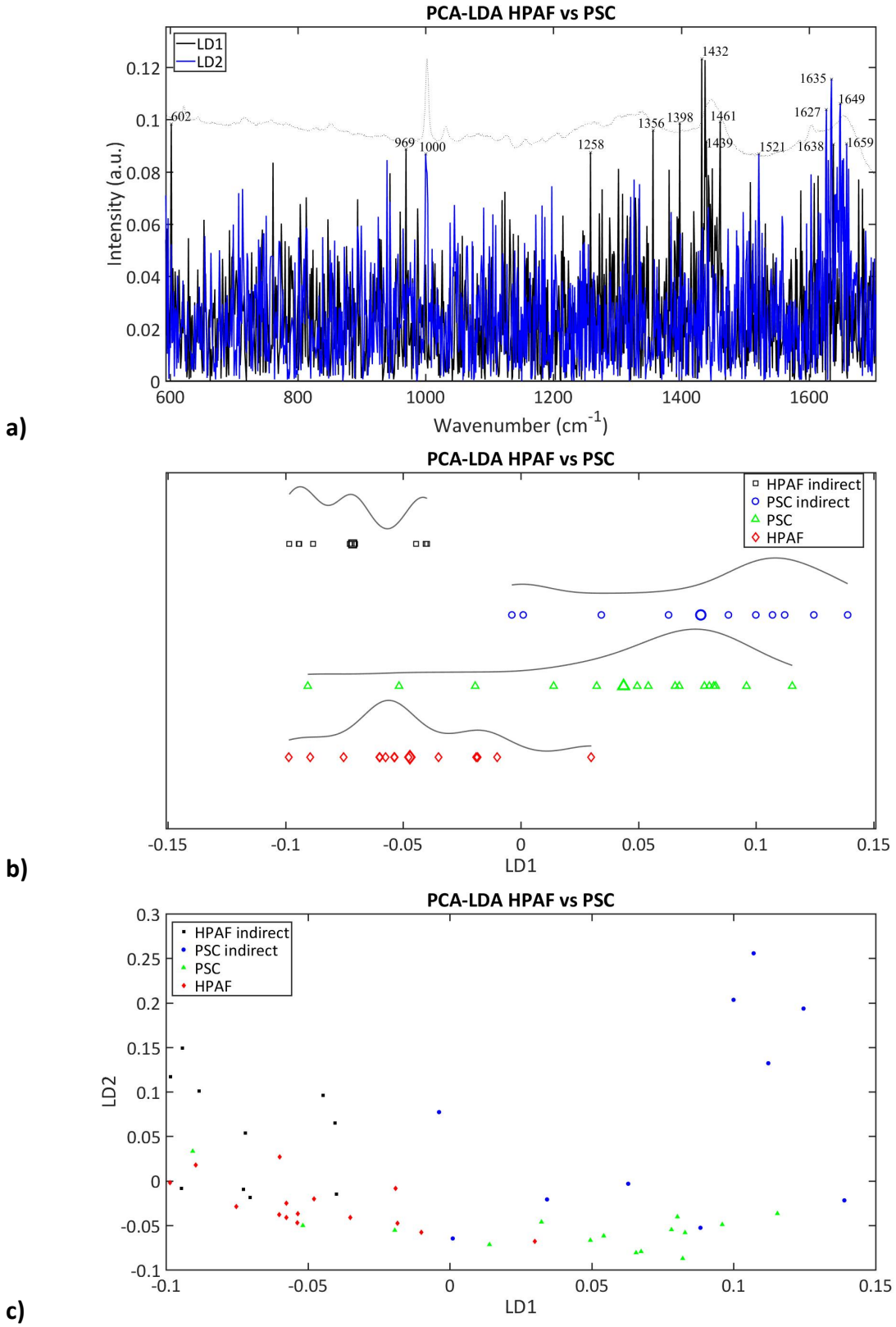

Figure 28:PCA-LDA analysis of 100% HPAF and 100% pancreatic stellate cells. a) PCA loadings plot b) PCA-LDA 2D scores plot c) PCA-LDA 1D scores plot. 'Indirect'' indicates cells grown in coculture in a wells plate, with cells sharing media but no contact between the cells.

PCA-LDA analysis separates the HPAF-II cells much more distinctly, although there is still much more heterogeneity among the PSCs and some overlap of these cells with the HPAF-II (Figure 28b, Figure 28c). This may be because the spectra have been taken of fundamental components present in both cells, such as cell membrane, and the structure of these components is essentially the same across cell types. Similarly to PCA, the separation between the cell types can be seen along LD1, with the heterogeneity of the PSC cells grown in wells plates seen along LD2. Using PCA-LDA analysis also brings out greater heterogeneity in the HPAF-II cells grown for experiments with cells grown in indirect contact; a separation also seen along LD2 (Figure 28b).

PCA-LDA attributes the separation between the cell types to amide III, adenine, cytosine (1258cm^{-1}), guanine (1356cm^{-1}), an C=O symmetric stretch (1398cm^{-1}) and a CH_2 bending mode or scissoring (1439cm^{-1}) (Figure 28a).(107) The greatest contribution to the variation, according to the PCA-LDA, appears to be due to a peak at 1432cm^{-1}, although this is not a true peak which can be identified in the raw spectra.

The separation within the groups of HPAF-II and PSC, seen along LD2 appear to be due to phenylalanine (1000cm^{-1}) or differences in collagen content, (1635cm^{-1}) (Figure 28a).(107) The peak at 1659cm^{-1} could be due to amide I vibration of collagen like proteins, amide C=O stretching absorption or glutathione.(107) These are expected differences between HPAF-II and PSCs as phenylalanine is a component of DNA and amide I is a protein, which are likely to differ because of essential differences in the phenotype of cells. The difference identified in collagen is also a known difference as PSCs are able to produce ECM proteins, including collagen, whereas cancer cells do not have this function.(108)

6.3 Cocultures in Direct Contact

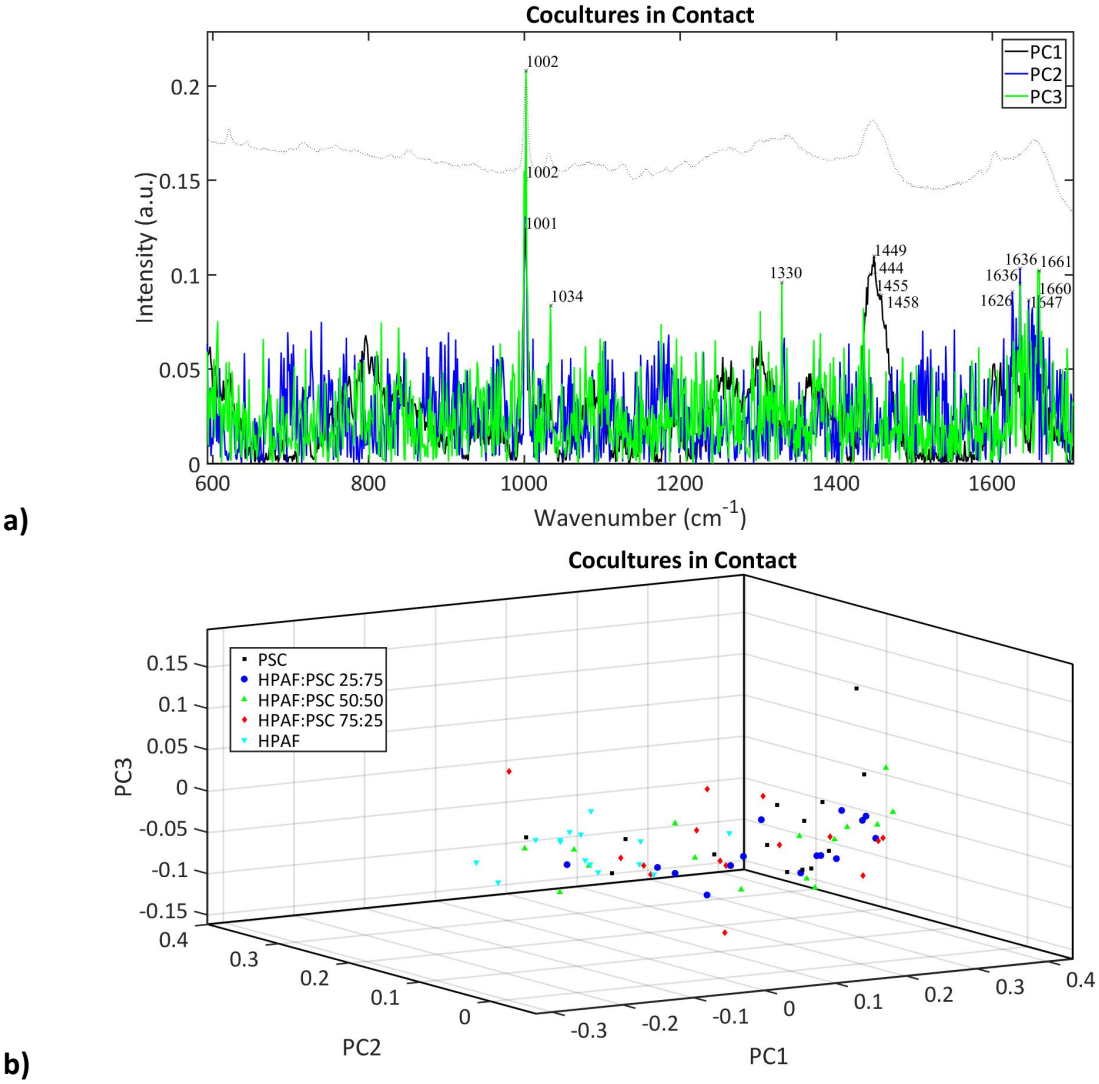

Figure 29:PCA analysis of cells in direct contact a) PCA loadings plot b) PCA 3D scores plot

Similarly to the PCA of uninfluenced HPAF-II and PSCs, the cocultures also show differences in phenylalanine, however it can be assumed that this is due to an innate difference between the cell types and not a result of the influence of the coculture environment. The variation along PC1 can also be seen due to C-H vibration in protein or lipid at peak 1449cm^{-1}, a cholesterol or lipid band seen at 1444cm^{-1}, deoxyribose associated with peak 1455cm^{-1} and differences in nucleic acid modes at peak 1458cm^{-1} (Figure 29a).(107) The comparison of uninfluenced HPAF-II with PSC showed a peak at 1448cm^{-1} which may have shifted to 1449cm^{-1} as a result of coculturing the cells, suggesting in cocultured cells there is more variation due to C-H vibration than due to

CH_2CH_3 deformation or collagen. Given this shift it could also be assumed that the innate difference between HPAF-II and PSCs is due to the CH_2CH_3 deformation as opposed to collagen content. Variation due to peaks at 1444cm^{-1}, 1455cm^{-1} and 1458cm^{-1} appear to have arisen as result of the influence of coculture (Figure 29a), suggesting coculturing cells causes changes to the expression or function of the cells.

Both PC2 and PC3 identify variation within the groups. As there is a similar pattern of separation within all groups, these peaks are possibly associated with differences between components or organelles common to all cells, dependent on the location within the cells from which the spectra were taken. Differences along PC2 are attributed to phenylalanine (1002cm^{-1}), lipids (1652cm^{-1}) and variations in the amide I band (1660cm^{-1}, 1626cm^{-1}, 1636cm^{-1}) (Figure 29a),(107) all of which are likely to vary in their presence and quantity dependent on the organelle or location in the cell from which the spectrum is acquired; it is feasible that PC2 identifies this natural variance within a cell. While the pattern of separation along PC2 and PC3 are similar, there is a greater spread of the data along PC3 than PC2. The most significant contribution to this spread is phenylalanine (1002cm^{-1}, 1034cm^{-1}) and amide I (1636cm^{-1}), which are also seen in PC2 (Figure 29a).(107) PC3 also identifies variation due to DNA and phospholipids (1330cm^{-1}) (Figure 29a).(107)

6.4 Cocultures in Indirect Contact

HPAF-II and PSCs, grown in indirect contact, separate mostly along PC1, with HPAF-II 100% cells separating from all other cells along PC2 (Figure 30b). There is significant overlap between spectra taken from HPAF-II grown at 50%, 75% and 100% proportions. HPAF-II cells grown at 25%, in coculture with 75% PSC, however, separate completely from all other HPAF-II groups, along PC1, separating even further than the groups of PSCs (Figure 30b). The PSCs from the same the coculture, on the other hand, show some overlap with the other groups of HPAF-II cells. Although they still overlap with the PSCs, there is much greater overlap with the HPAF-II cells.

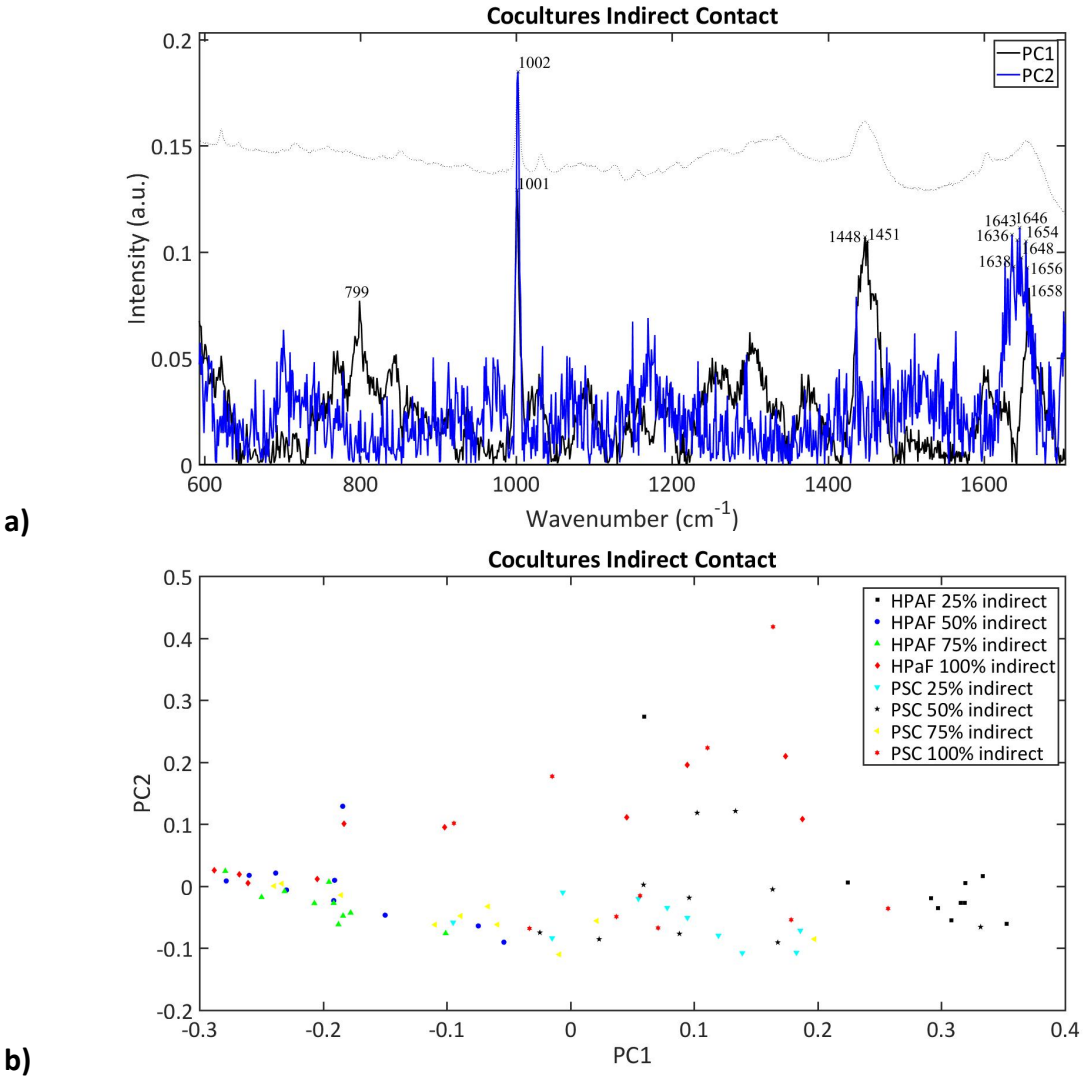

Figure 30:PCA analysis of cells in indirect contact, grown in a wells plate with an insert, . 'Indirect'' indicates cells grown in coculture in a wells plate, with cells sharing media but no contact between the cells, a) PCA loadings plot b) PCA 2D scores plot

This suggests that cells grown in indirect contact at a proportion of HPAF:PSC 25:75, have an influence on each other, creating differences in the HPAF-II cells by altering the backbone geometry and phosphate ion interactions (peak 799cm^{-1}), phenylalanine (1001cm^{-1}), CH_2CH_3 deformation (1448cm^{-1}, 1451cm^{-1}) and an amide I α-helix (1658cm^{-1}) (Figure 30a), although some of this variation is natural variation between HPAF-II and PSCs (Figure 27).(107) The differences between HPAF-II and PSC cells also appear to be due to the same peaks, as these also vary along PC1, suggesting that at a HPAF:PSC 25:75 proportion, the products secreted by PSCs and the subsequent interactions cause HPAF-II cells to change their phenotype to become

more similar to PSCs. It is difficult, however, to identify whether these changes are due to the proportions at which the cells are cocultured or the indirect nature of the interaction between the cell types.

The HPAF-II 100% cells separate from all other cell types, both HPAF-II grown in coculture and all PSCs, along PC2 (Figure 30b). This is mostly due to a difference in phenylalanine (1002cm^{-1}) and an amide I band and α-helix (1643cm^{-1}, 1646cm^{-1}, 1654cm^{-1}, 1656cm^{-1})(Figure 30a).(107) This suggests that in comparison to 'pure' HPAF-II cells, those which interact indirectly with PSCs, change their phenotype to some degree, through changes to phenylalanine and amide I, to become more similar to PSCs, although they can still be identified as a distinct group.

6.5 Comparison by Proportion

6.5.1 HPAF:PSC 25:75

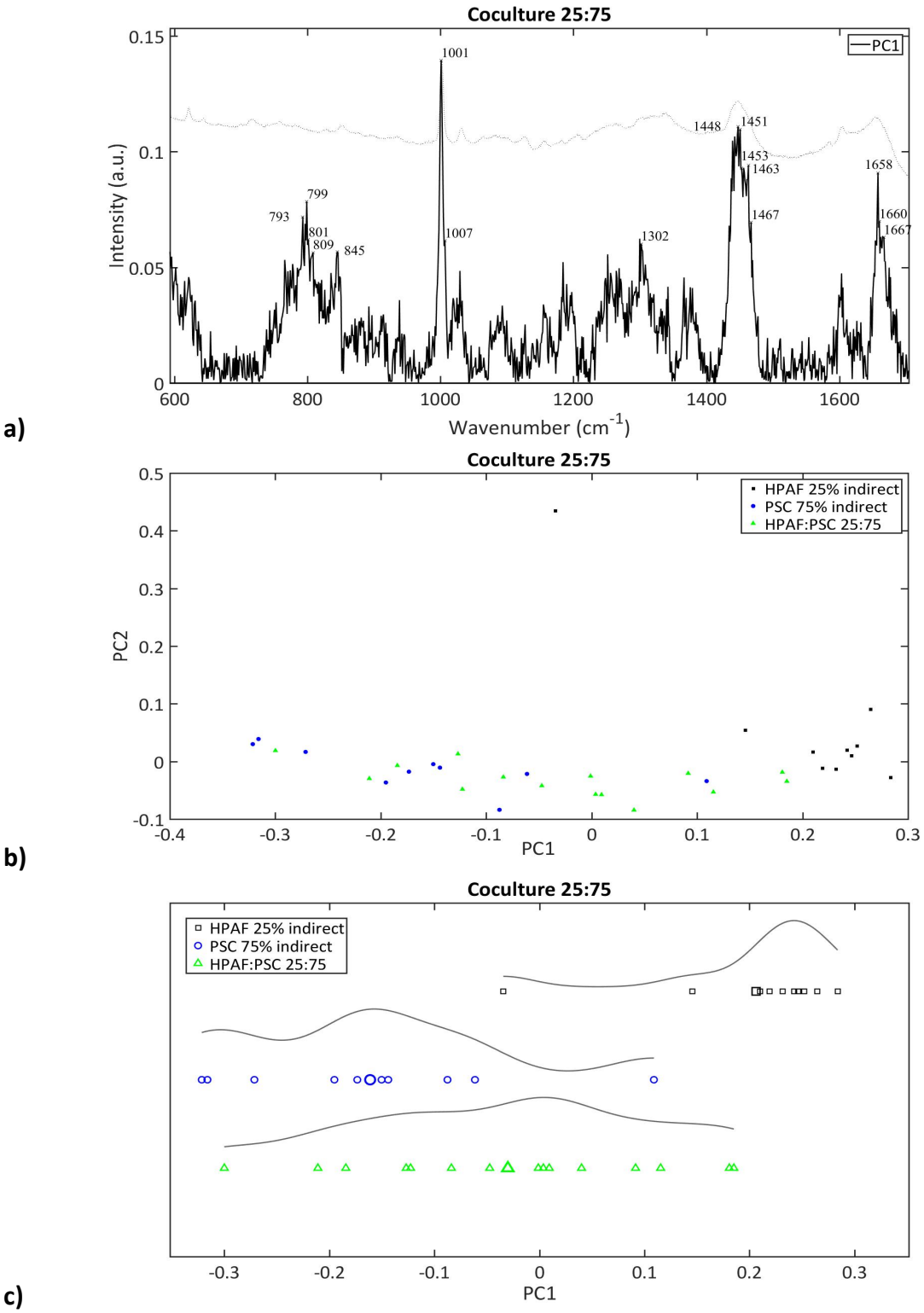

Figure 31:PCA analysis of cells grown at HPAF:PSC 25:75 proportions in direct contact and indirect contact. 'Indirect'' indicates cells grown in coculture in a wells plate, with cells sharing media but no contact between the cells a) PCA loadings plot b) PCA 2D scores plot, c) PCA 1D scores plot

Variation amongst cells grown at HPAF:PSC 25:75 can be seen entirely along PC1. There is clear separation of the HPAF 25% group, grown in indirect contact with PSC 75%, and more overlap between HPAF:PSC 25:75 grown in direct contact and the PSCs 75% (Figure 31c). This may suggest that indirect contact with PSCs increases variation in HPAF-II cells at a 25:75 proportion, more so than direct contact between the cells at the same proportion. This is surprising as it was hypothesised that the greater variety would be seen in cells growing in direct contact as there is both direct and indirect contact between these cells and so this would have a greater influence than just indirect contact. It may, however, suggest that there is a more complex relationship between the two cell types, with some pathways which may be inhibited by the direct contact between cells. Thus, the impact of such pathways is amplified when cells are grown in indirect contact, causing more alterations to the HPAF-II cells grown in indirect contact with PSCs than those in direct contact.

PCA suggests that some of the variation along PC1 is due to natural variation between PSCs and HPAF-II cells; peaks at 799cm^{-1}, 1001cm^{-1} and 1448cm^{-1} were seen on the loadings plot when comparing uninfluenced HPAF-II with uninfluenced PSCs (Figure 28a, Figure 31a). Growing cells in coculture, however, has identified further differences due to new peaks associated with changes to CH_2 (1302cm^{-1}) and amide I (1658cm^{-1}, 1660cm^{-1}, 1667cm^{-1}), which would suggest that these differences are a result of the influence of interaction between cells (Figure 31a).(107)

6.5.2 HPAF:PSC 50:50

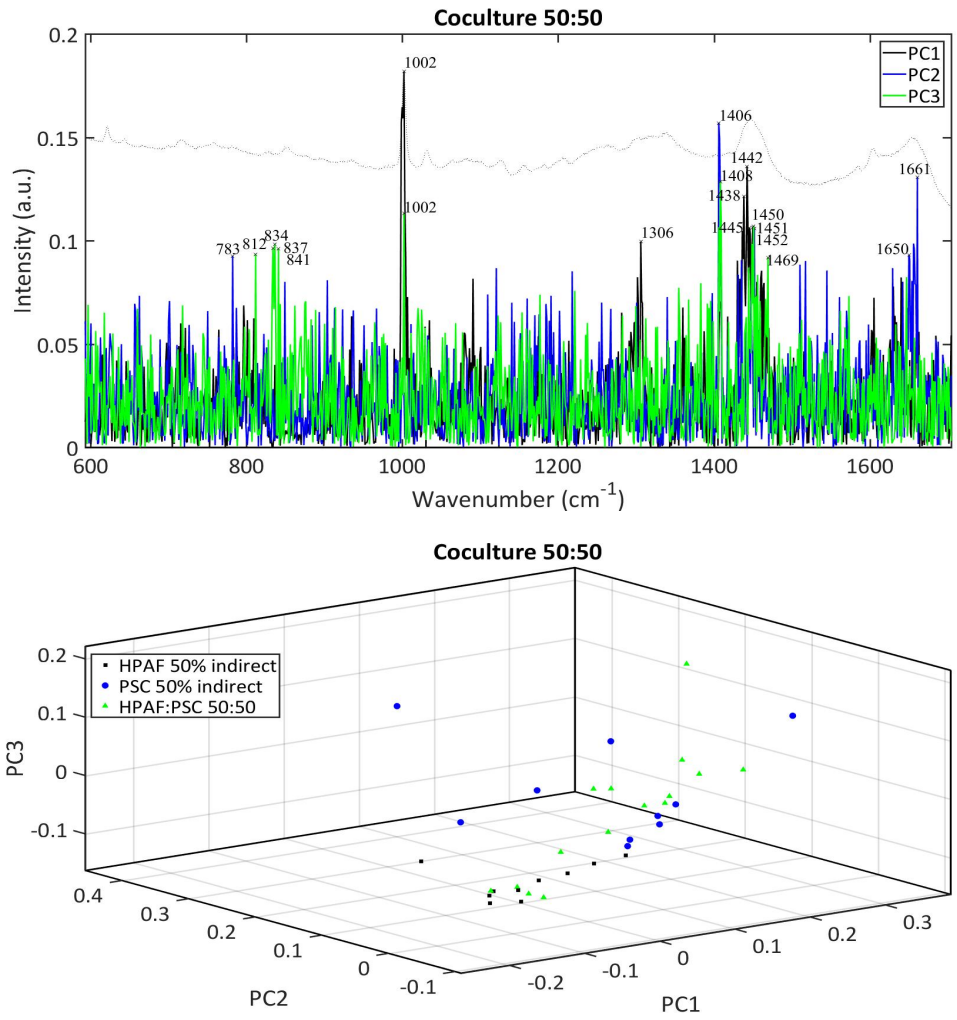

Figure 32:PCA analysis of cells grown at HPAF:PSC 50:50 proportions in direct contact and indirect contact, 'Indirect'' indicates cells grown in coculture in a wells plate, with cells sharing media but no contact between the cells a) PCA loadings plot b) PCA 3D scores plot

Along PC1, there is clear separation between HPAF-II and PSC, with spectra from the slide with HPAF:PSC 50:50 grown in direct contact showing an even spread along PC1, overlapping with both of the individual cell types (Figure 32b). This is expected as this slide contained both cell types and so the PC1 spread would suggest that PCA is able to separate out these cell types. There is also some separation between cell types along PC3 (Figure 32b). The loading plot suggests that much of this variation is due to natural variation between the cell types but peaks the peak at 1306cm^{-1}, associated with changes to CH_2, is due to the influence of the interaction between the cells (Figure 32a). This is a similar variation identified as a result of interaction of cells at a

25:75 proportion, which may suggest that coculturing HPAF-II and PSCs in any proportion causing changes in CH_2 groups in one or both of the cell types.

PC2 shows the heterogeneity within the PSC 50%, grown in indirect contact with 50% HPAF-II (Figure 32b). This degree of heterogeneity within the cell type is only seen in the cells grown in indirect contact and is not present in what could be assumed to be PSCs, based on their separation along PC1, from the cells grown in direct contact. This would suggest either, that being grown in direct contact with cancer cells reduces a natural heterogeneity present within PSCs, or growing PSCs indirectly in contact with cancer cells causes an interaction which allows them to proliferate in a way that creates this heterogeneity but which may be inhibited by the direct presence of cancer cells. Alternatively, this heterogeneity may be a difference in the PSCs themselves, potentially due to differences in passage, as was seen in PCA of 100% HPAF-II and 100% PSCs.

Some of the heterogeneity within the PSCs 50% in indirect coculture is also identified along PC3 (Figure 32b). PC3 also shows much more separation within the HPAF:PSC 50:50 group grown in direct contact, with some spectra showing very clear overlap with the HPAF-II 50% and the remaining spectra showing a similar pattern of heterogeneity as the PSC 50% group. As the PSCs showed greatest heterogeneity when uninfluenced (Figure 27b), this would suggest that some of this heterogeneity is natural. However, the coculture does appear to have an influence on the nature of the heterogeneity as when cocultured PCA attributes the differences to peaks at 783cm^{-1}, ν_s COO^- possibly in IgG (1406cm^{-1}), C=C in amide I (1650cm^{-1}) and 1661cm^{-1} along PC2 and phosphodiester (812cm^{-1}), polysaccharide structure (841cm^{-1}), a CH_2 bending mode in malignant tissue (1450cm^{-1}), CH_2CH_3 deformation (1451cm^{-1}) along PC3 (Figure 32a).(107) Whereas, the PCA of PSCs not in coculture suggest the heterogeneity is due to peaks at phenylalanine (1001cm^{-1}) and CH_2CH_3 deformation or collagen (1448cm^{-1}) (Figure 13a).(107) These results suggest that growing cells in coculture with indirect contact can have an influence on the cell phenotype. The fact that this heterogeneity is highlighted in cells in indirect contact and not those grown

in direct contact also suggests there may be a degree of inhibition which is more influential when the cells are in direct contact.

6.5.3 HPAF:PSC 75:25

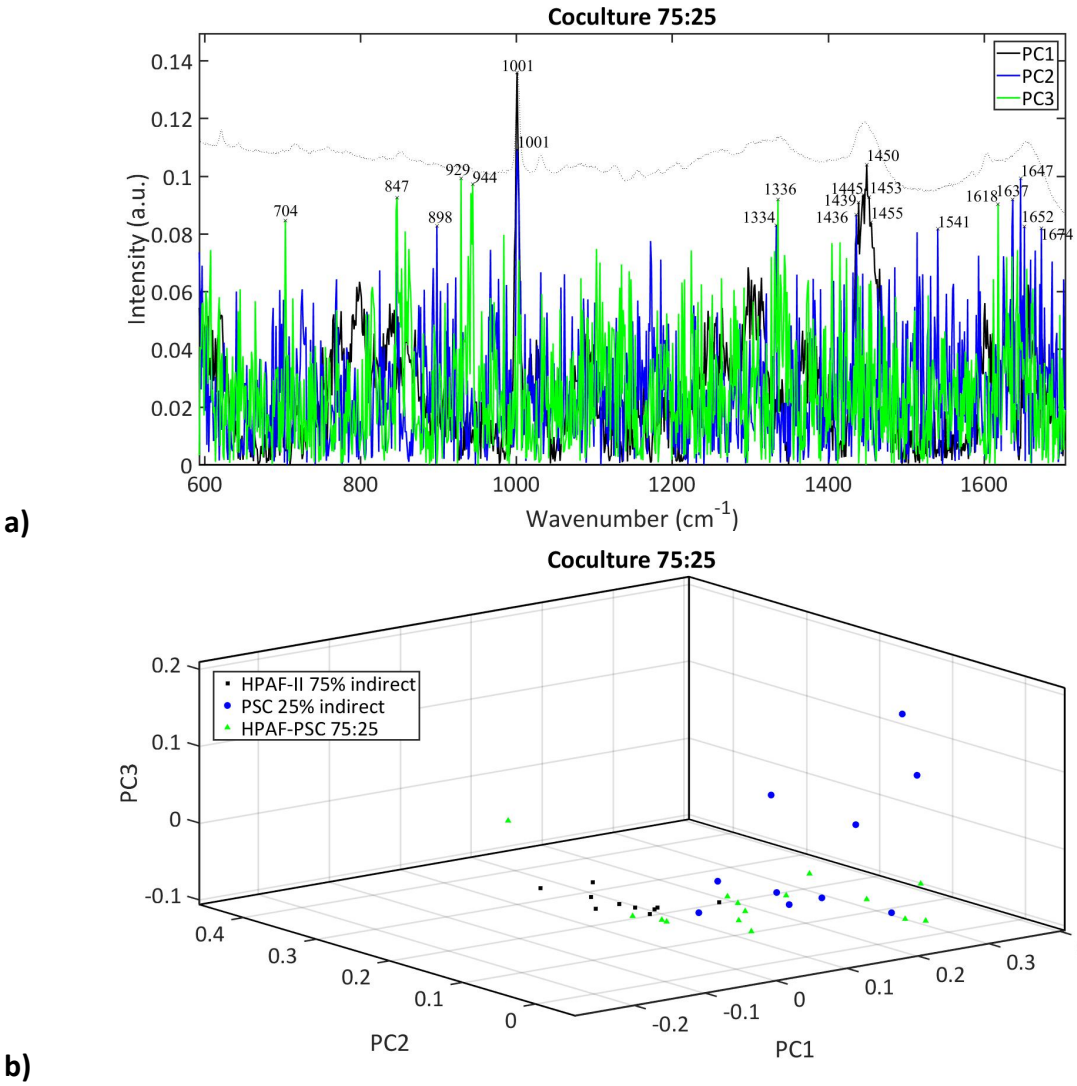

Figure 33:PCA analysis of cells grown at HPAF:PSC 75:25 proportions in direct contact and indirect contact, 'Indirect'' indicates cells grown in coculture in a wells plate, with cells sharing media but no contact between the cells a) PCA loadings plot b) PCA 3D scores plot

HPAF-II 75% cells when grown in indirect contact with PSC 25%, separate as a very distinct group along PC1, whereas there is overlap between the HPAF:PSC 75:25 grown in direct contact and PSCs 25% (Figure 33b). The distribution of spectra and classes along PC1 is very similar to the distribution of HPAF:PSC at a 25:75 proportion, with the HPAF cells grown in indirect contact with PSCs showing clear separation

from cells grown in direct contact, while PSCs show an expected overlap (Figure 31b, Figure 33b). While this could be because more spectra were taken from PSCs than HPAF-II on the slide, it could also suggest that the direct contact of HPAF-II and PSCs grown at this proportion causes changes to HPAF-II cells giving them characteristics similar to that of PSCs. Alternatively, indirect contact may allow for a change to HPAF-II cells which is otherwise inhibited by the direct contact between cells. PCA suggests these changes to the HPAF-II cells are in phenylalanine (1001cm^{-1}) CH_2 scissoring (1436cm^{-1}, 1439cm^{-1}, 1445cm^{-1}) a CH_2 bending mode found in malignant tissues (1450cm^{-1}), a protein band (1453cm^{-1}) (Figure 33a).(107) The peak at 1445cm^{-1} may be particularly significant as it has been shown to be associated with a number of changes to CH_2 and CH_2CH_3 bonds, in both proteins and lipids, some of which have been shown to be of diagnostic significance in normal and cancerous tissue of the nasopharynx.(107)

Comparison of the PCA scores plots, with cells grown at different proportions, shows differences in the way spectra taken from HPAF-II cells in indirect contact, as opposed to those grown in direct contact, separate and cluster along PC1. HPAF-II cells grown in indirect contact at a HPAF:PSC 25:75 and 75:25 proportion cluster separately to cells grown in direct contact, whereas those at a 50:50 proportion overlap (Figure 31b, Figure 32b, Figure 33b). It is unlikely that this separation of HPAF-II cells grown in indirect contact is simply because more spectra have been taken from PSCs on the slides with cells in direct contact, as the probability of doing so on a slide containing 75% HPAF-II cells is low. Therefore, coculturing HPAF-II and PSCs appears to have an impact on the cancer cells which causes some changes to their phenotype. However, as this separation of HPAF-II cells is not present at a HPAF:PSC 50:50 proportion, which makes it difficult to propose the type of change or reason they may occur.

The HPAF-II 75% group also clusters along PC3 but this cluster sits in the middle of spectra acquired from PSC 25% grown in indirect contact (Figure 33b). Along both PC1 and PC3 there is almost no overlap between HPAF-II 75% and HPAF:PSC 75:25, grown in direct contact, supporting the hypothesis that either direct contact with PSCs causes changes to HPAF-II as a result of the contact and direct interaction of the

cells or the indirect contact allows for changes to HPAF-II cells which are inhibited through direct contact between cells.

There is more heterogeneity of the PSC 25% along PC3 and the spectra from these cells overlap with all other cell types (Figure 33b). Similarly to cocultures in other proportions the PCA would suggest that in part this heterogeneity is a result of the influence of the coculture, as opposed to natural variance in the cells, as the peaks identified as causing these differences are different to those identified in the initial PCA of uninfluenced PSCs (Figure 28a, Figure 33b).

In comparison to the PCA loadings plot of the HPAF:PSC 50:50 coculture, which identified heterogeneity of PSC along PC2, (Figure 32a) changing the proportion of cells to HPAF:PSC 75:25 identifies differences along PC3 (Figure 33). It identifies the heterogeneity attributed to peaks in the nucleotide conformation (704cm^{-1}), C-C stretching (929cm^{-1}), guanine (1336cm^{-1}) and ν(C=C) in tryptophan or porphyrin (1618cm^{-1}) (Figure 33a). Interestingly, when the proportion of cells is changed from 50:50 to 75:25, the peaks attributed to causing heterogeneity within the cells change and there is no overlap between the peaks identified for the 2 proportions.

6.6. Cells and Tumour

Spectra taken from cell line cocultures were compared those taken from cancerous tumour tissue, taken from patient 1, to identify overlaps in the spectra, which shows which models were most similar to human tissue and so could be most useful for further research. Identifying differences between the models and tissue also identifies elements of the model which may need to be altered to create a model which functions most similarly to human tissue, working towards developing a model which allows for research that is more easily translated to clinical practice.

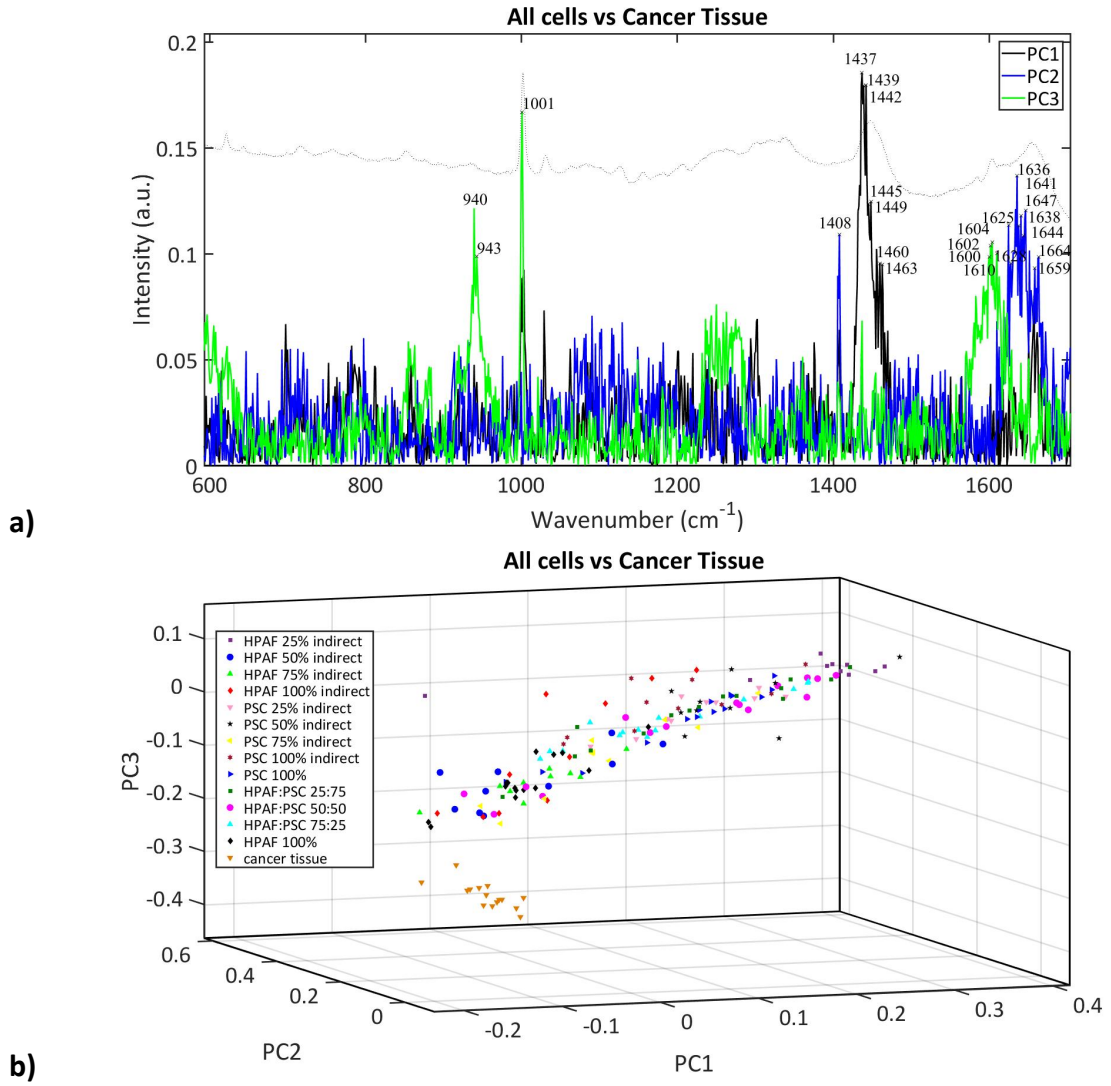

Figure 34:PCA comparing cells line models with cancerous tissue. 'Indirect'' indicates cells grown in coculture in a wells plate, with cells sharing media but no contact between the cells Spectra for cancer tissue were taken from fresh tissue from patient 1. a) PCA loadings plot b) PCA 3D scores plot

There is overlap between spectra taken from the tumour and the cell lines and in particular any spectra taken from HPAF-II cells, at any proportion other than HPAF 25%, along both PC1 and PC2 (Figure 34b). This is unsurprising as the tumour is likely to contain a significant proportion of cancer cells. There is much less overlap with the PSCs, which are ordinarily present in the tumour stroma, suggesting that the natural tumour environment alters these PSCs in a way which has not been replicated by the cell line models.

The tumour tissue separates very clearly along PC3, due to differences in skeletal modes including polysaccharides and amylose (940cm^{-1}, 943cm^{-1}), phenylalanine (protein assignment) (1602cm^{-1}) and cytosine (NH_2) (1610cm^{-1}) (Figure 34a),(107) which suggests there are factors in vivo which create these differences which have not been replicated by simply growing the relevant cell types in coculture.

This may in part be a result of the fact that patient 1 had an undifferentiated (anaplastic or sarcomatoid) carcinoma whereas HPAF-II cells are a PDAC cell line (Table 2). However, there is much more similarity between the tumour spectra and HPAF-II spectra, and the differences are in the PSCs. This suggests that cancer cells, even in different histological types of pancreatic cancer, are similar, whereas their interaction with and impact on PSCs differs, in part dependent on the tumour type. This highlights the complexity and importance of the relationship between cancer cells and PSCs and emphasises the need for a better understanding of these interactions, in the development and progression of pancreatic cancer, in order for there to be developments in research which will be successful when applied in a clinical setting.

6.7 SERS – mapping image analysis

Surface enhanced Raman spectroscopy (SERS) was used on cocultured cells, using the mapping set-up in a raster pattern, taking spectra every 5μm. Initial analysis showed great variety in peaks, dependent on the presence of nanoparticles, suggesting that SERS can identify very subtle changes within cells and extract specific organelle information in great detail.

The outline of the cells and presence of nanoparticles can be seen on the white light images (Appendix, Figure 41). The morphology of the cells was clearer when looking down the microscope than can be seen in the images, which allowed good visualisation of the cells and nanoparticles, which is obscured on the images due to the camera quality. Initial shading by PCA shows variation to be independent of the visible distribution or concentration of nanoparticles on the image (Figure 35). Darker shading showed visually higher signal to noise ratio, suggesting these were areas where nanoparticles had interacted with components of the cell, giving very specific organelle data. However, it is difficult to determine whether the variation seen is due to the presence of nanoparticles or differences within the cells. Moreover, as PCA is carried out on each image separately, it is not possible to compare and identify variation between the images.

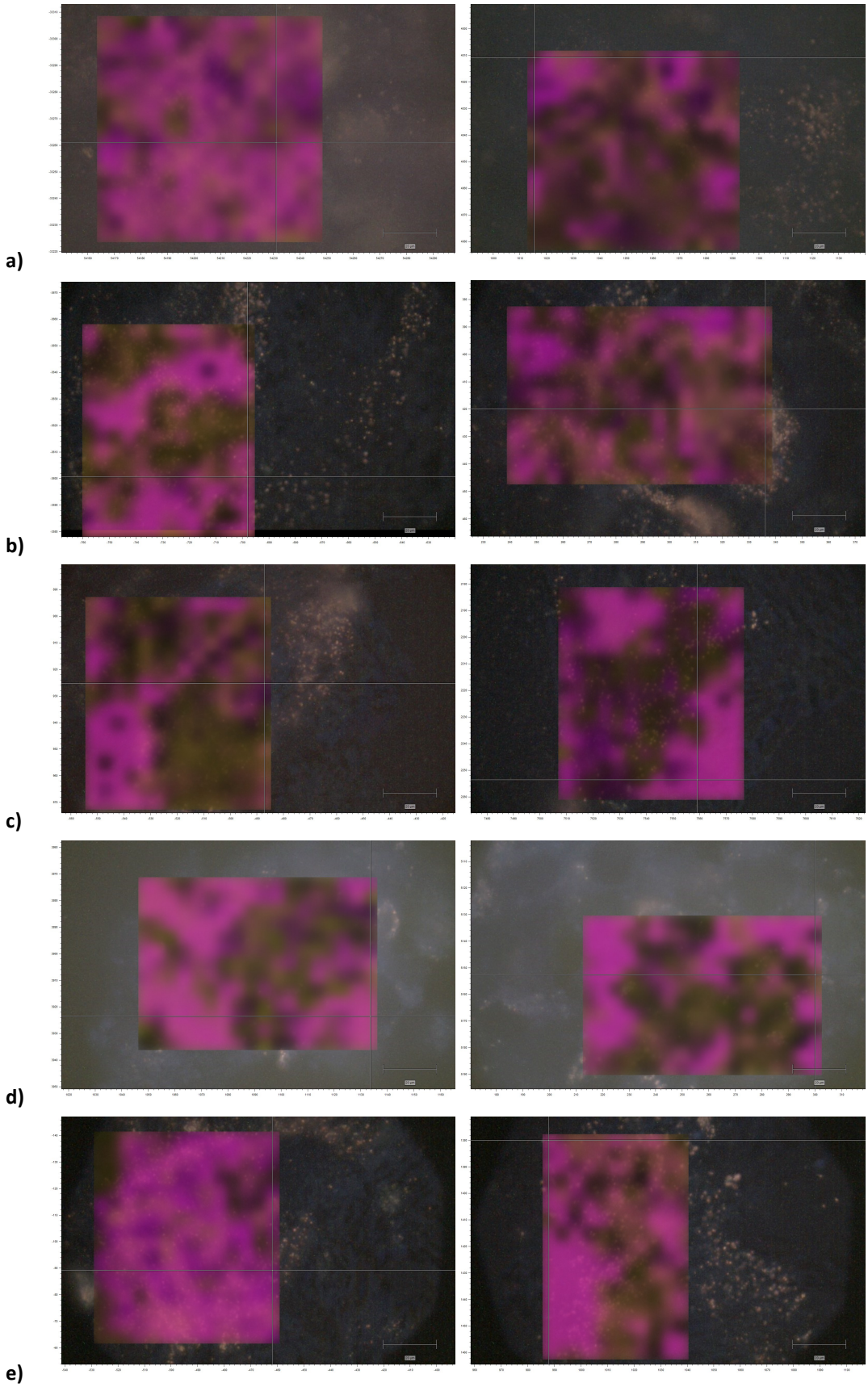

Figure 35:Raman shaded maps for cell cocultures with SERS showing shading by PCA. PC1 is seen in magenta and PC2 in yellow Scale bar 20μm. Maps were taken from 2 locations on each slide a) HPAF 25:75, b) HPAF 50:50, c) HPAF 75:25, d)HPAF 100% e) PSC 100%

Further, signal to baseline analysis identified regions according to specified peaks. The 600-800cm^{-1} and 1325-1345cm^{-1} ranges were used, both highlighting differences associated with DNA (Figure 35). Shading using 5-95% of the peak intensity range was used to reduce contribution from spectra with very low and very high intensity including regions where the receptor had been saturated, in turn highlighting SERS spectra.

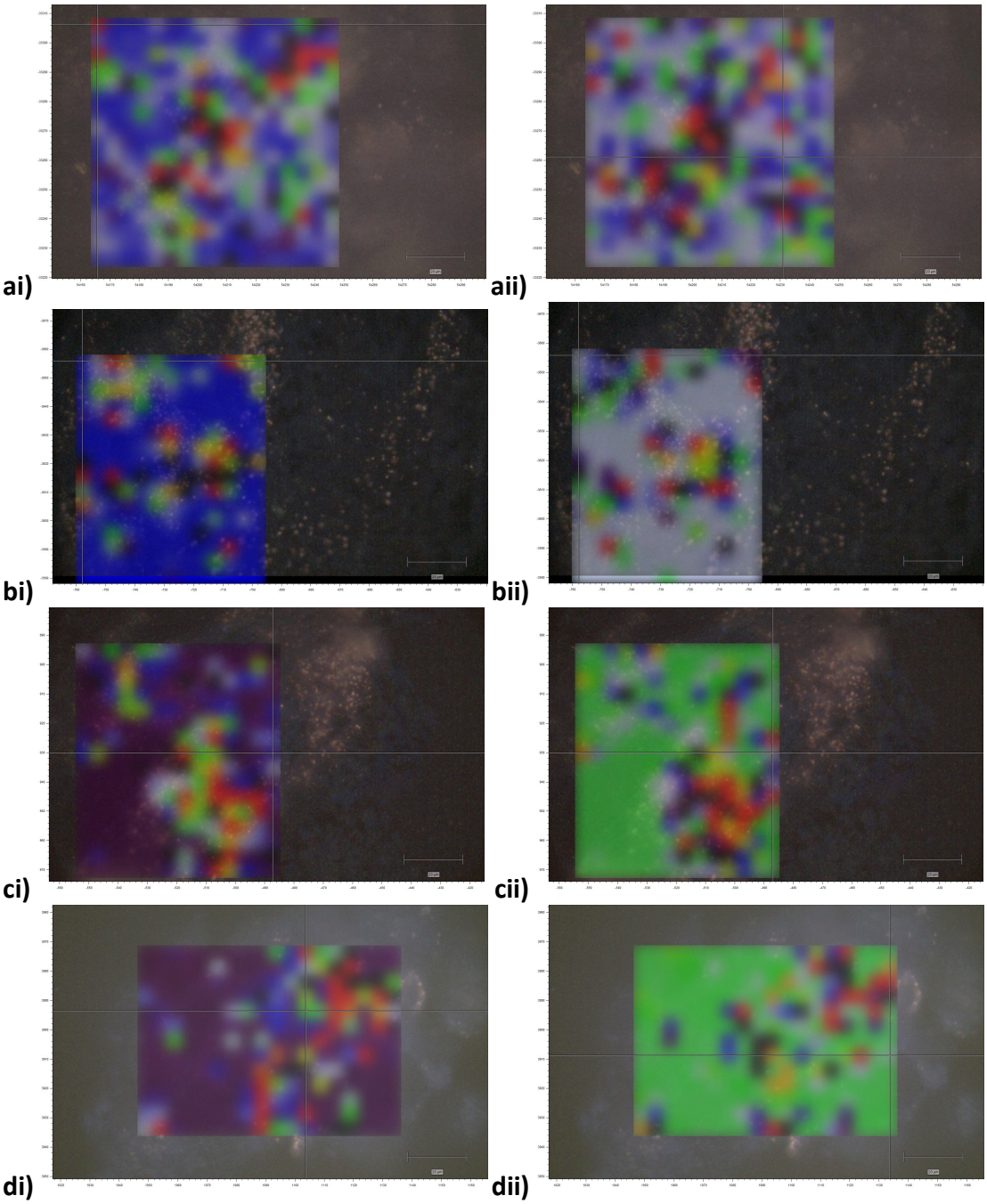

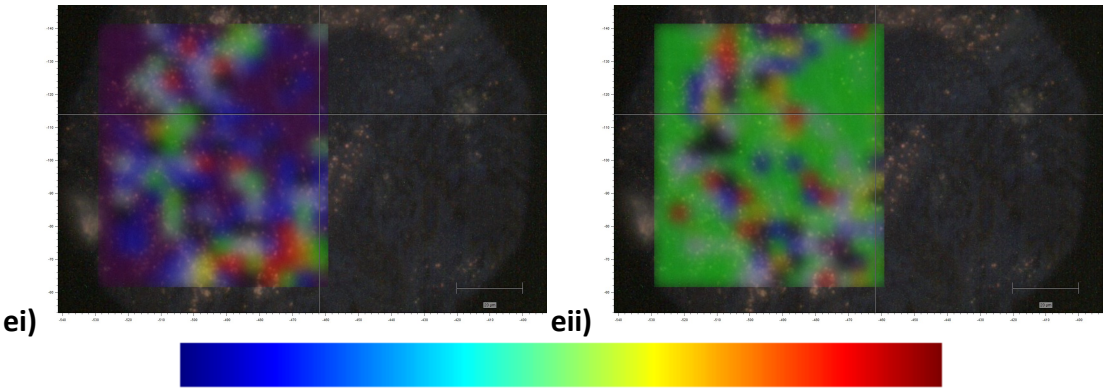

Figure 36: Raman shaded maps for cell cocultures grown in direct contact with SERS showing shading by signal to baseline analysis for wavenumbers i) 600-800cm^{-1} and ii)1325-1345cm^{-1}. Colour bar shown as reference for shading; blue shows lowest relative intensity and red the highest relative intensity within the image but shading is arbitrary and not numerically equal or comparable between images. Scale bar 20μm. ai) HPAF:PSC 25:75 600-800cm^{-1} shading aii) HPAF:PSC 25:75 1325-1345cm^{-1} shading , bi) HPAF 50:50 600-800cm^{-1} shading bii) HPAF:PSC 50:50 1325-1345cm^{-1} shading, ci) HPAF:PSC 75:25 600-800cm^{-1} shading cii) HPAF:PSC 75:25 1325-1345cm^{-1} shading, d)HPAF 100% 600-800cm^{-1} shading dii)HPAF 100% 1325-1345cm^{-1} shading ei) PSC 100% 600-800cm^{-1} shading eii) PSC 100% 1325-1345cm^{-1} shading

Shading by signal to baseline, allows some identification of regions of DNA. Comparison of images shaded by signal intensity of 600-800cm^{-1} and those shaded by the signal intensity of 1325-1345cm^{-1} ranges show overlap, particularly where the relative intensity is highest (Figure 36, Appendix, Figure 42). This shading therefore allows us to identify the location of the nuclei, based on the areas of high DNA intensity. However, what is difficult to identify are the changes to the spectra within each of the chosen regions of wavenumbers, which is likely to be more pertinent information in understanding the changes to the DNA which have occurred as a result of the coculture environment and so in understanding the impact the coculture on the cells. As shading is according to regions, changes within these regions are not evident.

While shading according to the intensity of a single peak and identifying how the presence of a single peak changes between images may show the changes in intensity within a single peak, this would reduce the amount of information seen within an image and risks missing information. Subtle shifts in the peak, which could highlight important information about cellular changes, would not be viewed on an image shaded by peak intensity and so could not be differentiated from peaks which

are of less significance. Moreover, it is difficult to know if low signal intensity, in a particular location, is because the relevant cell structure is not present in that location or due to insufficient presence of nanoparticles.

While regions of highest intensity overlap between images, what appear to be background regions on the image when shaded to 600-800cm^{-1} showing very low intensity, when shaded to 1325-1345cm^{-1} show higher intensity (Figure 36, Appendix, Figure 42). This may be because a number of peaks in the 1325-1345cm^{-1} are possibly associated with both nucleic acids and CH_2CH_3 wagging in collagen as well as the presence of phospholipids. If lower intensities, seen in the background, are identifying collagen this may suggest the beginnings of collagen deposition when coculturing the cells. However, there is little difference in the relative background intensities between different coculture proportions, which makes it difficult to propose how the coculture environment may be having an impact on any potential collagen deposition. Shading so the intensities are of numerical equivalence between images may give more insight into this, as it would allow for a direct comparison between different coculture proportions. This is difficult using the WiRE software, without arbitrarily altering the peak intensity range used, which could remove potentially important information.

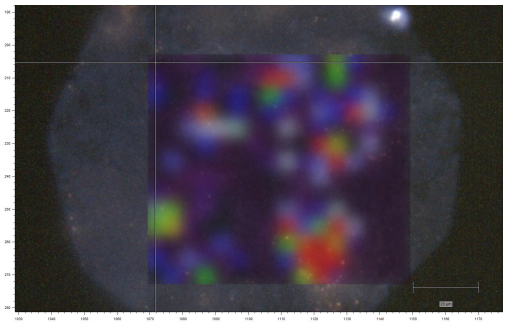

ai)

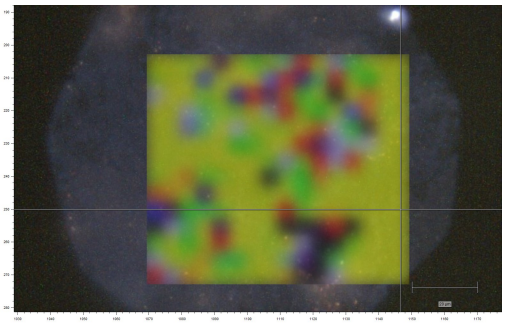

aii)

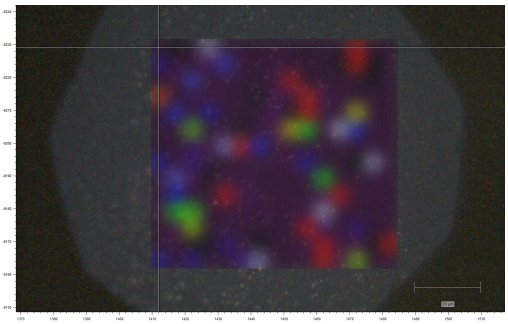

bi)

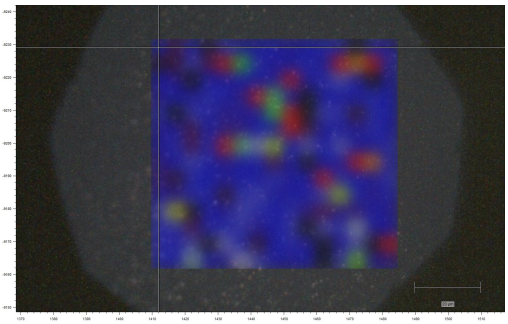

bii)

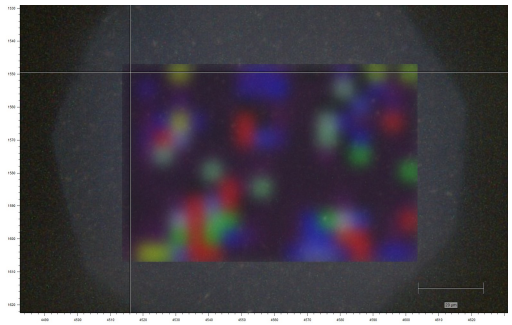

ci)

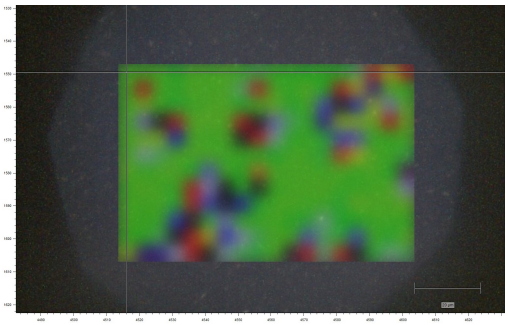

cii)

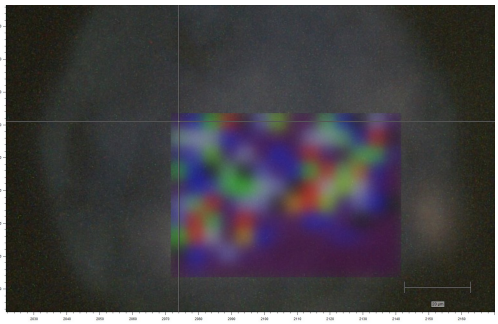

di)

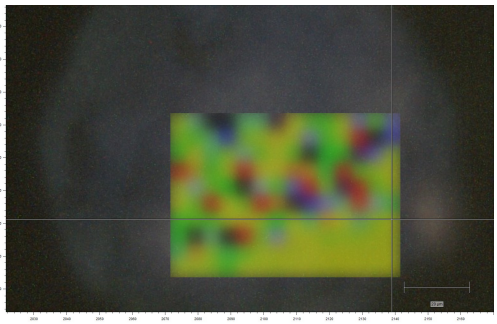

dii)

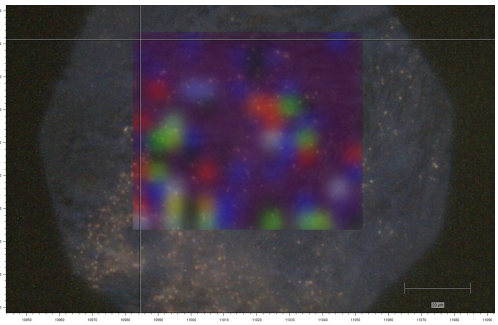

ei)

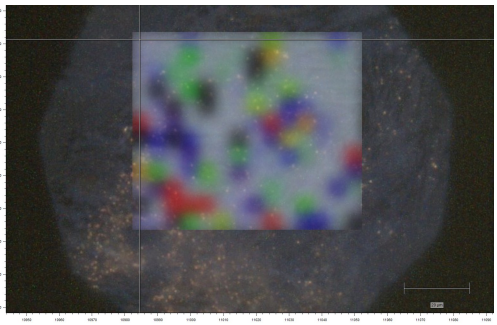

eii)

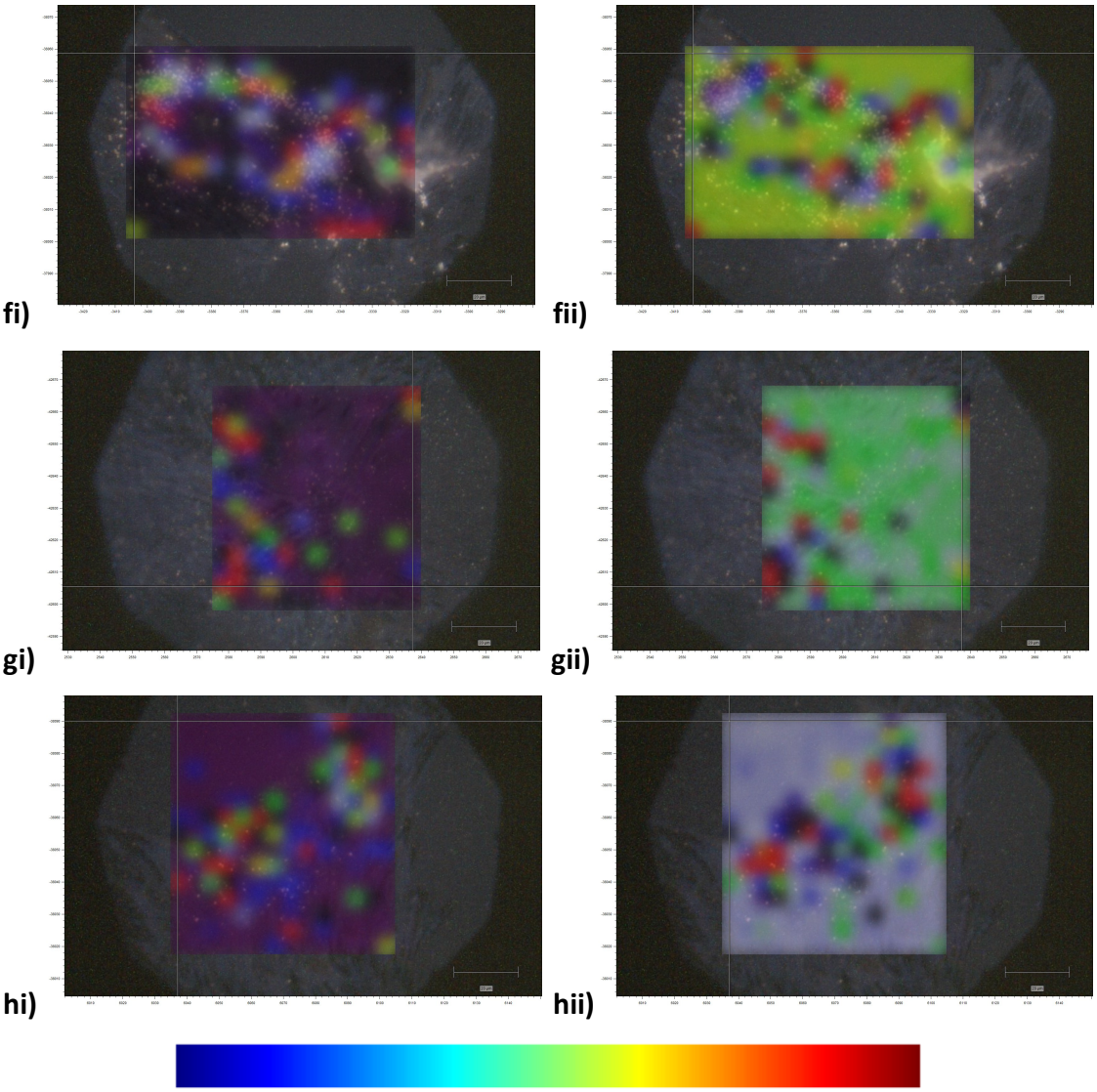

Figure 37: Raman shaded maps for cell cocultures grown in indirect contact with SERS showing shading by signal to baseline analysis for wavenumbers i)600-800cm^{-1} and ii) 1325-1345cm^{-1}. Colour bar shown as reference for shading; blue shows lowest relative intensity and red the highest relative intensity within the image but shading is arbitrary and not numerically equal or comparable between images. Scale bar 20μm. ai) HPAF 25% 600-800cm^{-1} shading aii) HPAF 25% 1325-1345cm^{-1} shading , bi) HPAF 50% 600-800cm^{-1} shading bii) HPAF 50% 1325-1345cm^{-1} shading, ci) HPAF 75% 600-800cm^{-1} shading cii) HPAF 75% 1325-1345cm^{-1} shading, d)HPAF 100% 600-800cm^{-1} shading dii)HPAF 100% 1325-1345cm^{-1} shading ei) PSC 100% 600-800cm^{-1} shading eii) PSC 100% 1325-1345cm^{-1} shading, fi) PSC 25% 600-800cm^{-1} shading fii) PSC 25% 1325-1345cm^{-1} shading , gi) PSC 50% 600-800cm^{-1} shading gii) PSC 50% 1325-1345cm^{-1} shading, hi) PSC 75% 600-800cm^{-1} shading hii) PSC 75% 1325-1345cm^{-1} shading.

Shading by signal to baseline for 600-800cm^{-1} and 1325-1345cm^{-1} for cells grown in indirect contact, showed greater differences than those grown in direct contact (Figure 37, Appendix, Figure 43). Although, there was some overlap between areas of highest relative intensity of the two regions, there were a number of locations showing highest intensity of wavenumber in the 600-800cm^{-1} region, which showed the lowest intensity of 1325-1345cm^{-1}; a difference which was not as apparent in the images of cocultures grown in direct contact (Figure 37, Appendix, Figure 43). Interestingly, the areas of highest intensity for 600-800cm^{-1} are often adjacent to areas with highest 1325-1345cm^{-1} intensity. This may suggest, in a single cell type, shading may be identifying differences within the nucleus based on differences between the nucleotide conformation and in nucleic acids. In contrast, the coculture of more than one cell type obscures this variation, potentially because of the interaction and attachment between cells impacting the distribution, especially where cells may grow on top of each other due to lack of space, or by causing changes to the DNA.

Much like the shading for cocultures grown in direct contact, the background when shaded according to signal of the 1325-1345cm^{-1} region, shows a higher relative intensity than the background with maps shaded to 600-800cm^{-1} (Figure 37, Appendix, Figure 43). There is however, much more variation in this background intensity in the single cells, although it is difficult to compare between images of different coculture proportions to determine the significance of this difference.

6.8 ELISA

Quantitative ELISA showed cells grown in indirect contact to produce much more SPARC than those grown in direct contact. In line with the literature, HPAF-II cells grown alone did not produce any SPARC, confirming that it is the PSCs in pancreatic tumours responsible for SPARC production (Figure 38).(44, 49, 50) PSCs alone also produced very little SPARC, compared to the production in cocultures, suggesting that the interaction between PSCs and HPAF-II stimulates SPARC production. This stimulation appears to occur regardless of whether the cells are in direct or indirect contact.

The significantly greater production of SPARC by cells grown in indirect contact may in part be a result of a higher seeding density and differences in passage of the stellate cells, when setting up coculture experiments. Alternatively, similarly to the variance seen in the PCA of the Raman spectra of cocultured cells, the direct contact between cells may inhibit cell proliferation and SPARC production in a way which does not occur when cells interact indirectly.

The serum sample (from patient 1) contained the highest concentration of SPARC, and very similar concentration to cells grown in indirect contact at HPAF:PSC 50:50 proportion (Figure 38). For cells grown in indirect contact, a 50:50 proportion produces the highest SPARC concentration, and for those grown in indirect contact 25:75 proportion produces the highest SPARC concentration, although the standard deviation bars suggest the 25:75 in indirect contact could produce more SPARC than a proportion 50:50 in indirect contact (Figure 38). Given the size of the standard deviation bars, especially for the 25:75 grown in indirect contact, further repeats may need to be done to validate these results.

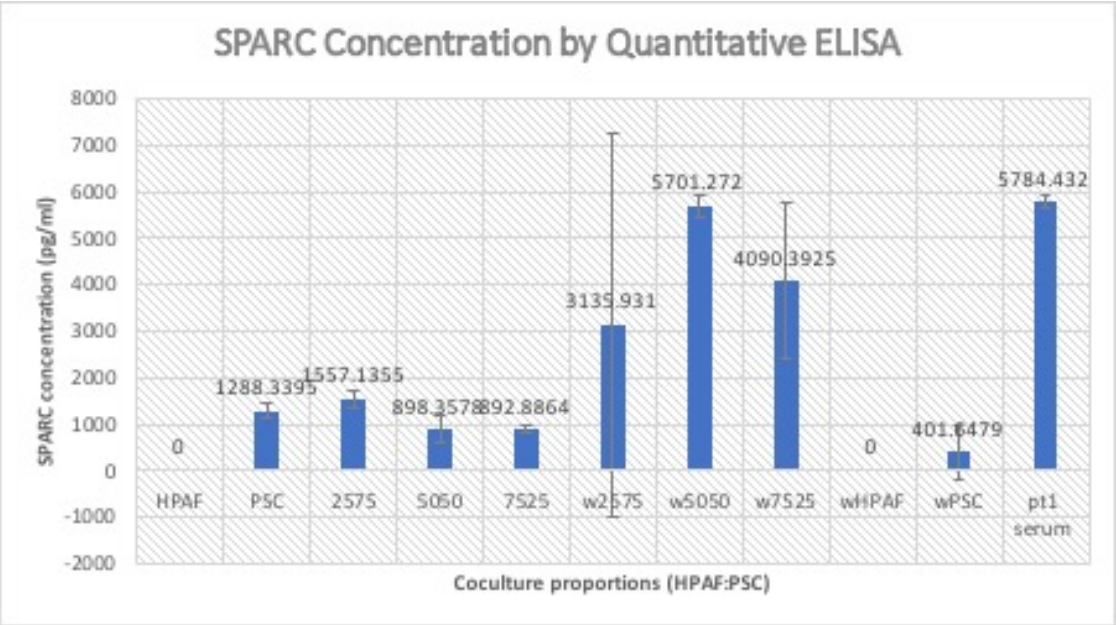

Figure 38: Bar chart, with standard deviation bars, showing SPARC concentration values using quantitative ELISA, from media from cell cocultures and serum from patient 1. 'w' indicates media taken from cocultures grown in indirect contact in wells plates with an insert.

Chapter 7 – Discussion

Raman spectroscopy has been used to identify a number of cancers, both at a diagnostic stage and during surgery to guide resection.(84, 91) However, the literature gives little insight into its potential use in pancreatic cancer. There has been very little research into identifying differences between cancerous and healthy tissue in pancreatic cancer using Raman spectroscopy and all of the current literature differentiating healthy pancreas from that which is diseased does so using animal models.(95, 96) There is some work aiming to identify a serum biomarker for pancreatic cancer, however, this is largely focussed on the development of nanoparticles and immunoassays to improve sensitivity and specificity, particularly of the MUC4 marker, as opposed the identification of a novel biomarker.(28, 92-94)

This study investigates the utility of Raman spectroscopy in differentiating healthy pancreas from cancers of the exocrine pancreas, using both human tissue and blood samples, ultimately aiming to identify novel biomarkers which could be used in screening, diagnosis or in the surgical guidance of resection margins. It further investigates the ability of Raman spectroscopy and SERS, to identify and provide information about the characteristics of pancreatic cancer, with a focus on cancer cells and PSCs and their interactions, in a 2D cell line model.

7.1 Importance of Collagen in Differentiating Healthy and Cancerous Tissue

Variation between cancerous and healthy tissue, in fresh tumours of the same pathological staging, is seen due to differences in proline and presence of nucleic acid in the tissue, and identified due to differences in collagen in fixed tissue. As PCA-LDA identified that collagen is most altered during the fixing process, the differences in collagen seen after accounting for differences in sample preparation may suggest that the composition and quantity of collagen varies between healthy and cancerous tissue, and potentially even between tumour types, in a way that is related to and allows identification of the malignant nature of the tissue. This variation, due to collagen, may be enhanced on PCA when tissue is fixed, as the cross-linking of

proteins caused by fixing has a greater impact on collagen proteins than other components in the tissue, therefore highlighting differences in the cancer which are caused by collagen.(85, 100) The higher intensity of the collagen peak in fixed cancerous tissue is visible on the pre-processed spectra.

The role and presence of collagen in pancreatic cancer is already well described in the literature. It is understood that human PDAC tumours have a high collagen content, with one study suggesting approximately 41% of the tumour area is composed of collagen in human sections.(109) In the healthy pancreas specific organized expression of collagen is needed for maintenance of epithelial structure and for healthy organ function and maintenance. However, pathological deposition of collagen causes fibrosis and plays a role in pancreatic carcinogenesis.(110) This study suggests that Raman spectroscopy may able to identify this excess deposition and change in collagen, which could in turn be used to identify tumour margins, and in the diagnosis of pancreatic cancer.

Importantly, pancreatic cancer cells increase Snail expression, in response to contact with collagen type 1, and Snail expression has been shown to be a regulator of EMT, an early and important change in the development of pancreatic cancer.(110, 111) Hence, the presence of collagen is an early feature in the development of pancreatic cancer and one which promotes the development and progression of pancreatic cancer. An ability to accurately and sensitively identify collagen presence at a stage when it is promoting EMT, a precancerous lesion, may allow for the development of a method which enables earlier detection of pancreatic cancer. Collagen alignment is also positively correlated with EMT expression and high collagen alignment has been shown to be an independent prognostic factor in PDAC.(112) Raman spectroscopy was able to attribute differences due to the twisting or wagging of CH_3CH_2 in collagen to identify differences between cancerous and normal tissue in both fresh and fixed tissue. Further identifying the degree to which this change was linked to the collagen alignment may be interesting further work. This could be achieved by comparing amide III to amide I ratio, which increases with increased collagen alignment and observing changes to the shape of the amide III band at 1270cm^{-1}.(113)

Collagen is also thought to promote cancer cell survival, as nutrient-derived PDAC cells are shown to take up collagens through a number of mechanisms.(109) This collagen can be broken down to become a source of proline, which is used as a source of nutrients in glucose depleted conditions and is able to fuel tricarboxylic acid cycle metabolism to generate ATP.(109) This is in line with data from this study which shows that in fresh tissue there is separation of cancerous and healthy tissue due to differences in proline; confirming and providing some explanation for the likely increased presence of proline, as opposed to any other amino acid, in cancerous tissue where it is not present in healthy tissue. It also suggests that the variation seen in fresh tissue, as due to proline, and those seen in fixed tissue, as due to collagen, may be linked. This adds weight to the hypothesis that variation between cancerous and healthy tissue, seen in fixed tissue as due to collagen, may be a result of this variation being enhanced and highlighted by the alterations to collagen that occur during fixation.

Sample preparation may have had impact on the variation seen between cancerous and healthy tissue, in fresh tissue due to peak 1662cm^{-1}, indicating nucleic acid in tissue, as it is known that formalin fixation induces changes in nucleic acids.(85) Pre-processed spectra show a lower intensity of the peak in healthy tissue and higher intensity in cancerous tissue, but a greater difference in intensity seen in fresh tissue than fixed. This suggests that this is an important change, but one which can only be identified using PCA in fresh tissue.

7.2 Utility of Raman Spectroscopy in Identifying Cancer Stages and Healthy Tissue

Comparison of scores plots of fresh tissue, with spectra classed by cancer type or by patient, shows that spectra thought to be taken from cancer overlap, regardless of which patient they are taken from. Spectra taken from normal and unknown tissue show much more difference between patients and are separate from cancer (Figure 16b, Figure 18b). This overlapping, central section at the mean of PC1 may suggest that changes due to cancer are such that the natural variance between patients is

reduced as tissue becomes malignant, creating a tissue type that is more homogenous both within and between patients. It could be proposed that the natural variance between patients is overtaken by a greater variance between cancer and healthy tissue, due to structural change including the production of collagen and resultant production of proline as well changes to the nucleic acid presence in the tissue: this is highlighted by PCA.

A comparison of the scores plots with spectra taken from tumour tissue identifies patient 4 as a very separate group (circled on Figures 7b and 8b), separating from all other tissue, regardless of whether this other tissue was cancerous, healthy or unknown, along PC2 in both fresh and fixed tissue. Also, as the tissue from patient 4 was a core biopsy it was not possible to identify if the tissue was cancerous or healthy and so was all classed as unknown. Notably patient 4 had the most advanced tumour, at stage IIb, whereas patient 1,2 and 3 had stage IIa tumours. This may suggest that Raman spectroscopy combined with PCA is able to identify a more advanced tumour, based on variations in collagen as well as DNA and lipid peaks. This strengthens the hypothesis that collagen is a structure which varies with the progression of pancreatic cancer and in a way which, using Raman spectroscopy, can be used to identify the presence and stage of the cancer.

Differences between cancerous and normal tissue can be identified in both fresh and fixed tissue due to structural changes in the tissue but the identifying cause of the variation changes dependent on the method of sample preparation. Clinically this could have remarkable potential as it could mean that tumours could be staged more accurately pre-operatively, therefore reducing the number of patients who are found to have non-resectable tumours during surgery and be used intraoperatively to increase the number of complete resections. Notably, at present it is also thought that 6-9% of pancreatic resections are done inappropriately for pancreatitis and so a more accurate preoperative method of diagnosis is imperative.(28) Equally, PCA shows there are still identifiable differences in fixed tissue which is useful for more thorough diagnosis of resection status and histologic type of the tumour after surgery, and for research purposes where it is useful to be able to preserve tissue.

The current method of identifying a tumour margin according to gross features of cancer, even with an experienced surgeon, is highly subjective and allows a high possibility of there being an incomplete tumour margin. One study indicated that if pathological assessment is detailed and standardized, margin involvement is found in >75% of pancreaticoduodenectomy specimens for pancreatic cancer.(114) Furthermore, there are difficulties in distinguishing between pancreatic, ampullary and distal bile duct cancers using histological methods, with frequent reclassification of the origin of the tumour, which also causes a wide range of rates of microscopic margin involvement in pancreaticoduodenectomy specimens, dependent on the pathological assessment.(105) This inconsistency in reporting means the clinical significance of margin involvement status in pancreatic cancer, and also ampullary and distal bile duct cancers, is unclear.(105) These difficulties in identifying both cancer type and tumour margins pose problems not only clinically for patients, as there can be uncertainty around diagnosis even after pathological assessment, but also for research as results are often compared to the current 'gold standard' of pathological assessment. Therefore, comparison of results between studies using human tissue could be of limited value.

This presents an even greater need to identify a method of distinguishing between cancer types and identifying the tumour margin with much greater accuracy than is currently available, both intraoperatively and during histopathological assessment. Although a great deal of further work is needed, Raman spectroscopy could be a potential method by which this could be achieved, possibly by identifying the presence and changes to collagen in the tissue. In addition, the results of this study show promise for the application of Raman spectroscopy to blood samples, to identify between types of pancreatic cancer.

7.3 Potential use of Raman Spectroscopy on Blood Samples

Spectra taken from blood samples, both with and without the use of AuNP, showed extremely clear natural variance between patient samples, with no overlap of 95%

confidence ellipses. As there was a sample from each cancer type, it could suggest that some of the variance was the result of differences in cancer, although it is difficult to discern if the differences are due to the cancer types or the patients themselves. It is possible that both factors play a role. There are a number of clinically insignificant variables which may be causing this variance; the simplest and most likely of which is ABO blood typing, the status of which was unknown for all of the patients.

A recent study showed variation between blood types using Raman spectroscopy.(115) However, laser tweezers Raman spectroscopy was used in order to achieve this result, in order to trap and manipulate cells in a way that would consistently exploit these differences, to avoid the impact of the Brownian motion of cells in an aqueous solution.(115) Conversely, the current study utilised this Brownian motion to acquire spectra from a range of components in the blood, thus reducing the impact any single variable related to a single component in the blood, such as ABO type, might have on variation. Despite including this variety of blood components in each sample, the spectra taken from each sample were very tightly clustered, with very clear separation seen between samples.

Differences between blood type were seen as a decrease in Raman signal at 1224cm^{-1} in blood type AB compared to other groups and changes to the shape of the spectral range at 1500-1700cm^{-1}, including the 1620cm^{-1} ν(C=C) bond.(115) These 2 peaks were the only ones suggested to contribute to differences in blood type, which overlapped with peaks identified on the PCA loadings plot from this study as causing variation between blood samples, indicating that the variations seen between blood samples are not just because of differences in blood type. Moreover, it was noted in the literature that the differences between Type A, Type B and Type AB are slight, whereas in the results, PCA identifies very significant differences between the samples.(115)

Equally, each patients' comorbid conditions, diet and the time of day at which the sample was taken, amongst other factors could add to the variation between the

samples. It is however, impossible to control for every potential factor and having more samples in the study may identify some of these confounders. Moreover, when blood samples are taken for clinical purposes, these factors cannot be controlled for and so identifying the degree to which the cancer contributes to the variation as opposed to the contribution of other factors would be important for clinical translation. The small sample size and lack of healthy controls or those with pancreatitis is a key limitation in this study, making it difficult to identify the degree to which this variation is disease specific. However, PCA evidently identifies clear variation between blood samples, in a way that cannot be attributed to blood type alone. Therefore, acquiring a larger sample size, including control samples, would be the next step in understanding the potential utility of Raman spectroscopy in the diagnosis of pancreatic cancer using blood samples and identifying which peaks in these spectra are specific to or due to pancreatic cancer.

The PCA loadings plot for blood samples identified peaks at 1556cm-1 and 1563cm-1, as peaks which contributed to the variation between blood samples with and without the addition of AuNP. These peaks do not have a clear association in the current literature,(107) and the relative importance of these peaks in unknown. However, given that there has been considerable research on the use of Raman spectroscopy on blood, which has not identified these peaks, could suggest that these peaks are unique to blood samples taken from patients with pancreatic cancer and are substances which are being enhanced with the use of SERS.(116)

In order to understand the utility of Raman spectroscopy and identify peaks which are specific to pancreatic cancer, it may be helpful to identify features which are similar between tumour tissue and blood. This would indicate if there are any molecules which are secreted by the tumour into the blood. PCA showed clear variation, with no overlap between a blood sample and tissue sample taken from the same patient, which is likely to be because there are significant differences between the samples as they are different types of tissue. Hence, it is likely that any secreted molecules make up a comparatively small part of the samples that their contribution

to the similarities in the spectra are masked by the great variation in other tissue components, especially using PCA which primarily identifies variation.

7.4 Potential Biomarkers – SPARC and Collagen

While it is currently possible to identify similarities and differences in a single known peak, this is dependent on first knowing which peak and associated molecule is linked to pancreatic cancer. SPARC has been shown to be present in tumour tissue and in serum samples, with an identified link between SPARC concentration in the serum and tumour size.(74) Therefore, it may be useful in further work to utilise Raman spectroscopy to identify and quantify the presence of SPARC in tissue and serum, as it is known that this is a molecule present in both samples. This would be comparable to quantitative ELISA testing and if able to be utilised would be a faster method of quantifying serum SPARC concentration, as the spectrum took only 10 minutes to acquire and required no sample preparation.

Using the presence of SPARC, alongside the presence of collagen as identified in this study, may also create a highly specific marker for the tumour margin in pancreatic cancer. Importantly, unlike collagen which is found in the basement membrane in healthy pancreatic tissue, there is no SPARC expression in the normal pancreas but this expression arises in invasive PDAC and remains throughout metastasis, although it is restricted to the stroma of the tumour.(50, 53) Therefore, using a combination of SPARC and collagen as important spectral features, may create a highly specific set of spectral markers to identify tumour margin. SPARC has also previously been identified as being upregulated in the initial stages of acinar destruction and lost in the final stages of acinar destruction and during acinar to duct metaplasia; events which are known to precede PanIN and PDAC.(52) Therefore, being able to identify the point of highest SPARC expression intraoperatively would also indicate the point at which metaplastic changes had begun and so indicate the edge of the resection margin, with greater accuracy, which may enable sufficient resection to the reduce the rate of recurrence of the disease.

This study has not found specific peaks associated or indicative of the presence of SPARC in the tumours. However, it has been identified by immunohistochemical staining, in the literature, suggesting the molecule is present in tumour tissue.(44, 49) SPARC also has a follistatin-like domain, which is rigidly stabilized by five disulphide bonds and contains a β-hairpin subdomain.(45) The presence of disulphide bonds may be able to characterise the molecule, however these are associated with a peaks at 509cm^{-1}, 535cm^{-1} and 540cm^{-1}, which was outside of the spectral range in this study. Therefore, there may be value in including this region of the spectral range in future work.

7.5 Relationship Between HPAF-II cells and PSCs

The presence of SPARC in cell line cocultures was also identified using quantitative ELISA. Identifying SPARC distribution, using immunohistochemistry, on the cell line cocultures would also have been an interesting comparison to the immunohistochemistry of the tumours and given information about the influence of different proportions of HPAF-II:PSCs on the expression and distribution of SPARC. However, in the current study the cells were inadequately fixed to the slides to enable immunohistochemical staining.

Quantitative ELISA showed that HPAF-II cells did not produce any SPARC but that the presence of cancer cells was necessary for maximal SPARC production. This indicates that there is a complex relationship between HPAF-II cells and PSCs, requiring the presence but not the direct contact of both cell types to stimulate SPARC production. The complexity of the relationship between cancer cells and PSCs identified in the literature and the incompletely understood formation and role of stroma produced by PSCs is acknowledged as a remaining an area of difficulty in the development of a therapeutic target for pancreatic cancer.(12, 110) While PSCs are shown to enhance the malignant phenotype of cancer cells, removal of PSCs has been shown to promote pancreatic cancer in mouse models.(110)

The complexity of the relationship between HPAF-II and PSCs was also identified in data acquired from Raman spectra. Coculturing cells at any proportion created spectral differences in both HPAF-II and PSCs beyond the natural differences between uninfluenced HPAF-II and PSCs, suggesting there are biochemical changes to the cells themselves. In cocultures grown at HPAF:PSC 25:75 and 75:25 proportions, HPAF-II cells grown in indirect contact with PSCs showed complete separation from both PSCs and HPAF-II cells grown in direct contact with PSCs. This suggests that either the direct contact with PSCs causes cancer cells to acquire characteristics resulting in them becoming more similar to PSCs or that the indirect contact with PSCs induces a change in HPAF-II which is otherwise not present in direct contact between the cell types. While previous studies have identified that the cell culture supernatant from pancreatic cancer cells triggers production of ECM proteins and proliferation of PSCs and that culturing of cancer cells with PSC supernatant enhances rate of growth, proliferation and migration of cancer cells,(12, 103, 117) biochemical changes to the cells themselves have not previously been described.

Activated PSCs are thought to produce 641 proteins, as opposed to 46 proteins secreted by quiescent PSCs, including matricellular proteins such as SPARC and a number of extracellular-matrix proteins, including collagen, stimulated by PDGF, TGF-β and FGF-2.(103, 108) These growth factors are also able to promote the proliferation of cancer cells, through the activation of the Akt and MAPK signalling pathways, and are likely to have been present in the coculture media. (108, 117) Activation of PSCs has also been shown to be stimulated by growth factors, including PDGF, TGF-β and FGF-2, from injured acinar cells and cancer cells.(103) Hence the two cell types have a synergistic relationship where they are able to promote one another's activation and proliferation.

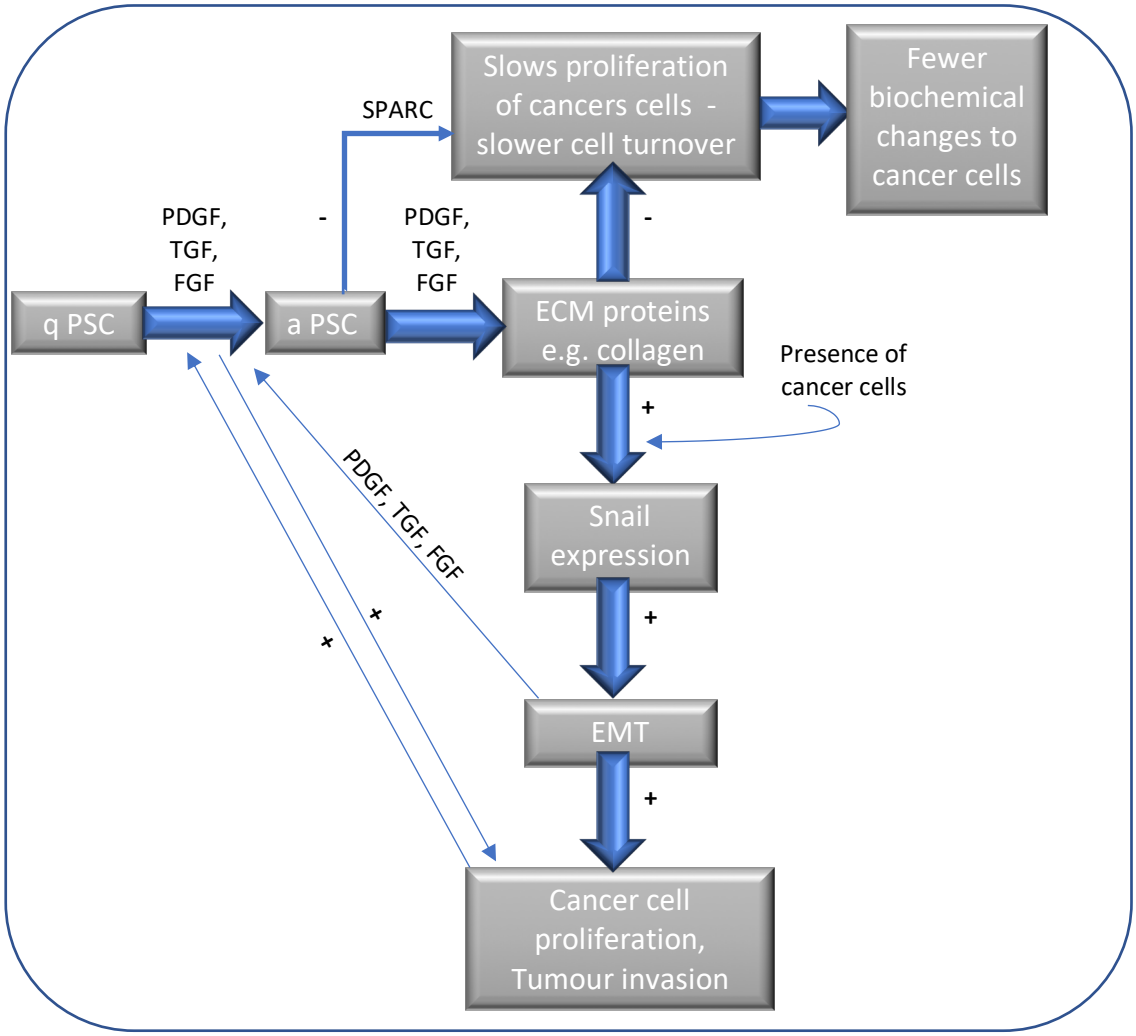

Figure 39: Diagram created by H. Bham showing proposed interactions between HPAF-II and PSCs, drawing together processes from the literature. Quiescent PSCs (qPSC) are activated by platelet derived growth factor (PDGF), tumour growth factor-β (TGF) and fibroblast growth factor-2 (FGF).(103) Activated PSCs (aPSC), stimulated by PDGF, TGF and FGF secrete matricellular and ECM proteins, including collagen and SPARC.(49, 103) Presence of collagen and its contact with cancer cells increases Snail expression causing epithelial mesenchymal transition (EMT), which sensitises surrounding healthy tissue to tumour invasion, causing cancer cell proliferation.(110, 111) Injured acinar cells (resulting from ADM and EMT) and cancer cells produce, PDGF, TGF and FGF causing further activation and proliferation of PSCs.(103) Physical presence of collagen and production of SPARC also slow proliferation of cancer cells, reducing the rate of cell turnover, meaning there are fewer biochemical changes to the cells.(47, 59, 110)

However, recent evidence suggests that the presence of stroma and production of collagen, may have a protective role in pancreatic cancer.(45, 59, 64, 110) It is thought the production of collagen and fibrosis restricts the growth of the tumour. In order to do so, it may slow the proliferation of cancer cells, meaning fewer biochemical changes occur due to reduced cell turnover. This would mean that when

cells are grown in direct contact the presence of collagen slows the growth of cancer cells causing fewer changes to the cell (Figure 39). Cells grown in indirect contact with PSCs would still be exposed to growth factors in the shared media and so be able to proliferate as a result of the relevant signalling pathways, but without exposure to collagen meaning the growth of the cells would not be inhibited (Figure 39). This would create a higher rate of cell turnover and greater biochemical change, creating the variation seen on PCA between HPAF-II cells grown in direct and in indirect contact with PSCs. If the higher relative intensity of 1325-1345cm^{-1} peaks, compared to 600-800cm^{-1} peaks in the background of coculture maps suggest the possible beginnings of stroma formation, and so presence of collagen, this would corroborate the hypothesis.

While this variation between HPAF-II cells grown in direct and in indirect contact was not seen in the 50:50 proportion, this may be explained by the production of SPARC seen on quantitative ELISA. The 50:50 proportion, in indirect contact produced the highest concentration of SPARC, which is thought to have a tumour suppressor function and has been shown to reduce the rate of cancer cell proliferation.(47) The presence of this tumour suppressor at this concentration in the media may have been sufficient to promote apoptosis and slow proliferation of the HPAF-II, even without the presence of collagen, for cells in indirect contact, preventing the biochemical changes from occurring to the same degree (Figure 39). Hence, cocultures in indirect contact at this proportion showed less variation than at other proportions.

Comparison between cell line cocultures and cancerous tumour tissue, shows clear differences along PC3 are due to differences in carbohydrates and proteins, which suggests there are factors in vivo which create these differences that have not been replicated in this coculture study. Although in vivo conditions are extremely difficult to replicate, especially in a 2D model, some of these differences may be caused by the lack of other important cell types such as tumour associated macrophages. (12) These cells have also been shown to be able to promote both an anti-tumorigenic and pro-tumorigenic response, which is thought to be dependent on the ratio of

tumour cells to macrophages.(12) PSCs have also been described as a heterogenous population, and this heterogeneity is unlikely to be reflected in a cell line model.(59)

7.6 Strengths and Limitations

This is the first study to use Raman spectroscopy on human tissue to identify variation between healthy and cancerous pancreatic tissue. It is also the first to use Raman spectroscopy and SERS without immunoassay on blood from patients to attempt to identify features which may be linked to the presence and type of pancreatic cancer. Although the study has a very small sample size and a lack of control blood samples, creating difficulty when drawing conclusions, it does identify variation between cancerous and healthy tissue, based on differences in nucleic acid content, proline and collagen. It further identifies clear natural variance in blood samples from different patients, with different types of cancer, which can be attributed to more than differences in blood type. These observations have significant potential clinical utility if the results can be validated in a larger study.

Previous studies have demonstrated properties and interaction of HPAF-II and PSCs in coculture, both in direct contact and culturing using the supernatant of the opposite cell type.(103, 117) However, this is the first study to coculture HPAF-II and PSCs in indirect contact, using an insert in a wells plate, creating an environment with concurrent presence and interaction but not the direct contact of the cells. It is also the first to identify variation and characteristics of the cells related to pancreatic cancer using Raman spectroscopy.

The results of quantitative ELISA of SPARC, while comparable between cocultures of different proportions in the same environment, should be interpreted tentatively when looking at differences between cells grown in direct compared to cells grown in indirect contact. This is due to differences in the seeding density of cells, when setting up this experiment. Repeating this experiment, with cells seeded at the same density for both coculture in direct and indirect contact would give more comparable results.

The use of SERS and mapping images in comparing the impact of coculture could be of great value, as SERS extracted highly specific and varied spectra, which is likely to give very specific data about components of the cells. However, the analysis of the data was very limited and the inability to compare between different maps offers limited comparison between cocultures of differing proportions and environments.

7.7 Further Work

7.7.1 Analysis of SERS data

The difficulties in analysing SERS data because of the variety and single molecule sensitivity of spectra are described by Pavillion et al.(118) The SERS signal is dependent on the local presence and aggregation of nanoparticles and their interaction with the local molecular environment. Moreover, it is known that the 'best spectra' are often not found where they might be expected in the AuNP distribution, even in the presence of nanoparticles.(118) This means only a fraction of the data collected is of interest, and so there is a need to reduce the dataset to only include the relevant spectra to enable more specific analysis.

An algorithm has been developed by Pavillion et al, which enables detection, extraction and clustering of the most relevant SERS spectra, which are present on a localisation map.(118) The algorithm retains spatial information, making it possible to trace spectra from their location on the map, and has been used on live cells, showing its applicability to biological samples.(118) While the information itself is of great value, the reduced dataset can also be used for further analysis such as PCA.(118)

This algorithm could of great value when analysing the SERS maps from coculture experiments, allowing identification of pertinent similarities and differences in the spectra of individual components of the cells. There is an ongoing collaboration with authors of Pavillion et al 2013 to adapt the algorithm, making it compatible with SERS data from this study, to enable further analysis of the data.

7.7.2 Further experiments with Cocultures

Given the identifiable differences between differing proportions of HPAF:PSC, extending this experiment to include more proportions, for example 90:10, would validate the impact PSCs have on HPAF-II cells and may identify the threshold at which this impact occurs. Using a variety of pancreatic cancer cell lines may also be valuable as the varying genotypes and phenotypes of the available pancreatic cancer cell lines have been shown to vary and give differing results when detecting tumorigenicity and angiogenesis.(119) The HPAF-II cell line is also a well differentiated cell line, from a 44 year old male with distant metastasis, unlike the patients in this study who were both older and had moderately differentiated tumours.(119) Using an additional cell line may therefore be of value, especially if the aim is to identify changes concurrent with the early interaction of PSCs and HPAF-II and their role in the development of PDAC, when patients would not have metastasis. The addition of tumour associated macrophages may also be valuable, as these have been shown to play an important role in tumorigenesis and have been shown to be viable in coculture.(120) The use of alternative cell lines and the addition of tumour associated macrophages may also make the cocultures more comparable to the human samples.

Coculture of HPAF-II and PSC in this study appears to secrete ECM proteins, including collagen, which is identified as being of importance after data analysis, after the cells were grown for 7 days. This study proposes the hypothesis that interaction between the cell types and biochemical changes to the cells are possibly related to deposition of collagen and production of SPARC and their inhibiting effects on cancer cell proliferation (Figure 39). HPAF-II cells have also been shown to produce tumours in mice 100 days after orthotopic injection, however, it is likely that ECM production occurs much earlier than this.(119) Further work understanding when the ECM is produced, with a focus on collagen production and when it begins to have an impact on the cell characteristics would be valuable in further understanding the interaction between HPAF-II and PSCs. Scanning the cells at different time points during the 7 days would also identify the point at which the most collagen is secreted and if this secretion is limited at any stage. Determining the timepoint at which the collagen

secretion and alignment is most similar to that in tumour samples would also help to validate any cell line model and understand its ability to function in a way similar to a tumour. Improving this functionality enables the production of cell line models which are closer to in vivo conditions, aiding the applicability and translation of research, such as drug testing, to clinical conditions and practice.

7.7.3 Optimisation of Immunohistochemistry

This study also attempted to identify SPARC expression from cell cocultures using immunohistochemical staining, however the cells were inadequately fixed to the CaF_2 slides to enable staining. This may in part have been a result of using CaF_2 slides, which, although needed for optimum Raman spectra, are not ordinarily used for staining techniques. A previous study has however used alternative slides and clamped these to an aluminium plate to enable both immunofluorescence and Raman spectroscopy on the same sample of cells.(121) Another study has also shown potential for Raman spectroscopy of cells grown on polymer substrates such as agar, which may be particularly useful as these substrates are more able to imitate natural microenvironments such as ECM. (122) However, this is done by subtracting the Raman signal of the polymer substrate from the overall Raman spectrum, which may result in variable quality of the spectra. (122)

These alternative methods may enable both immunohistochemical staining and Raman spectroscopy of cell cocultures, providing more information, particularly about the morphology of the cells, and a comparison between information identified by different techniques. However, it is known that the Raman signature from polymer substrates can create noise in the Raman signal,(122) and this limitation would need to be carefully considered and balanced with the advantages of growing cells on a polymer substrate.

Moreover, the immunohistochemistry technique also needs to be optimised, for both cell samples and tumour tissue, as the SPARC antigen was not detected in the tumour tissue in this study. This may include altering the antibody dilutions, increasing

incubation periods and optimising antigen retrieval times as well as ensuring samples remain on the slides while being processed.

7.7.4 Development of a SERS based Immunoassay

The development of a SERS based immunoassay, identifying SPARC would also be valuable and an interesting comparison to histological techniques, in further research around the importance of SPARC, particularly in the early stages of pancreatic cancer. Such a development would also have great potential clinical utility, if SPARC was to be validated as a reliable marker for screening or diagnosis of pancreatic cancer. The development of nanoparticles, with improved sensitivity and specificity, for clinical use is already an extensive area of research and has been an essential part of the research around the use of Raman spectroscopy in other cancers.(123) It is also research which has attracted some attention in the use of Raman spectroscopy in pancreatic cancer, although the focus has largely been on the CA19-9 and MUC4 biomarkers.(28, 92, 94)

Another study, in mice, showed the potential to use injected SERRS nanostars to detect tumour margins at resections.(96) It identified that SERRS nanostars accumulated in the tumour stroma and within epithelial tumour cells and were also found in and able to identify PanIN lesions, showing high specificity for malignant tissues.(96) This suggests that pancreatic cancer lesions are able to take up SERRS nanostars and so a tumour margin could be identified very clearly in patients injected with these preoperatively. However, this uptake might vary between mice and human patients and require development of a nanoparticle which is both non-toxic and can be easily excreted, especially as it is known that some nanoparticles are toxic.(124) This could require significant work before there is potential for clinical translation. This study, however, demonstrates the potential of Raman spectroscopy, which is known to be safe in vivo, to differentiate between cancerous and healthy human tissue, without the use of nanoparticles, in pancreatic cancer. The development of a probe to detect these changes intraoperatively, would be an important step for translation to clinical practice.

7.7.5 Combining Clinical and Spectroscopic Techniques

In the context of pancreatic cancer, combining spectroscopic techniques, including SERS and SORS with clinical techniques such as ERCP and endoscopy could allow for the development of a more sensitive or specific diagnostic technique. The potential for these techniques to be combined has been widely researched and the development of probes for clinical use is an ongoing field with great potential.(125) A probe, which can be attached to an endoscope, has been developed to detect changes in the oesophagus, suggesting there is potential to develop a similar probe for use in ERCP or EUS.(125)

Conclusion

Pancreatic cancer presents an increasing mortality burden, with few of the recent developments in treatment having a significant impact on the poor survival rates. The significant mortality burden can in part be attributed to difficulties in detection of the disease, during diagnosis, surgery and pathological assessment; 80% of cancers are diagnosed at an advanced and unresectable stage and 95% of cancers recur within 2 years of resection.(1, 38) Lack of accuracy during histopathological assessment also causes problems for research as there is limited comparability between studies.(105) This presents a significant need for the advent of a new technology, with greater accuracy and potential clinical utility.

Raman spectroscopy has been widely researched for its potential biomedical applications.(85) It has further been used in the detection and surgical guidance of a number of cancers, although its application to pancreatic cancer is very limited.(91)

The aim of this study was to demonstrate the potential utility of Raman spectroscopy in identifying the development of pancreatic cancer and differences between healthy and cancerous pancreatic tissue.

Using a 2D cell line model this study highlights the complexity of the relationship between cancer cells and PSCs. It identifies SPARC production using ELISA, showing

the need for the presence of both cell types for maximal production and suggests a role for collagen in inhibiting cancer cell proliferation. The interactions between HPAF-II and PSCs are thought to cause biochemical changes to cancer cells, which were identified using Raman spectroscopy. Cells grown in indirect contact showed greater variation than those grown in direct contact, with particular changes observed in cancer cells grown in indirect contact with PSCs. Although an unexpected result, the data from this study, alongside processes drawn from the literature, propose a hypothesis for the interaction between cancer cells and PSCs, suggesting that the physical presence of collagen may limit the rate of cancer cell proliferation and so the number of biochemical changes, due to reduced cell turnover.

This study also demonstrates that Raman spectroscopy is able to differentiate healthy from cancerous tissue in the exocrine pancreas, using both fresh and fixed human tumour resection samples. It shows that cancerous tissue shows greater homogeneity both within the tissue itself and between patients. It could be proposed that this homogeneity is created by the deposition of collagen and natural variance between patients is overtaken by a greater variance characterised by the presence of collagen and identified by PCA. Moreover, this study suggests that Raman spectroscopy may be able to differentiate different stages of pancreatic cancer. Significant variation between blood samples from patients with different types of pancreatic cancer were also observed and, although patient characteristics are likely to play a role, part of this variation is thought to be attributable to the differences in cancer types.

Although the small sample size is a significant limitation in this study, this is the first study to demonstrate the potential utility of Raman spectroscopy in pancreatic cancer and therefore warrants further investigation. It demonstrates clear variation between cancerous and healthy tissue as well as significant variation between blood samples. Validating these results in a bigger study could be pivotal in utilising Raman spectroscopy to improve both the diagnosis and management of pancreatic cancer, to improve survival rates and reduce the mortality burden currently associated with the disease.

References

1. Ilic M, Ilic I. Epidemiology of pancreatic cancer. World journal of gastroenterology. 2016;22(44):9694.
2. Cancer Research UK. Pancreatic Cancer Incidence Statistics 2018 [Available from: http://www.cancerresearchuk.org/health-professional/cancer-statistics/statistics-by-cancer-type/pancreatic-cancer/incidence.
3. Moore KL, Dalley AF, Agur AM. Clinically oriented anatomy: Lippincott Williams & Wilkins; 2013.
4. Longnecker DS, Gorelick F, Thompson ED. Anatomy, Histology, and Fine Structure of the Pancreas. The Pancreas: An Integrated Textbook of Basic Science, Medicine, and Surgery. 2018:10-23.
5. Skandalakis J. Small Intestine Chapter 16. Surgical Anatomy– The Embryologic and Anatomic Basis of Modern Surgery vol II. Athens, Greece2004. p. 1095-150.
6. Agur AMR LM, Grant JCB. Grant's Atlas of Anatomy 13th ed 13 ed. London, UK Lippincott Williams and Wilkins; 2013.
7. Lowe JS, Anderson PG. Stevens & Lowe's Human Histology E-Book: With STUDENT CONSULT Online Access: Elsevier Health Sciences; 2014.
8. Hruban RH, Fukushima N. Pancreatic adenocarcinoma: update on the surgical pathology of carcinomas of ductal origin and PanINs. Modern Pathology. 2007;20(1s):S61.
9. Chen W. Ductal adenocarcinoma, NOS. PathologyOutlines.com 2017 [Available from: http://www.pathologyoutlines.com/topic/pancreasductal.html. .
10. Hong S-M, Goggins M, Wolfgang CL, Schulick RD, Edil BH, Cameron JL, et al. Vascular invasion in infiltrating ductal adenocarcinoma of the pancreas can mimic pancreatic intraepithelial neoplasia: a histopathologic study of 209 cases. The American journal of surgical pathology. 2012;36(2):235.
11. Artinyan A, Soriano PA, Prendergast C, Low T, Ellenhorn JD, Kim J. The anatomic location of pancreatic cancer is a prognostic factor for survival. Hpb. 2008;10(5):371-6.
12. Khalafalla FG, Khan MW. Inflammation and Epithelial-Mesenchymal Transition in Pancreatic Ductal Adenocarcinoma: Fighting Against Multiple Opponents. Cancer growth and metastasis. 2017;10:1179064417709287.
13. Klöppel G, Lingenthal G, Von Bülow M, Kern H. Histological and fine structural features of pancreatic ductal adenocarcinomas in relation to growth and prognosis: studies in xenografted tumours and clinico-histopathological correlation in a series of 75 cases. Histopathology. 1985;9(8):841-56.
14. Cancer Research UK. TNM staging for Pancreatic Cancer 2017 [Available from: http://www.cancerresearchuk.org/about-cancer/pancreatic-cancer/stages-types-grades/tnm-staging.
15. Sobin LH, Gospodarowicz MK, Wittekind C. TNM classification of malignant tumours: John Wiley & Sons; 2011.
16. Edge SB, Cancer AJCo. AJCC cancer staging handbook: from the AJCC cancer staging manual: Springer New York; 2010.
17. Khan MA, Azim S, Zubair H, Bhardwaj A, Patel GK, Khushman M, et al. Molecular drivers of pancreatic cancer pathogenesis: looking inward to move forward. International journal of molecular sciences. 2017;18(4):779.

18. Lee AYL, Dubois CL, Sarai K, Zarei S, Schaeffer DF, Sander M, et al. Cell of origin affects tumour development and phenotype in pancreatic ductal adenocarcinoma. Gut. 2018.
19. Farrow B, Sugiyama Y, Chen A, Uffort E, Nealon W, Mark Evers B. Inflammatory mechanisms contributing to pancreatic cancer development. Annals of surgery. 2004;239(6):763-9; discussion 9-71.
20. National Institute for Health and Care Excellence. Suspected cancer recognition and referral: site or type of cancer 2018 [Available from: https://pathways.nice.org.uk/pathways/suspected-cancer-recognition-and-referral/suspected-cancer-recognition-and-referral-site-or-type-of-cancer#content=view-node%3Anodes-gastrointestinal-tract-upper-cancers.
21. Pannala R, Basu A, Petersen GM, Chari ST. New-onset diabetes: a potential clue to the early diagnosis of pancreatic cancer. The lancet oncology. 2009;10(1):88-95.
22. Tempero MA, Malafa MP, Al-Hawary M, Asbun H, Bain A, Behrman SW, et al. Pancreatic adenocarcinoma, version 2.2017, NCCN clinical practice guidelines in oncology. Journal of the National Comprehensive Cancer Network. 2017;15(8):1028-61.
23. Lévy P, Domínguez-Muñoz E, Imrie C, Löhr M, Maisonneuve P. Epidemiology of chronic pancreatitis: burden of the disease and consequences. United European gastroenterology journal. 2014;2(5):345-54.
24. National Institute for Health and Care Excellence. Pancreatic cancer in adults: diagnosis and management 2018 [Available from: https://www.nice.org.uk/guidance/ng85/chapter/Recommendations#diagnosis.
25. Toft J, Hadden WJ, Laurence JM, Lam V, Yuen L, Janssen A, et al. Imaging modalities in the diagnosis of pancreatic adenocarcinoma: A systematic review and meta-analysis of sensitivity, specificity and diagnostic accuracy. European journal of radiology. 2017;92:17-23.
26. van Veldhuisen E, Vogel JA, Klompmaker S, Busch OR, van Laarhoven HW, van Lienden KP, et al. Added value of CA19-9 response in predicting resectability of locally advanced pancreatic cancer following induction chemotherapy. HPB. 2018.
27. E Poruk K, Z Gay D, Brown K, D Mulvihill J, M Boucher K, L Scaife C, et al. The clinical utility of CA 19-9 in pancreatic adenocarcinoma: diagnostic and prognostic updates. Current molecular medicine. 2013;13(3):340-51.
28. Banaei N, Foley A, Houghton JM, Sun Y, Kim B. Multiplex detection of pancreatic cancer biomarkers using a SERS-based immunoassay. Nanotechnology. 2017;28(45):455101.
29. Dusch N, Weiss C, Ströbel P, Kienle P, Post S, Niedergethmann M. Factors predicting long-term survival following pancreatic resection for ductal adenocarcinoma of the pancreas: 40 years of experience. Journal of Gastrointestinal Surgery. 2014;18(4):674-81.
30. Benassai G, Quarto G, Perrotta S, Furino E, Benassai G, Amato B, et al. Long-term survival after curative resection for pancreatic ductal adenocarcinoma–Surgical treatment. International Journal of Surgery. 2015;21:S1-S3.
31. Barreto SG, Pandanaboyana S, Ironside N, Windsor JA. Does revision of resection margins based on frozen section improve overall survival following pancreatoduodenectomy for pancreatic ductal adenocarcinoma? A meta-analysis. HPB

: the official journal of the International Hepato Pancreato Biliary Association. 2017;19(7):573-9.
32. Hank T, Hinz U, Tarantino I, Kaiser J, Niesen W, Bergmann F, et al. Validation of at least 1 mm as cut-off for resection margins for pancreatic adenocarcinoma of the body and tail. British Journal of Surgery. 2018.
33. Torgeson A, Garrido-Laguna I, Tao R, Cannon GM, Scaife CL, Lloyd S. Value of surgical resection and timing of therapy in patients with pancreatic cancer at high risk for positive margins. ESMO open. 2018;3(1):e000282.
34. Yin Z, Zhou Y, Hou B, Ma T, Yu M, Zhang C, et al. Revision of Surgical Margin under Frozen Section to Achieve R0 Status on Survival in Patients with Pancreatic Cancer. Journal of Gastrointestinal Surgery. 2018;22(9):1565-75.
35. Mois E, Graur F, Al-Hajjar N, Zaharie F, Bartos A, Bodea R, et al. Microscopically positive (R1) resections do not affect survival in pancreatic head cancer. Annali italiani di chirurgia. 2017;88:491-6.
36. Sugiura T, Uesaka K, Mihara K, Sasaki K, Kanemoto H, Mizuno T, et al. Margin status, recurrence pattern, and prognosis after resection of pancreatic cancer. Surgery. 2013;154(5):1078-86.
37. Pahk E, Jesin R, Kluger Y, Epelbaum R, Lachter J. Predictors of Early Recurrence of Adenocarcinoma of the Head of the Pancreas after Curative Resection. JOP Journal of the Pancreas. 2015;16(6).
38. Barugola G, Falconi M, Bettini R, Boninsegna L, Casarotto A, Salvia R, et al. The determinant factors of recurrence following resection for ductal pancreatic cancer. JOP. 2007;8(1 Suppl):132-40.
39. Vaz J, Ansari D, Sasor A, Andersson R. SPARC: a potential prognostic and therapeutic target in pancreatic cancer. Pancreas. 2015;44(7):1024.
40. Yu IS, Cheung WY. A Contemporary Review of the Treatment Landscape and the Role of Predictive and Prognostic Biomarkers in Pancreatic Adenocarcinoma. Canadian journal of gastroenterology & hepatology. 2018;2018:1863535.
41. Zhang Y, Yang C, Cheng H, Fan Z, Huang Q, Lu Y, et al. Novel agents for pancreatic ductal adenocarcinoma: emerging therapeutics and future directions. Journal of hematology & oncology. 2018;11(1):14.
42. Loosen SH, Neumann UP, Trautwein C, Roderburg C, Luedde T. Current and future biomarkers for pancreatic adenocarcinoma. Tumour biology : the journal of the International Society for Oncodevelopmental Biology and Medicine. 2017;39(6):1010428317692231.
43. Han W, Cao F, Chen M-b, Lu R-z, Wang H-b, Yu M, et al. Prognostic value of SPARC in patients with pancreatic cancer: a systematic review and meta-analysis. PloS one. 2016;11(1):e0145803.
44. Infante JR, Matsubayashi H, Sato N, Tonascia J, Klein AP, Riall TA, et al. Peritumoral fibroblast SPARC expression and patient outcome with resectable pancreatic adenocarcinoma. Journal of Clinical Oncology. 2007;25(3):319-25.
45. Neuzillet C, Tijeras-Raballand A, Cros J, Faivre S, Hammel P, Raymond E. Stromal expression of SPARC in pancreatic adenocarcinoma. Cancer and Metastasis Reviews. 2013;32(3-4):585-602.
46. Spratlin JL, Mulder KE. Looking to the future: biomarkers in the management of pancreatic adenocarcinoma. International journal of molecular sciences. 2011;12(9):5895-907.

47. Guweidhi A, Kleeff J, Adwan H, Giese NA, Wente MN, Giese T, et al. Osteonectin influences growth and invasion of pancreatic cancer cells. Annals of surgery. 2005;242(2):224.
48. Rahman M, Chan AP, Tai IT. A peptide of SPARC interferes with the interaction between caspase8 and Bcl2 to resensitize chemoresistant tumors and enhance their regression in vivo. PloS one. 2011;6(11):e26390.
49. Sato N, Fukushima N, Maehara N, Matsubayashi H, Koopmann J, Su GH, et al. SPARC/osteonectin is a frequent target for aberrant methylation in pancreatic adenocarcinoma and a mediator of tumor-stromal interactions. Oncogene. 2003;22(32):5021.
50. Bloomston M, Ellison EC, Muscarella P, Al-Saif O, Martin EW, Melvin WS, et al. Stromal osteonectin overexpression is associated with poor outcome in patients with ampullary cancer. Annals of surgical oncology. 2007;14(1):211-7.
51. Zhivkova-Galunska M, Adwan H, Eyol E, Kleeff J, Kolb A, Bergmann F, et al. Osteopontin but not osteonectin favors the metastatic growth of pancreatic cancer cell lines. Cancer biology & therapy. 2010;10(1):54-64.
52. Reding T, Wagner U, Silva AB, Sun L-K, Bain M, Kim S-Y, et al. Inflammation-dependent expression of SPARC during development of chronic pancreatitis in WBN/Kob rats and a microarray gene expression analysis. Physiological genomics. 2009;38(2):196-204.
53. Gundewar C, Sasor A, Hilmersson KS, Andersson R, Ansari D. The role of SPARC expression in pancreatic cancer progression and patient survival. Scandinavian journal of gastroenterology. 2015;50(9):1170-4.
54. Hong S-M, Kelly D, Griffith M, Omura N, Li A, Li C-P, et al. Multiple genes are hypermethylated in intraductal papillary mucinous neoplasms of the pancreas. Modern Pathology. 2008;21(12):1499-507.
55. Gao J, Song J, Huang H, Li Z, Du Y, Cao J, et al. Methylation of the SPARC gene promoter and its clinical implication in pancreatic cancer. Journal of Experimental & Clinical Cancer Research. 2010;29(1):28.
56. Mao Z, Ma X, Fan X, Cui L, Zhu T, Qu J, et al. Secreted protein acidic and rich in cysteine inhibits the growth of human pancreatic cancer cells with G1 arrest induction. Tumor Biology. 2014;35(10):10185-93.
57. Seux M, Peuget S, Montero M, Siret C, Rigot V, Clerc P, et al. TP53INP1 decreases pancreatic cancer cell migration by regulating SPARC expression. Oncogene. 2011;30(27):3049-61.
58. Rossi MK, Gnanamony M, Gondi CS. The 'SPARC' of life: Analysis of the role of osteonectin/SPARC in pancreatic cancer (Review). International journal of oncology. 2016;48(5):1765-71.
59. Park H, Lee Y, Lee H, Kim JW, Hwang JH, Kim J, et al. The prognostic significance of cancer-associated fibroblasts in pancreatic ductal adenocarcinoma. Tumour biology : the journal of the International Society for Oncodevelopmental Biology and Medicine. 2017;39(10):1010428317718403.
60. Korc M. Pancreatic cancer–associated stroma production. The American Journal of Surgery. 2007;194(4):S84-S6.
61. Yu X-Z, Guo Z-Y, Di Y, Yang F, Ouyang Q, Fu D-L, et al. The relationship between SPARC expression in primary tumor and metastatic lymph node of resected pancreatic

cancer patients and patients' survival. Hepatobiliary & Pancreatic Diseases International. 2017;16(1):104-9.
62. Al-Batran S-E, Geissler M, Seufferlein T, Oettle H. Nab-paclitaxel for metastatic pancreatic cancer: clinical outcomes and potential mechanisms of action. Oncology research and treatment. 2014;37(3):128-34.
63. Nagathihalli NS, Castellanos JA, Shi C, Beesetty Y, Reyzer ML, Caprioli R, et al. STAT3 mediated remodeling of the tumor microenvironment results in enhanced tumor drug delivery in a mouse model of pancreatic cancer. Gastroenterology. 2015;149(7):1932.
64. Sasson AR, Wetherington RW, Hoffman JP, Ross EA, Cooper H, Meropol NJ, et al. Neoadjuvant chemoradiotherapy for adenocarcinoma of the pancreas. International journal of gastrointestinal cancer. 2003;34(2-3):121-7.
65. Mantoni TS, Schendel RR, Rödel F, Niedobitek G, Al-Assar O, Masamune A, et al. Stromal SPARC expression and patient survival after chemoradiation for non-resectable pancreatic adenocarcinoma. Cancer biology & therapy. 2008;7(11):1806-15.
66. Moffitt RA, Marayati R, Flate EL, Volmar KE, Loeza SGH, Hoadley KA, et al. Virtual microdissection identifies distinct tumor-and stroma-specific subtypes of pancreatic ductal adenocarcinoma. Nature genetics. 2015;47(10):1168-78.
67. Ormanns S, Haas M, Baechmann S, Altendorf-Hofmann A, Remold A, Quietzsch D, et al. Impact of SPARC expression on outcome in patients with advanced pancreatic cancer not receiving nab-paclitaxel: A pooled analysis from prospective clinical and translational trials. British journal of cancer. 2016;115(12):1520-9.
68. Miyoshi K, Sato N, Ohuchida K, Mizumoto K, Tanaka M. SPARC mRNA expression as a prognostic marker for pancreatic adenocarcinoma patients. Anticancer research. 2010;30(3):867-71.
69. Von Hoff DD, Ramanathan RK, Borad MJ, Laheru DA, Smith LS, Wood TE, et al. Gemcitabine plus nab-paclitaxel is an active regimen in patients with advanced pancreatic cancer: a phase I/II trial. Journal of Clinical Oncology. 2011;29(34):4548.
70. Sinn M, Sinn B, Striefler J, Lindner J, Stieler J, Lohneis P, et al. SPARC expression in resected pancreatic cancer patients treated with gemcitabine: results from the CONKO-001 study. Annals of Oncology. 2014;25(5):1025-32.
71. Hidalgo M, Plaza C, Musteanu M, Illei P, Brachmann CB, Heise C, et al. SPARC Expression Did Not Predict Efficacy of nab-Paclitaxel plus Gemcitabine or Gemcitabine Alone for Metastatic Pancreatic Cancer in an Exploratory Analysis of the Phase III MPACT Trial. Clinical cancer research : an official journal of the American Association for Cancer Research. 2015;21(21):4811-8.
72. Fan X, Mao Z, Ma X, Cui L, Qu J, Lv L, et al. Secreted protein acidic and rich in cysteine enhances the chemosensitivity of pancreatic cancer cells to gemcitabine. Tumor Biology. 2016;37(2):2267-73.
73. Blogowski W, Dolegowska K, Deskur A, Dolegowska B, Starzyńska T. An Attempt to Evaluate Selected Aspects of “Bone–Fat Axis” Function in Healthy Individuals and Patients With Pancreatic Cancer. Medicine. 2015;94(32).
74. Papapanagiotou A, Sgourakis G, Karkoulias K, Raptis D, Parkin E, Brotzakis P, et al. Osteonectin as a screening marker for pancreatic cancer: A prospective study. Journal of International Medical Research. 2018:0300060518772413.

75. Farrow B, Sugiyama Y, Chen A, Uffort E, Nealon W, Evers BM. Inflammatory mechanisms contributing to pancreatic cancer development. Annals of surgery. 2004;239(6):763.
76. Weeks ME, Hariharan D, Petronijevic L, Radon TP, Whiteman HJ, Kocher HM, et al. Analysis of the urine proteome in patients with pancreatic ductal adenocarcinoma. PROTEOMICS-Clinical Applications. 2008;2(7-8):1047-57.
77. Davis VW, Schiller DE, Eurich D, Bathe OF, Sawyer MB. Pancreatic ductal adenocarcinoma is associated with a distinct urinary metabolomic signature. Annals of surgical oncology. 2013;20(3):415-23.
78. Debernardi S, Massat NJ, Radon TP, Sangaralingam A, Banissi A, Ennis DP, et al. Noninvasive urinary miRNA biomarkers for early detection of pancreatic adenocarcinoma. American journal of cancer research. 2015;5(11):3455.
79. Fischer R, Breidert M, Keck T, Makowiec F, Lohrmann C, Harder J. Early recurrence of pancreatic cancer after resection and during adjuvant chemotherapy. Saudi journal of gastroenterology: official journal of the Saudi Gastroenterology Association. 2012;18(2):118.
80. Ryall CL, Viloria K, Lhaf F, Walker AJ, King A, Jones P, et al. Novel Role for Matricellular Proteins in the Regulation of Islet β Cell Survival THE EFFECT OF SPARC ON SURVIVAL, PROLIFERATION, AND SIGNALING. Journal of Biological Chemistry. 2014;289(44):30614-24.
81. Kos K, Wong S, Tan B, Gummesson A, Jernas M, Franck N, et al. Regulation of the fibrosis and angiogenesis promoter SPARC/osteonectin in human adipose tissue by weight change, leptin, insulin, and glucose. Diabetes. 2009;58(8):1780-8.
82. Gonzalez-Solis J, Luevano-Colmenero, GH, Vargas-Mancilla, J. Surface enhanced Raman spectroscopy in breast cancer cells. Laser therapy. 2013;22(1):37-42.
83. Kelly JG, Trevisan J, Scott AD, Carmichael PL, Pollock HM, Martin-Hirsch PL, et al. Biospectroscopy to metabolically profile biomolecular structure: a multistage approach linking computational analysis with biomarkers. Journal of proteome research. 2011;10(4):1437-48.
84. Cialla-May D, Zheng X-S, Weber K, Popp J. Recent progress in surface-enhanced Raman spectroscopy for biological and biomedical applications: from cells to clinics. Chemical Society Reviews. 2017;46(13):3945-61.
85. Smith R, Wright KL, Ashton L. Raman spectroscopy: an evolving technique for live cell studies. Analyst. 2016;141(12):3590-600.
86. Huang J, Liu S, Chen Z, Chen N, Pang F, Wang T. Distinguishing Cancerous Liver Cells Using Surface-Enhanced Raman Spectroscopy. Technology in cancer research & treatment. 2016;15(1):36-43.
87. Lever J, Krzywinski M, Altman N. Points of significance: Principal component analysis. Nature Publishing Group; 2017.
88. Raschka S. 'Linear Discriminant Analysis bit by bit'. Disponible en: sebastianraschka com/Articles/2014_python_lda html. 2014.
89. Fearn T. Discriminant Analysis In: Chalmers J, Griffiths P, editors. Handbook of Vibrational Spectrscopy 3. 5 ed. New York, USA John Wiley and Sons 2002. p. 2086-93.
90. García-Flores A, Raniero L, Canevari R, Jalkanen KJ, Bitar R, Martinho H, et al. High-wavenumber FT-Raman spectroscopy for in vivo and ex vivo measurements of breast cancer. Theoretical Chemistry Accounts. 2011;130(4-6):1231-8.

91. Santos IP, Barroso EM, Schut TCB, Caspers PJ, van Lanschot CG, Choi D-H, et al. Raman spectroscopy for cancer detection and cancer surgery guidance: translation to the clinics. Analyst. 2017;142(17):3025-47.
92. Granger JH, Granger MC, Firpo MA, Mulvihill SJ, Porter MD. Toward development of a surface-enhanced Raman scattering (SERS)-based cancer diagnostic immunoassay panel. Analyst. 2013;138(2):410-6.
93. Krasnoslobodtsev AV, Torres MP, Kaur S, Vlassiouk IV, Lipert RJ, Jain M, et al. Nano-immunoassay with improved performance for detection of cancer biomarkers. Nanomedicine : nanotechnology, biology, and medicine. 2015;11(1):167-73.
94. Wang G, Lipert RJ, Jain M, Kaur S, Chakraboty S, Torres MP, et al. Detection of the potential pancreatic cancer marker MUC4 in serum using surface-enhanced Raman scattering. Analytical chemistry. 2011;83(7):2554-61.
95. Zhou QL, Rong X, Wei F, Luo RQ, Liu H. Different Raman spectral patterns of primary rat pancreatic beta cells and insulinoma cells. Journal of biomedical optics. 2015;20(4):047001.
96. Harmsen S, Huang R, Wall MA, Karabeber H, Samii JM, Spaliviero M, et al. Surface-enhanced resonance Raman scattering nanostars for high-precision cancer imaging. Science translational medicine. 2015;7(271):271ra7.
97. Engvall E, Perlmann P. Enzyme-linked immunosorbent assay (ELISA) quantitative assay of immunoglobulin G. Immunochemistry. 1971;8(9):871-4.
98. Lequin RM. Enzyme immunoassay (EIA)/enzyme-linked immunosorbent assay (ELISA). Clinical chemistry. 2005;51(12):2415-8.
99. Suvarna KS, Layton C, Bancroft JD. Bancroft's Theory and Practice of Histological Techniques E-Book: Elsevier Health Sciences; 2018.
100. Thavarajah R, Mudimbaimannar VK, Elizabeth J, Rao UK, Ranganathan K. Chemical and physical basics of routine formaldehyde fixation. Journal of oral and maxillofacial pathology: JOMFP. 2012;16(3):400.
101. Lin D, Feng S, Pan J, Chen Y, Lin J, Chen G, et al. Colorectal cancer detection by gold nanoparticle based surface-enhanced Raman spectroscopy of blood serum and statistical analysis. Optics express. 2011;19(14):13565-77.
102. Han H, Yan X, Dong R, Ban G, Li K. Analysis of serum from type II diabetes mellitus and diabetic complication using surface-enhanced Raman spectra (SERS). Applied Physics B. 2009;94(4):667-72.
103. Bachem MG, Schünemann M, Ramadani M, Siech M, Beger H, Buck A, et al. Pancreatic carcinoma cells induce fibrosis by stimulating proliferation and matrix synthesis of stellate cells. Gastroenterology. 2005;128(4):907-21.
104. Martin FL, Kelly JG, Llabjani V, Martin-Hirsch PL, Patel II, Trevisan J, et al. Distinguishing cell types or populations based on the computational analysis of their infrared spectra. Nature protocols. 2010;5(11):1748.
105. Verbeke CS, Gladhaug IP. Resection margin involvement and tumour origin in pancreatic head cancer. The British journal of surgery. 2012;99(8):1036-49.
106. Movasaghi Z, Rehman S, Rehman IU. Raman spectroscopy of biological tissues. Applied Spectroscopy Reviews. 2007;42(5):493-541.
107. Talari ACS, Movasaghi Z, Rehman S, Rehman IU. Raman spectroscopy of biological tissues. Applied Spectroscopy Reviews. 2015;50(1):46-111.

108. Nielsen MFB, Mortensen MB, Detlefsen S. Key players in pancreatic cancer-stroma interaction: cancer-associated fibroblasts, endothelial and inflammatory cells. World journal of gastroenterology. 2016;22(9):2678.
109. Olivares O, Mayers JR, Gouirand V, Torrence ME, Gicquel T, Borge L, et al. Collagen-derived proline promotes pancreatic ductal adenocarcinoma cell survival under nutrient limited conditions. Nature communications. 2017;8:16031.
110. Hamada S, Masamune A. Elucidating the link between collagen and pancreatic cancer: what's next? : Taylor & Francis; 2018.
111. Shields MA, Dangi-Garimella S, Redig AJ, Munshi HG. Biochemical role of the collagen-rich tumour microenvironment in pancreatic cancer progression. Biochemical Journal. 2012;441(2):541-52.
112. Drifka CR, Loeffler AG, Mathewson K, Keikhosravi A, Eickhoff JC, Liu Y, et al. Highly aligned stromal collagen is a negative prognostic factor following pancreatic ductal adenocarcinoma resection. Oncotarget. 2016;7(46):76197.
113. Kerns JG, Buckley K, Churchwell J, Parker AW, Matousek P, Goodship AE. Is the collagen primed for mineralization in specific regions of the turkey tendon? An investigation of the protein–mineral interface using Raman spectroscopy. Analytical chemistry. 2016;88(3):1559-63.
114. Verbeke CS, Menon KV. Redefining resection margin status in pancreatic cancer. Hpb. 2009;11(4):282-9.
115. Lin D, Zheng Z, Wang Q, Huang H, Huang Z, Yu Y, et al. Label-free optical sensor based on red blood cells laser tweezers Raman spectroscopy analysis for ABO blood typing. Optics express. 2016;24(21):24750-9.
116. Atkins CG, Buckley K, Blades MW, Turner RF. Raman spectroscopy of blood and blood components. Applied spectroscopy. 2017;71(5):767-93.
117. Hwang RF, Moore T, Arumugam T, Ramachandran V, Amos KD, Rivera A, et al. Cancer-associated stromal fibroblasts promote pancreatic tumor progression. Cancer research. 2008;68(3):918-26.
118. Pavillon N, Bando K, Fujita K, Smith NI. Feature-based recognition of Surface-enhanced Raman spectra for biological targets. Journal of biophotonics. 2013;6(8):587-97.
119. Deer EL, González-Hernández J, Coursen JD, Shea JE, Ngatia J, Scaife CL, et al. Phenotype and genotype of pancreatic cancer cell lines. Pancreas. 2010;39(4):425.
120. Kuen J, Darowski D, Kluge T, Majety M. Pancreatic cancer cell/fibroblast co-culture induces M2 like macrophages that influence therapeutic response in a 3D model. PloS one. 2017;12(7):e0182039.
121. Klein K, Gigler AM, Aschenbrenner T, Monetti R, Bunk W, Jamitzky F, et al. Label-free live-cell imaging with confocal Raman microscopy. Biophysical journal. 2012;102(2):360-8.
122. Sinjab F, Sicilia G, Shipp DW, Marlow M, Notingher I. Label-free Raman hyperspectral imaging of single cells cultured on polymer substrates. Applied spectroscopy. 2017;71(12):2595-607.
123. Ravanshad R, Karimi Zadeh A, Amani AM, Mousavi SM, Hashemi SA, Savar Dashtaki A, et al. Application of nanoparticles in cancer detection by Raman scattering based techniques. Nano Reviews & Experiments. 2018;9(1):1373551.
124. Elsaesser A, Howard CV. Toxicology of nanoparticles. Advanced drug delivery reviews. 2012;64(2):129-37.

125. Stevens O, Petterson IEI, Day JC, Stone N. Developing fibre optic Raman probes for applications in clinical spectroscopy. Chemical Society Reviews. 2016;45(7):1919-34.

Appendix

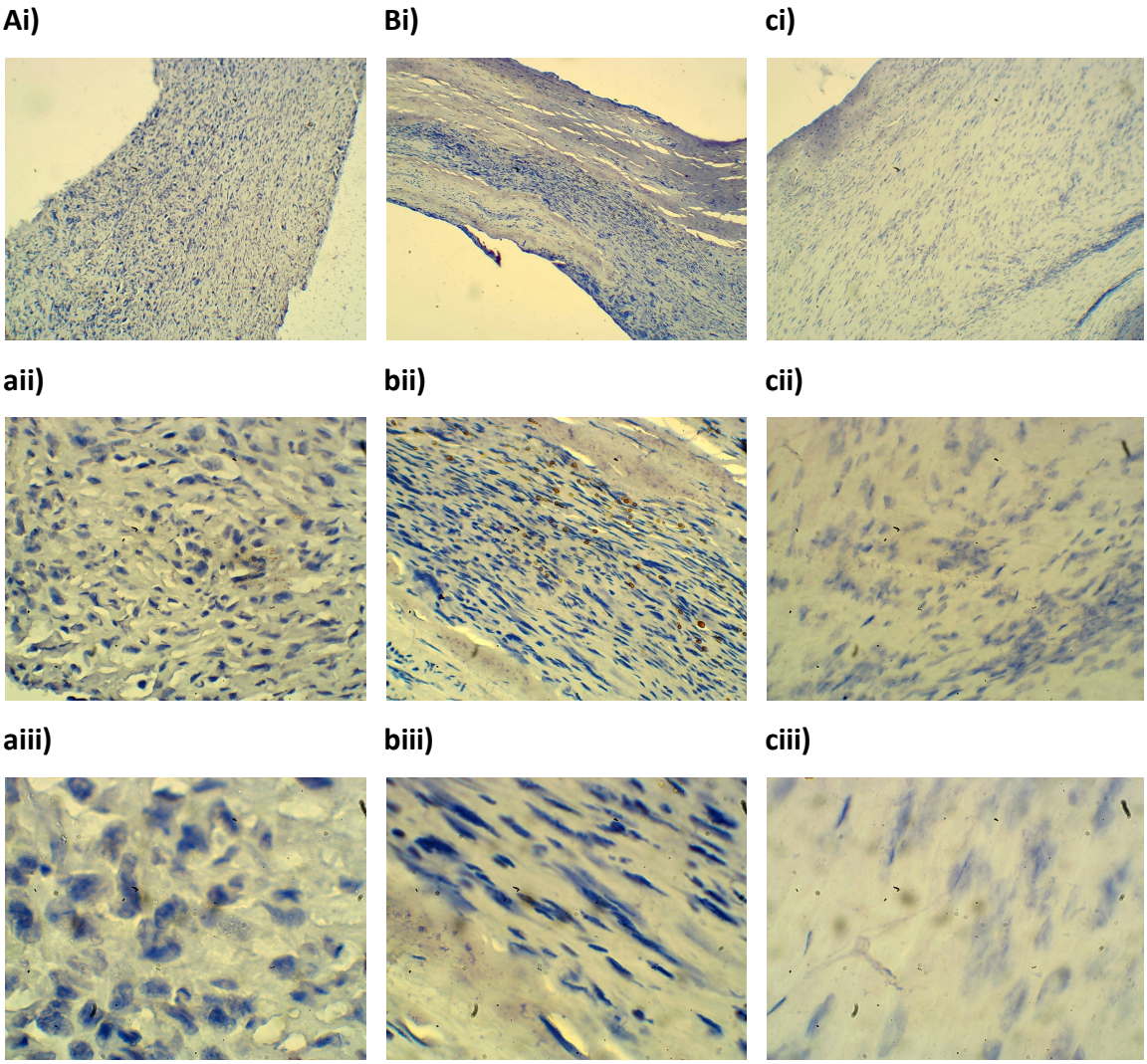

Figure 40: immunohistochemical staining of tumour tissue. The lack of a brown stain suggests no SPARC antigen was detected, suggesting the technique needs to be optimised. ai) patient 1 x10, aii) patient 1 x40 aiii) patient 1 x100 bi) patient 2 x10, bii) patient 2 x40 biii) patient 2 x100 ci) patient 3 x10, cii) patient 3 x40 ciii) patient 3 x100

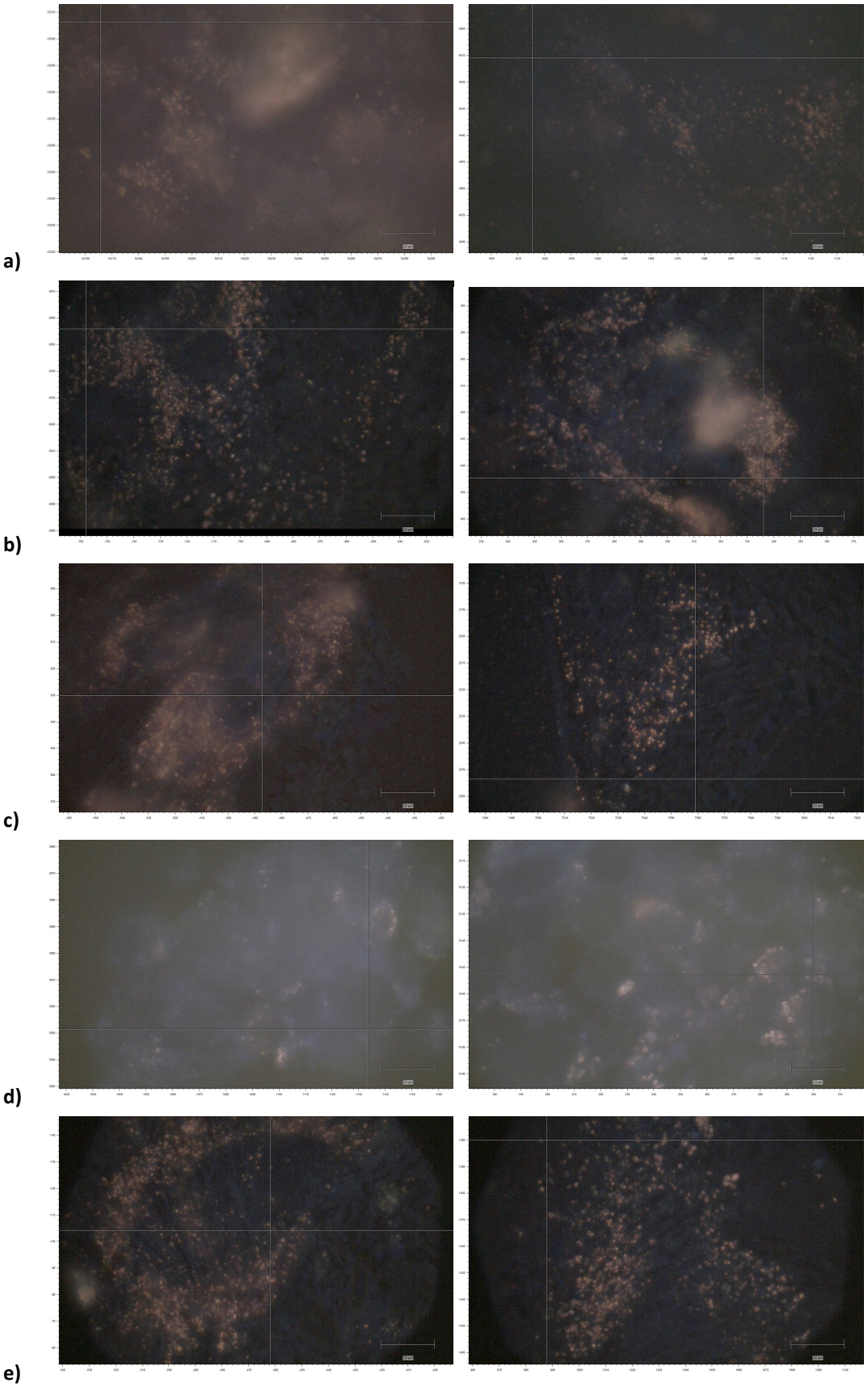

Figure 41: white light images for cell cocultures with SERS showing cell outlines and presence of nanoparticles. Scale bar 20μm a) HPAF 25:75, b) HPAF 50:50, c) HPAF 75:25, d)HPAF 100% e) PSC 100%

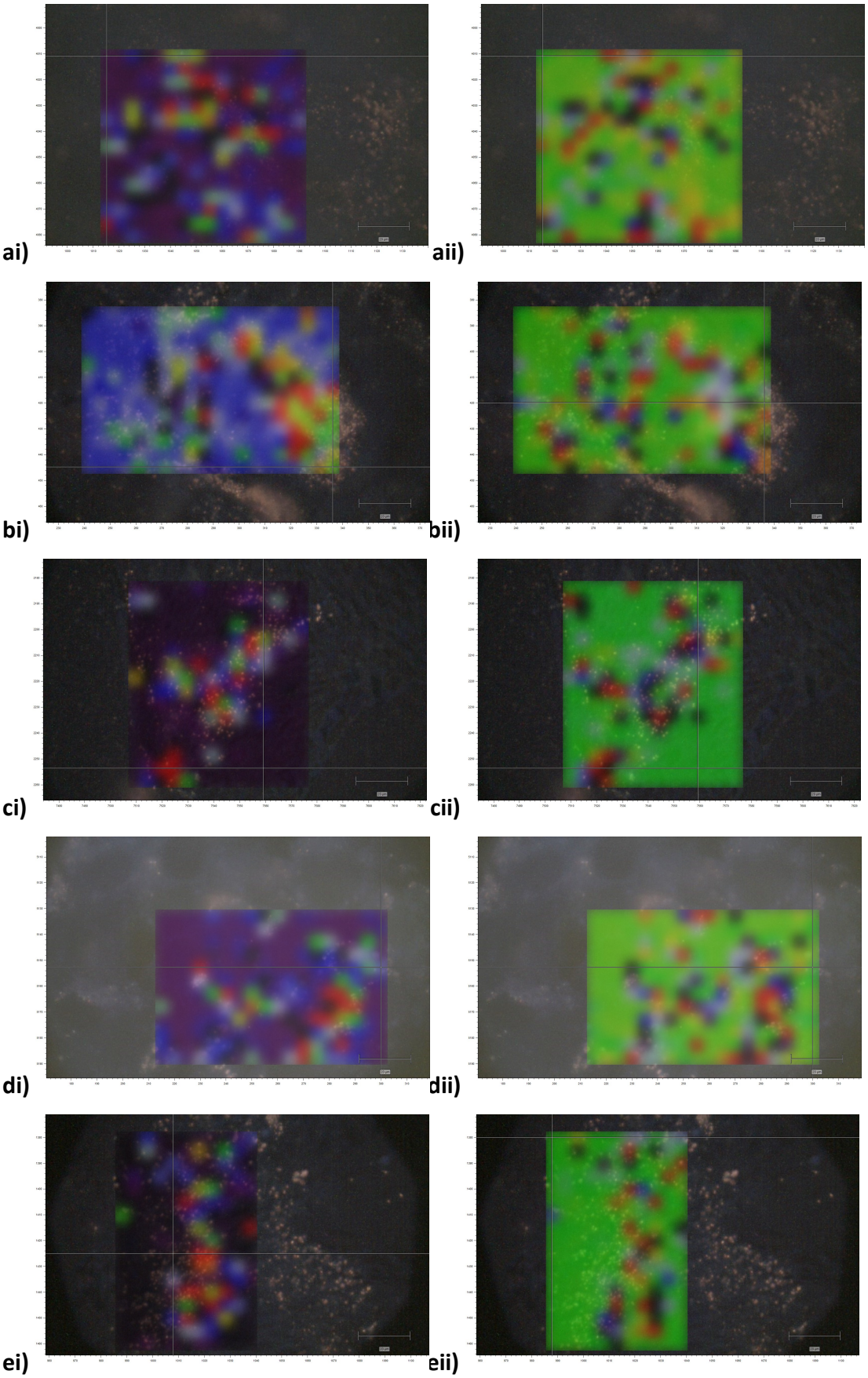
ai)
aii)
bi)
bii)
ci)
cii)
di)
dii)
ei)
eii)

Figure 42: Raman shaded maps for cell cocultures grown in direct contact with SERS showing shading by signal to baseline analysis for wavenumbers i) 600-800cm^{-1} and ii)1325-1345cm^{-1}. Colour bar shown as reference for shading; blue shows lowest relative intensity and red the highest relative intensity within the image but shading is arbitrary and not numerically equal or comparable between images. Scale bar 20μm. ai) HPAF:PSC 25:75 600-800cm^{-1} shading aii) HPAF:PSC 25:75 1325-1345cm^{-1} shading , bi) HPAF 50:50 600-800cm^{-1} shading bii) HPAF:PSC 50:50 1325-1345cm^{-1} shading, ci) HPAF:PSC 75:25 600-800cm^{-1} shading cii) HPAF:PSC 75:25 1325-1345cm^{-1} shading, d)HPAF 100% 600-800cm^{-1} shading dii)HPAF 100% 1325-1345cm^{-1} shading ei) PSC 100% 600-800cm^{-1} shading eii) PSC 100% 1325-1345cm^{-1} shading

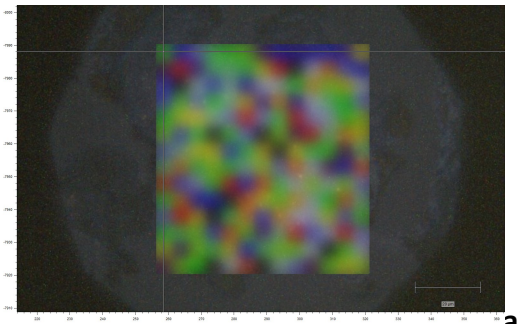
ai)

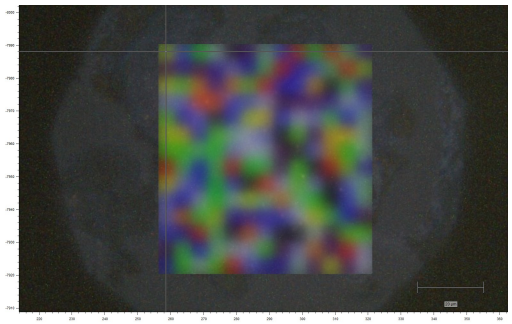
aii)

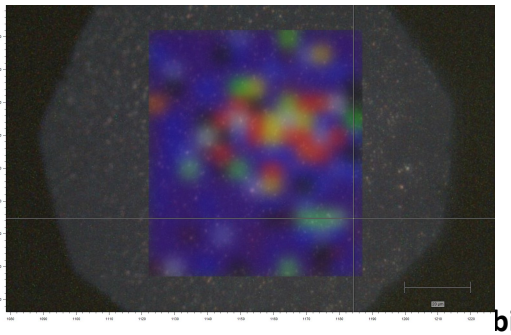
bi)

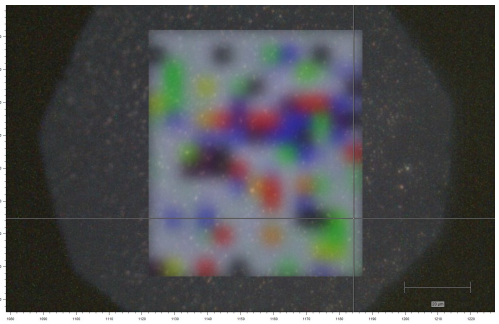
bii)

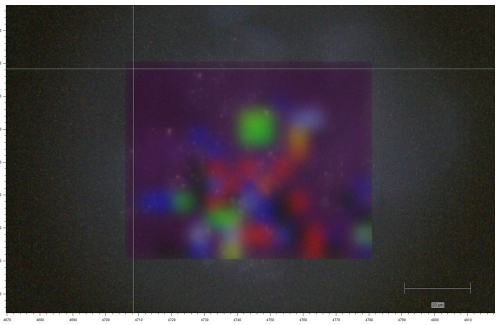
ci)

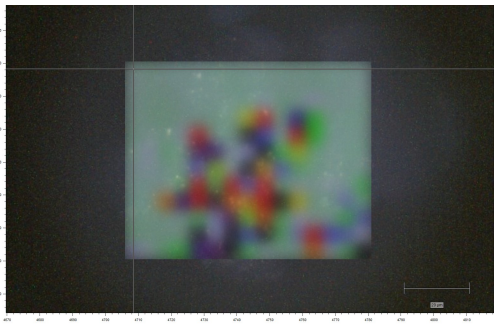
cii)

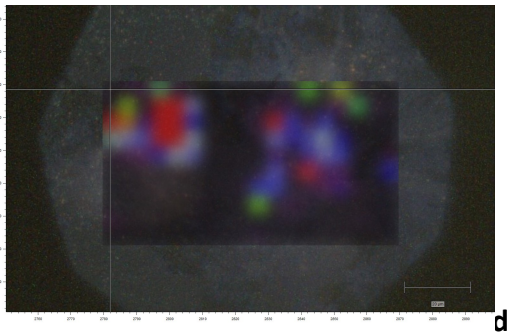
di)

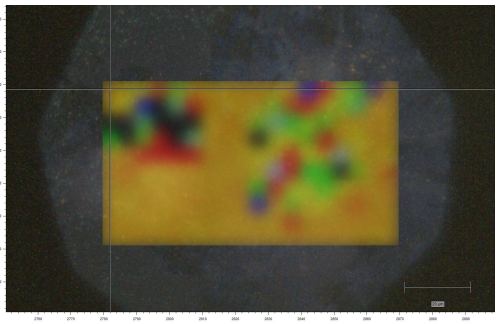
dii)

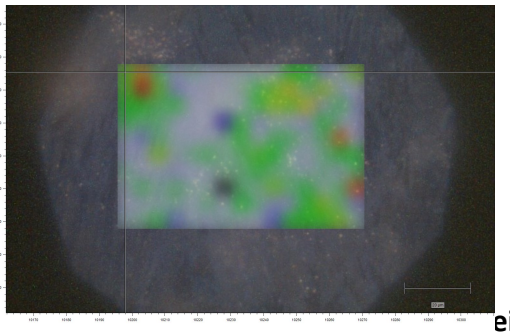
ei)

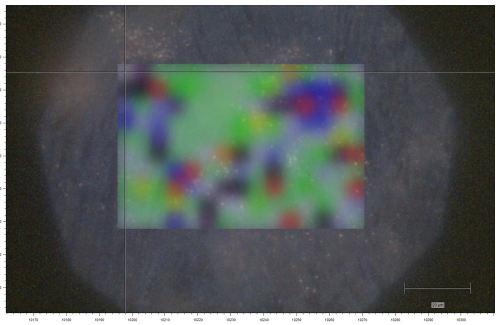
eii)

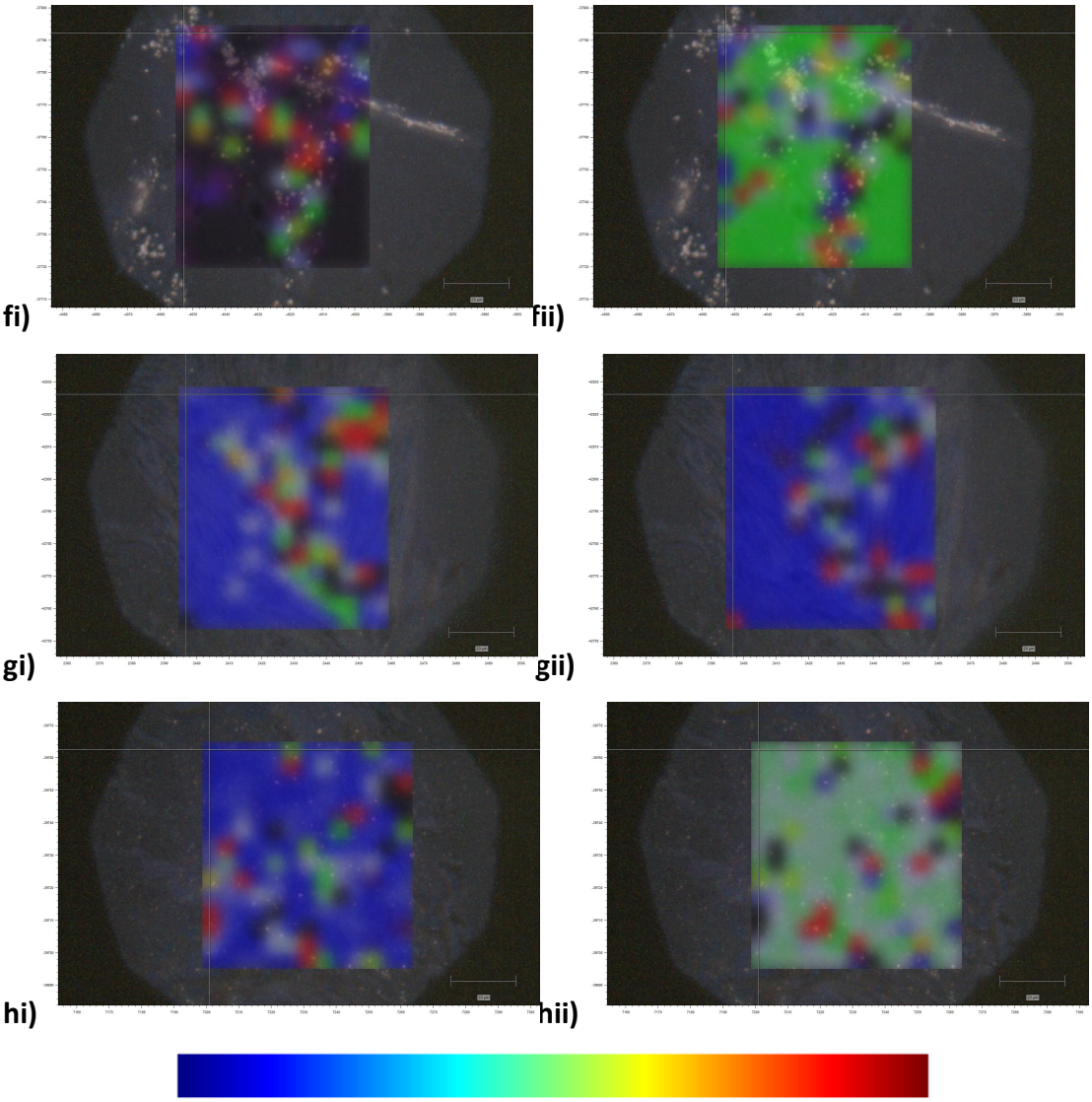

Figure 43: Raman shaded maps for cell cocultures grown in indirect contact with SERS showing shading by signal to baseline analysis for wavenumbers i)600-800cm^{-1} and ii) 1325-1345cm^{-1}. Colour bar shown as reference for shading; blue shows lowest relative intensity and red the highest relative intensity within the image but shading is arbitrary and not numerically equal or comparable between images. Scale bar 20μm. ai) HPAF 25% 600-800cm^{-1} shading aii) HPAF 25% 1325-1345cm^{-1} shading , bi) HPAF 50% 600-800cm^{-1} shading bii) HPAF 50% 1325-1345cm^{-1} shading, ci) HPAF 75% 600-800cm^{-1} shading cii) HPAF 75% 1325-1345cm^{-1} shading, d)HPAF 100% 600-800cm^{-1} shading dii)HPAF 100% 1325-1345cm^{-1} shading ei) PSC 100% 600-800cm^{-1} shading eii) PSC 100% 1325-1345cm^{-1} shading, fi) PSC 25% 600-800cm^{-1} shading fii) PSC 25% 1325-1345cm^{-1} shading , gi) PSC 50% 600-800cm^{-1} shading gii) PSC 50% 1325-1345cm^{-1} shading, hi) PSC 75% 600-800cm^{-1} shading hii) PSC 75% 1325-1345cm^{-1} shading.